

1-1-1997

The mathematical modelling of the Ross River Virus transmission

Yoon-Hong Choi
Edith Cowan University

Follow this and additional works at: <https://ro.ecu.edu.au/theses>



Part of the [Immunology and Infectious Disease Commons](#)

Recommended Citation

Choi, Y. (1997). *The mathematical modelling of the Ross River Virus transmission*. <https://ro.ecu.edu.au/theses/896>

This Thesis is posted at Research Online.
<https://ro.ecu.edu.au/theses/896>

Edith Cowan University

Copyright Warning

You may print or download ONE copy of this document for the purpose of your own research or study.

The University does not authorize you to copy, communicate or otherwise make available electronically to any other person any copyright material contained on this site.

You are reminded of the following:

- Copyright owners are entitled to take legal action against persons who infringe their copyright.
- A reproduction of material that is protected by copyright may be a copyright infringement. Where the reproduction of such material is done without attribution of authorship, with false attribution of authorship or the authorship is treated in a derogatory manner, this may be a breach of the author's moral rights contained in Part IX of the Copyright Act 1968 (Cth).
- Courts have the power to impose a wide range of civil and criminal sanctions for infringement of copyright, infringement of moral rights and other offences under the Copyright Act 1968 (Cth). Higher penalties may apply, and higher damages may be awarded, for offences and infringements involving the conversion of material into digital or electronic form.

**The Mathematical Modelling of
the Ross River Virus Transmission**

BY

Yoon Hong Choi

BSc (Mathematics), MSc (Mathematics)

A Thesis Submitted for the Award of

Doctor of Philosophy

at the Faculty of Science, Technology and Engineering

Edith Cowan University

Date of Submission : February, 1997

USE OF THESIS

The Use of Thesis statement is not included in this version of the thesis.

Abstract

Ross River virus is one of the most severe communicable diseases in Australia. During the 1995/96 outbreak of Ross River virus in south-western Australia, over 1,300 human cases were reported. Since the symptoms of the disease are sometimes too weak to be diagnosed, it is important to determine the number of humans who actually contracted the virus during outbreaks.

To do this, several mathematical models with different hypotheses are constructed and analysed mathematically. The threshold mathematical conditions of these models suggest that as well as the size of the vector mosquito population, the population size and length of viraemia periods of host populations and the infection rates between the hosts and vectors play the main roles in the transmission.

Several parameters in the transmission are currently unknown, so only simple models of RRV transmission are computer-simulated. Some of the unknown parameters are extrapolated from published studies of other arboviruses. The sensitivities of the models to some of the unknown parameters are also examined.

Simulation results indicate the sero-conversion rates and ratios of clinical to subclinical human infections during the outbreaks which occurred in the Peel and Leschenault districts in Southwestern Australia.

To

My Family

DECLARATION

"I certify that this thesis does not incorporate without acknowledgement any material previously submitted for a degree or diploma in any institution of higher education; and that to the best of my knowledge and belief it does not contain any material previously published or written by another person except where due reference is made in the text"

Signature:

Date: 25/8/97

Acknowledgements

There are many people I must thank for the support and encouragement that has been offered to me throughout this course.

Foremost, I wish to thank my supervisors, Dr. Catherine Comiskey, Associate Professor James Cross and Dr. Malcolm Anderson for providing constant guidance and constructive criticism.

My special thanks go to Dr. Michael Lindsay, University of Western Australia, who during his busy schedule, allowed me to use his data on Ross River virus. He also provided me with his remarkable microbiological knowledge.

I am immensely indebted to Dr. Dong Won Yu, Chung-Ang University, South Korea who guided me with his mathematical knowledge so that I could finish my thesis.

I would like to express my gratitude to Australian Government for offering me a scholarship to complete this study. I would also like to thank Professor Anthony Watson and Edith Cowan University for enabling me to attend and present papers at a number of conferences during this course.

Numerous colleagues at the Edith Cowan University have offered me their good friendship and warmth to continue my study during this course : among them are Stephan Bettermann, Marek Koscielecki, Andrew Mehnert, Damon Whyte, Suresh Tripathi and Saarah Farag.

Finally, but most deeply, I would also like to express my sincere gratitude to my family. Very special thanks go to my mother for her consistent love and

encouragement. I am dubious that I could finish my study without her love and support. I would also like to thank my sisters for their support.

My deepest appreciation goes to my lovely wife, Kyungmin Lee, for her endless love, patience, support and encouragement during my study.

Table of Contents

Use of Theses	i
Title Page	ii
Abstract	iii
Dedication	iv
Declaration	v
Acknowledgement	vi

Chapter

1. Introduction	1
1.1 Background	1
1.1.1 Ross River virus	2
1.1.2 Affected regions	3
1.1.3 Hosts and vectors of the Ross River virus	3
1.1.4 Seasonal trend	4
1.1.5 Medical symptoms	5
1.1.6 Distribution of patients	5
1.1.7 Prevention	6
1.1.8 Economic aspects	7
1.2 Data collection	7
1.3 Overview of thesis	8
1.4 Limitations of the research	9
1.5 Significance of the research	10

2. A brief introduction to population dynamics in epidemics	12
2.1 A brief history of population dynamics in epidemics	12
2.2 The basic deterministic model	15
2.3 Equilibrium values for the basic deterministic model	22
2.4 Host-Vector model	26
2.5 The Equilibrium Values for the Host-Vector model	31
2.6 Some specific models for malaria	33
2.6.1 Kingsolver's model	34
2.6.2 Moreira's model	37
2.6.3 Dye and Hasibeder's model	38
2.6.4 Discussion of Malaria models	40
3. The Host-Vector model for the RRV	43
3.1 The basic model with one host and one vector	44
3.2 The basic model with two hosts and one vector	55
3.3 The General model for RRV transmission	65
4. The host-vector model for the RRV with continuous natural infection on mosquito population	73
4.1 The basic model with one host and one vector with continuous natural infection	75
4.2 The basic model with two hosts and one vector	78
4.3 The general model for the RRV transmission	80

5. Parameter Estimation for the Simulation	83
5.1 Simulation models	85
5.2 Human population	85
5.3 Mosquito population	87
5.4 Infection rates β_1, β_2	92
6. Simulation Results	94
6.1 Simulation results for the 1991/92 outbreak in the Peel district	94
6.1.1 Estimating the parameters for the <i>Aedes camptorhynchus</i> population	96
6.1.2 Simulation result for the models (3.1.1) and (4.1.1)	100
6.1.3 Simulation results using different starting dates for the outbreak	108
6.1.4 Ten year simulation	111
6.1.5 Simulation results for the 1991/93 outbreak in the Peel district	113
6.1.6 Simulation results with a variable human exposure rate	115
6.2 Simulation results for the 1995/96 outbreak in the Peel district	117
6.3 Simulation results for the 1995/96 outbreak in the Leschenault district	124
6.3.1 Estimating the parameters for the <i>Aedes camptorhynchus</i> population	124
6.3.2 Simulation results of the different transmission rates	129

6.4 Discussion of simulation results	132
7. Conclusion	136
7.1 Summary	136
7.2 Future directions	138
References	141
Appendix	147
A.1. The computer program	147
A.2. The computer program listings	147

CHAPTER 1.

INTRODUCTION

Mathematical modelling is widely used in the study of complex systems in biology. The methods of population dynamics, and in particular the theory of systems of nonlinear differential equations, have been applied increasingly to problems in epidemiology. Numerous mathematical models have been constructed and simulated to determine the spread, cause and cost of outbreaks of communicable diseases such as AIDS, gonorrhea, malaria, rubella, etc.

The aim of this thesis is to build deterministic models that reflect the ecological cycle and transmission of the Ross River virus and to analyse them mathematically. Furthermore, this thesis presents the results of simulations based on outbreaks that occurred in several South Coastal districts in Western Australia.

1.1. Background

This section presents a brief introduction to the Ross River virus including its definition, history, medical symptoms, affected regions, the distribution of patients, ecological cycle, protection, and its economic aspects.

1.1.1. Ross River virus

Ross River virus (RRV) is an aetiological agent of a disease in humans known as epidemic polyarthritis (EPA) (Doherty *et al.*, 1963b). The disease is

the most common arboviral illness in humans in Australia with between several hundred and several thousand cases reported annually (CDI, 1991; CDI, 1992). RRV is an alphavirus in the family Togaviridae (Doherty *et al.*, 1963b, Strauss, 1991).

The first description of RRV was an "unusual epidemic" that occurred in Narrandera, New South Wales during 1928 (Nimmo, 1928). It is believed that this was not the first time RRV disease occurred in Australia. RRV was first isolated from mosquitoes trapped on the Ross River, near Townsville, North Queensland by Doherty and co-workers in 1963 (Doherty *et al.*, 1963a). Since then, it has become clear that mosquitoes are the only vectors of the virus (Kay *et al.*, 1987; Kay *et al.*, 1989). Most outbreaks occurred after periods of heavy rains and there is a seasonal trend in outbreaks. It was later found in the Northern Territory and Queensland that outbreaks among troops during World War II were reported by army medical personnel. The disease was given various names until in 1946 Dowling called it epidemic polyarthritis - a term that can be applied to diseases caused by a few of the alphaviruses. Later variations of the name arose from the site of the virus isolation of Ross River in northern Queensland.

1.1.2. Affected regions

Since Doherty isolated the virus, a number of outbreaks of RRV disease have occurred in the Murray Valley (Anderson & French 1957), Queensland (Doherty *et al.*, 1971), the central and coastal regions of New South Wales (Gard *et al.*, 1973; Hawkes *et al.*, 1985), South Australia (Mudge *et al.*, 1980),

Victoria (Campbell *et al.*, 1989), the Northern Territory (Merianos *et al.*, 1992; Tai *et al.*, 1993), south-western Australia (Lindsay, 1995), and the Pilbara and Kimberly regions in Western Australia (Lindsay, 1993b). Recently cases of Ross River virus disease have been reported throughout all mainland states of Australia and in several Pacific islands, such as the Solomon Islands and Papua New Guinea. During 1979 and 1980 massive outbreaks involving tens of thousands of people occurred in the Fiji Islands, American Samoa, the Cook Islands, and Funua and Wallis Islands and New Caledonia (Lindsay *et al.*, 1993a).

1.1.3. Hosts and vectors of the Ross River virus

The arthropod-borne animal viruses (arboviruses) have the ability to multiply in arthropod, as well as vertebrate, tissues and possess characteristic biochemical properties. The virus cycle also involves native and introduced animals. Most studies show that a wide range of nonmigratory, terrestrial animals, particularly marsupials, are the most likely vertebrate reservoirs or amplifiers of RRV (Mackenzie, *et al.*, 1994). Infected humans may also be responsible for transporting the virus over long distances as birds are not thought to be susceptible to infection. This is thought to be the means of introduction and spread of RRV during the outbreak in the Pacific Islands in 1979-80.

Since Doherty's first isolation of the Ross River virus from *Aedes vigilax*, the virus has been isolated from field specimens of 21 different mosquito species belonging to five genera. In Western Australia, the Ross River virus has been isolated from nine different mosquito species. *Culex annulirostris* is

thought to be the most important vector species in most inland areas in eastern Australia. *Aedes vigilax* is a major vector in coastal areas of New South Wales, Queensland, and the Northern Territory. *Aedes camptorhynchus* is the dominant salt-marsh breeding species and has yielded several isolates of the virus in coastal regions of Victoria and Tasmania and parts of South Australia. *Aedes vigilax* is a dominant species in coastal areas of the West Kimberley, north-west of Western Australia. The main vector of the Ross River virus in the south-west of Western Australia is *Aedes camptorhynchus*, which is thought to be restricted to cooler coastal regions of Australia and Western Australia (Lindsay, 1996).

1.1.4. Seasonal trend

RRV disease occurs in most years in many coastal areas of Australia. Most outbreaks occur after periods of heavy rain and there is a seasonal trend in outbreaks (Fig. 1.1). When mosquitoes reach plague proportions significant outbreaks may occur.

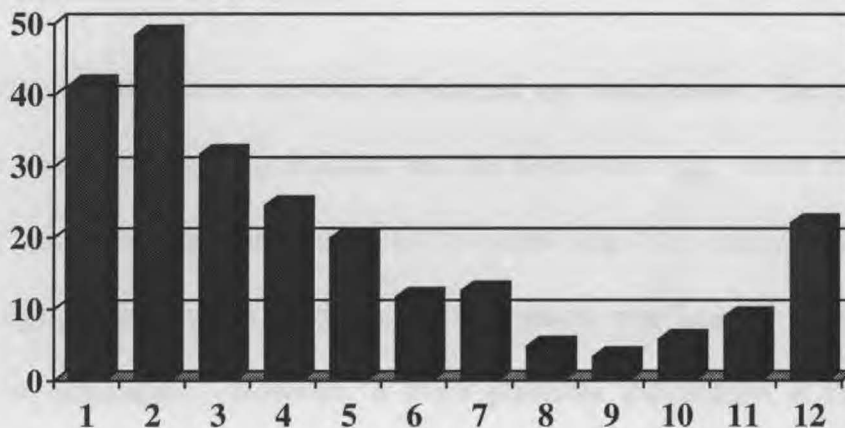


**Fig. 1.1 Average number of cases in WA each month, 1984-1993
(inclusive). (Lindsay, 1995)**

1.1.5. Medical symptoms

The disease is self-limited and characterized by arthritic pain - primarily in the wrist, knee, ankle, small joints of the extremities - rash, fever, and myalgia, which may last from days to months. Affected adults are unable to work in this period. Onset of arthritis may be followed by a maculopapular rash mainly affecting the trunk and limbs. Fever is sometimes absent. Cervical lymphadenopathy occurs frequently (Australia, Weekly Epidemiological Record, 1994). The incubation period is thought to range between 7 and 9 days. During the biggest outbreak of RRV infection in Western Australia between November 1988 and June 1989 only 27% of patients had recovered completely within 6 months of the onset of symptoms and up to 57% still experienced at least intermittent joint symptoms (Condon *et al.*, 1994).

1.1.6. Distribution of patients

The distribution of patients shows a bell-shaped age distribution. The age group that was most frequently infected was the 30-50 year olds. More than half of the cases were aged between 25 and 50 years (Fig. 1.2). The younger and older age groups possibly experienced lower attack rates because of less exposure to mosquitoes. However, a more plausible explanation is that children often do not manifest the typical symptoms of EPA and the elderly may be immune through previous infection. In addition, there are proportionally more females than males in Australia (female/male ratio 1.12/1) (Tai *et al.*, 1993). However, in Western Australia there are proportionally more males than females and this is reflected in Figure 1.2.

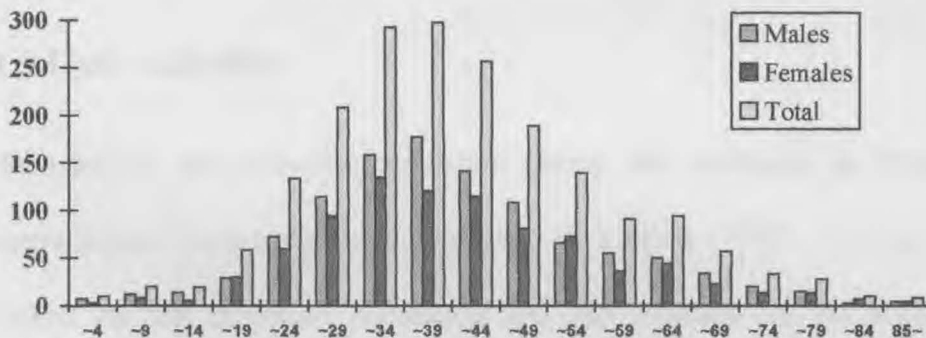


Figure 1.2. Notifications of RRV by age and sex, WA, 1985-1994

(Does not include 13 notifications). (Lindsay, 1995)

1.1.7. Prevention

No vaccine is available for Ross River virus infection, and prevention of the disease is based upon reducing the risk of exposure to infective mosquito bites (Australia, Weekly Epidemiological Record, 1994). The prevention of

mosquito-borne polyarthrititis relies on reduced exposure to mosquitoes through personal protection and environmental control. Personal protection, through the use of mosquito screens, long loose clothing and the use of repellents containing no more than 20% diethyltoluamide (DEET), is advised (Wolstenholme, 1992).

1.1.8. Economic aspects

The cost of the 1979-1980 Pacific epidemic of Ross River virus has not been estimated; however, the cost of the 1983-1984 outbreak in New South Wales was estimated at about \$3 million. The cost of RRV to the community in Western Australia (WA) alone between 1984 and 1996 was conservatively estimated at \$9.7 million. In Queensland, diagnostic serology costs \$500,000 annually (Kay, *et al.*, 1989).

1.2.Data collection

Samples of the mosquito population during the outbreaks in Western Australia have been collected and analysed by Lindsay (1995). Lindsay has worked on the mosquito population and the isolation of the RRV in mosquitoes in Western Australia since January 1987 as part of his doctoral studies on 'Ecology and epidemiology of Ross River virus in Western Australia'.

A database has been constructed to record the incidence, timing and place of exposure of cases of RRV disease in Western Australia. Data has been provided by all medical practitioners throughout the south-west of Western Australia who were registered with the Medical Board of Western Australia

on the 29th July 1986 (Lindsay, 1995). Comparing the real notifications from the database with the results of simulations, the likely ratio of clinical to subclinical human infections and the sero-conversion rate after the outbreaks can be estimated.

1.3. Overview of Thesis

Since Bernoulli's first epidemic model (1790), a variety of mathematical models have been developed to determine the spread, cause and cost of epidemic outbreaks. Chapter 2 gives a brief history of the application of population dynamics to epidemics. This chapter also introduces some basic deterministic models relevant to the RRV model. Furthermore, the mathematical properties of the models, which have been analysed by Bailey (1975), are discussed. In this chapter, three epidemic models for malarial transmission due to Kingsolver (1987), Moreira (1992), and Dye and Hasibeder (1988) are also introduced and discussed.

Chapter 3 discusses the mathematical models of RRV transmission with a single natural infection in the mosquito population while Chapter 4 considers those models with continuous natural infections in the mosquito population. In Chapters 3 and 4, three mathematical models of RRV transmission with single and continuous natural infection in the mosquito population are built with varying degrees of complexity. Later, the mathematical analysis of the models mentioned is undertaken, especially the threshold conditions and the stability conditions for the equilibrium points.

Chapter 5 introduces two types of simulation models for RRV transmission with a single or continuous natural infection in the mosquito population. This

chapter also presents the methods used to estimate the parameters describing the host and mosquito populations and their interactions with each other. Several numerical methods used to estimate the parameter values and to run the simulations are also presented in this chapter.

Chapter 6 presents the results of simulations of actual RRV outbreaks in some South Coastal districts in Western Australia.

Finally, Chapter 7 provides a general conclusion of this thesis and outlines areas for future research. The C program that implements the simulation for RRV transmission in this thesis is presented in the Appendix.

1.4. Limitations of the Research

Many of the parameters of RRV transmission are unknown and only limited field data are available. Therefore, the value of many of the parameters must rely on estimates provided by personal communication with microbiologists or entomologists. Some numerical methods are also used to estimate parameter values. For example, it is known that the mortality and recruitment rates of the mosquito population depend on different environmental conditions such as temperature, humidity, the tides, etc. However, research on the effects of these environmental factors on the transmission has not been completed. Also, the study of the extrinsic incubation period of mosquitoes with RRV is not completed. The range of possible values of the mortality rate and extrinsic incubation period for the mosquito population has been included on the basis of personal communication with Lindsay. The recruitment rate is extended from the field measurements of the total mosquito population by assuming a

sinusoidal mortality rate. The RRV has been identified in twenty-one different mosquito species belonging to five genera. Each mosquito species has a different life cycle and so different parameter values for the RRV transmission. However, the difficulty of getting the parameter values for all the mosquito species compels us to use a simple model incorporating only the main mosquito species involved in the transmission.

1.5. Significance of the Research

The RRV disease is conservatively estimated to have cost the Western Australian community A\$9.7 million between 1984 and 1996 (based on cost per case calculated by Geelhoed (1995) and incidences of the disease (Lindsay, 1995, Lindsay, unpublished data)). Given the cost of the epidemic and the numbers infected we believe that there is an urgent need for more research into the spread of this virus and in particular into mathematical and simulation studies of its spread through the Australian population.

In the light of the simulation results this thesis discusses the likely ratio of clinical to subclinical human infections of RRV and the sero-conversion rate after RRV outbreaks in Western Australia. To determine the likely ratio of clinical to subclinical human infections is especially significant for public health policy. Since the symptoms of the RRV disease are different for each patient, only some patients with severe symptoms have been notified with medical authenticics while others have not been.

Currently, there is no vaccine available for the RRV. Therefore, the only means of preventing human infection is to use surveillance methods to warn of outbreaks, with appropriate mosquito control and media warnings when

necessary. One means of predicting such outbreaks is to mathematically model transmission cycles of the disease and to carry out computer simulations of epidemic transmission.

CHAPTER 2.

A BRIEF INTRODUCTION TO POPULATION DYNAMICS IN EPIDEMICS

This chapter gives a brief history of the application of population dynamics to epidemics together with some examples. In particular, some basic epidemic models relevant to the RRV model are introduced and, following the work of Bailey (1975), are analysed. Additionally, some specific host-vector models for malaria are introduced and discussed.

2.1. A BRIEF HISTORY OF POPULATION DYNAMICS IN EPIDEMICS

The mathematical analysis of epidemics has been studied for a long time with a variety of models developed to determine the spread and cause of epidemic outbreaks. An epidemic is defined as a disease affecting or tending to attack many individuals in a population, community, or region at the same time. It is also any outbreak of a disease, which is regarded as an isolated phenomenon. On the other hand, a disease that is endemic is defined as belonging to or restricted to a particular locality or region. Recurrent epidemics tend to have some specific oscillations, which can be due to limit cycle behaviour or seasonal variation. It is generally believed that the first epidemic model was constructed by Bernoulli (1760). The model, involving a nonlinear ordinary differential equation, considered the effect of cow-pox inoculation on the spread of smallpox. The model was used to assess the practical advantages of a vaccination control programme.

In the early twentieth century, Hamer (1906), Ross (1911) and Moshkovski (1950) formulated specific theories about the transmission of infectious diseases. Hamer (1906) postulated the contact rate between susceptibles and infectives. In a deterministic model of an infectious disease, the population consists of two disjoint groups : the susceptible group and the infective group. The susceptible group are individuals who have not been infected by the disease. The infective group are individuals who are infected and able to transmit the disease. By using this idea, Hammer could prove the existence of periodic recurrences. This result has become the most important concept in this area. Kermack and McKendrick (1927) established the famous threshold theorem which is a cornerstone of modern theoretical epidemiology. The threshold theorem of epidemiology states that if the number of susceptibles exceeds a certain threshold value, then an epidemic outbreak will occur. The threshold theorem of the simple deterministic model is discussed in the following section, 2.2.

Soper (1929) first studied deterministic models of the periodicity of recurrent outbreaks of measles. The fact that simple models gave only damped waves discouraged him. Wilson and Worcester (1941 and 1945) made further investigations along similar lines. Consequently, Bartlett (1953-1960) reconsidered the problem and began with a discrete model to serve to carry the neutrally stable model into damped oscillations. Bartlett made several advances by formulating a more realistic stochastic model. May (1976) gave an overview for the development of the aspect of dynamical systems theory.

Capasso (1993) has examined the stability of a very general class of mathematical models of epidemic systems.

Over the past three decades biomathematicians have been concerned with probabilistic models. In recent work, they are emphasising the application of control theory to epidemic models, the study of the spatial spread of diseases, the investigation of the mechanisms underlying recurrent epidemic behaviour, and the extension of the threshold theory to encompass more complex deterministic and stochastic models.

The matter of homogeneity and heterogeneity of populations in epidemic system is an important part of mathematical models. Since the parameter values involved in the epidemic system are difficult to get, most mathematical models of epidemics assume that the populations are homogeneously mixing (Muench, 1959). However, the populations in real epidemics mix heterogeneously and the results are generally different. Recently, the study of spatial heterogeneity and dispersal in epidemic systems has been done by many researchers such as Hethcote and van Ark (1987). Furthermore, the study of age structured epidemic models have been the subject of much research.

In the following sections, we introduce a basic deterministic model and a basic host-vector model. These are important as they form the basis for all subsequent models of the RRV. These sections are based on Bailey (1975); however, we include full detail of the mathematical analysis of his models including a discussion of the equilibrium values.

2.2. THE BASIC DETERMINISTIC MODEL

In the basic deterministic model of an infectious disease, the total population, n , is divided into three disjoint groups. The susceptible group, $x(t)$, consists of those who have not contracted the disease. The infective group, $y(t)$, consists of those who are able to transmit the disease. Finally, the removal group, $z(t)$, consists of those who are removed by recovery or death.

There are three basic assumptions in the model.

1. The total population has a constant size n in the time interval considered. Changes in the population due to birth, death and migration are assumed to be negligible.

2. The population is homogeneously mixing. The host and vector populations are not divided by social behaviour and mix together homogeneously. The rate of occurrence of new infectives is proportional to both the number of susceptibles and the number of infectives. Thus the number of infections in time Δt is $\beta xy\Delta t$, where β is the infection rate.

3. Due to death or recovery from the disease, individuals are removed from the infective group, $y(t)$, at a rate proportional to the number of infectives. Hence, the number of removals due to death or recovery in time Δt is $\gamma y\Delta t$, where γ is the removal rate.

The basic differential equations following from these assumptions are

$$\begin{cases} \frac{dx}{dt} = -\beta xy, \\ \frac{dy}{dt} = \beta xy - \gamma y, \\ \frac{dz}{dt} = \gamma y, \end{cases} \quad (2.2.1.)$$

where $\rho = \frac{\gamma}{\beta}$ is the relative removal rate and the initial condition for (x, y, z) when $t = 0$ is $(x_0, y_0, 0)$.

If y_0 is small, x_0 will be approximately equal to n . Unless $\rho < x_0$ no epidemic can start to build up as this requires $[dy/dt]_{t=0} > 0$. That is,

$$\frac{dy}{dt} = \beta y(x - \frac{\gamma}{\beta}) = \beta y(x - \rho) > 0 \text{ at } t = 0.$$

Eliminating y from the first and third equations of (2.2.1) by division gives

$$\frac{dx}{dz} = -\frac{x}{\rho} \text{ or } x = x_0 e^{\left(-\frac{z}{\rho}\right)}. \quad (2.2.2.)$$

Substituting (2.2.2) into the third equation of (2.2.1), we obtain

$$\frac{dz}{dt} = \gamma(n - x - z) = \gamma \left(n - z - x_0 e^{\left(-\frac{z}{\rho}\right)} \right). \quad (2.2.3.)$$

Here $e^{\left(-\frac{z}{\rho}\right)}$ can be expanded by Taylor's series to $1 - \frac{z}{\rho} + \frac{z^2}{2\rho^2} - \xi$, where ξ

is the remainder term. Therefore,

$$\frac{dz}{dt} \approx \gamma \left\{ n - x_0 + \left(\frac{x_0}{\rho} - 1 \right) z - \frac{x_0}{2\rho^2} z^2 \right\}, \quad (2.2.4.)$$

as described in Bailey (1975).

Assume that z/ρ is small and that $x_0/\rho - 1$ is also small. This will occur near the threshold $\rho = x_0$.

The removal group $z(t)$ in (2.2.4) can be solved as

$$\left. \begin{aligned} z &= \frac{\rho^2}{x_0} \left\{ \frac{x_0}{\rho} - 1 + \alpha \tanh \left(\frac{1}{2} \alpha \gamma t - C' \right) \right\}, \\ \text{where } \alpha &= \left(\left(\frac{x_0}{\rho} - 1 \right)^2 + \frac{2x_0 y_0}{\rho^2} \right)^{\frac{1}{2}}, \\ \text{and } C' &= \tanh^{-1} \frac{1}{\alpha} \left(\frac{x_0}{\rho} - 1 \right), \end{aligned} \right\} \quad (2.2.5.)$$

as summarised by Bailey (1975).

The *epidemic curve*, which is defined by the rate of change with respect to time of the total number of removals, is therefore given by

$$\frac{dz}{dt} = \frac{\gamma \alpha^2 \rho^2}{2x_0} \operatorname{sech}^2 \left(\frac{1}{2} \alpha \gamma t - C'' \right).$$

So, if $t \rightarrow \infty$ in (2.2.5), then the total numbers of removals becomes

$$z_{\infty} = \frac{\rho^2}{x_0} \left\{ \frac{x_0}{\rho} - 1 + \alpha \right\}.$$

If $2x_0y_0/\rho^2$ is small compared with $\left\{x_0/\rho - 1\right\}^2$, then

$$\alpha = \left\{ \left(\frac{x_0}{\rho} - 1 \right)^2 + 2x_0y_0/\rho^2 \right\}^{\frac{1}{2}} \approx \frac{x_0}{\rho} - 1, \text{ when } \frac{x_0}{\rho} > 1.$$

Hence we obtain

$$z_{\infty} = \frac{\rho^2}{x_0} \left\{ \frac{x_0}{\rho} - 1 + \left(\frac{x_0}{\rho} - 1 \right) \right\} = 2\rho \left(1 - \frac{\rho}{x_0} \right). \quad (2.2.6.)$$

We can also get (2.2.6) by setting $\frac{dz}{dt} = 0$ and letting $x_0 \approx n$ in (2.2.4).

There is no true epidemic if $x_0 < \rho$. Let us suppose that

$$x_0 = \rho + v, \text{ where } v > 0. \quad (2.2.7.)$$

Substituting (2.2.7) in (2.2.6) shows that the total size of epidemic is approximately $2v$ since

$$z_0 \approx 2\rho \left(1 - \frac{\rho}{x_0} \right) = 2\rho \left(1 - \frac{\rho}{\rho + v} \right) = 2v \frac{\rho}{\rho + v}.$$

We therefore obtain the following **Threshold Theorem of epidemiology** (Kermack and McKendrick (1927)).

Let $x_0 = \rho + v$ and assume that ρ/v is very small compared to 1. Then, the number of individuals who ultimately contract the disease is $2v$. In other words, the level of susceptibles is reduced to a point as far below the threshold as it originally was above it.

Kendall (1956) undertook a more mathematically precise treatment of the model (2.2.1). Let the infection rate be a function, $\beta(z)$. Then (2.2.2) is replaced by

$$x = x_0 \exp\left(-\frac{1}{\gamma} \int_0^z \beta(w) dw\right),$$

which together with (2.2.1), gives

$$\frac{dz}{dt} = \gamma \left(n - z - x_0 \exp\left(-\frac{1}{\gamma} \int_0^z \beta(w) dw\right) \right). \quad (2.2.8.)$$

Equation (2.2.8) is the same as the approximation appearing in (2.2.4) if

$$\beta(z) = \frac{2\beta}{\left(1 - z/\rho\right) + \left(1 - z/\rho\right)^{-1}}.$$

Here, $\beta(0) = \beta$ and $\beta(z) < \beta$ when $0 < z < \rho$. Furthermore, if $z > \rho$, the model will be quite unrealistic, since we should then have a negative infection rate.

Returning now to (2.2.3), we consider the equation

$$n - z - x_0 e^{-z/\rho} = 0. \quad (2.2.9.)$$

Let the unique negative and positive roots of (2.2.8) be $-\eta_1$ and η_2 , respectively. Then we can integrate (2.2.9) to give

$$t = \frac{1}{\gamma} \int_0^z \frac{dw}{n - w - x_0 \exp\left(-\frac{1}{\gamma} \int_0^w \beta(u) du\right)}, \quad 0 \leq z < \eta_2. \quad (2.2.10.)$$

This gives a formal solution for the epidemic curve. The whole of the epidemic curve for $0 \leq t < \infty$ is involved since the integral in (2.2.10) diverges

when $z \rightarrow \eta_2$, and therefore $z_\infty = \eta_2$. Unfortunately the integral also diverges at the lower limit as $x_0 \rightarrow n$, so that in this case an infinite time elapses before the epidemic starts. The latter difficulty is overcome by changing the origin to the point where $x = \rho$, which may be called the *centre* of the epidemic. Since $\frac{d}{dt}\left(\frac{dz}{dt}\right) = \gamma^2 y \left(\frac{x}{\rho} - 1\right)$, the *peak* of epidemic curve occurs at the centre.

From the second equation in (2.2.1), we see that the maximum number of infectives also occurs at the same time. We now write $x_0 = \rho$ and still choose to take $z_0 = 0$ without loss of generality.

The numerical value of $z(t)$ is the number of removals in $(0, t)$ for $t > 0$ and in $(t, 0)$ if $t < 0$. The corresponding parametric solution is thus

$$t = \frac{1}{\gamma} \int_0^z \frac{dw}{y_0 - w + \rho(1 - e^{-w/\rho})}.$$

Since $n = y_0 + x_0 + z_0 = y_0 + \rho + 0$,

$$\frac{dz}{dt} = \gamma \left\{ y_0 - z - \xi_1 + \rho \left(1 - e^{-(z+\xi_1)/\rho} \right) \right\},$$

where $-\infty < t < \infty$ and $-\xi_1 < z < \xi_2$. Here the quantities $-\xi_1$ and ξ_2 are the unique negative and positive roots, respectively, of

$$y_0 - z + \rho(1 - e^{-z/\rho}) = 0.$$

Let $N = \rho + y_0 + \xi_1$ be the initial number of susceptibles in the population.

Thus, when $t = -\infty$, the groups of the population are $(x, y, z) = (N, 0, -\xi_1)$, while when $t = \infty$, they are $(x, y, z) = (N - Ni, 0, Ni - \xi_1)$, where the intensity of the epidemic, i , is defined by,

$$i = \frac{\xi_1 + \xi_2}{N}.$$

The intensity of the epidemic is the proportion of the total number of susceptibles that finally contracts the disease.

From the modified form of the second equation in (2.2.2), we have

$$x = Ne^{-(z+\xi_1)/\rho}. \quad (2.2.11.)$$

Then when $t = \infty$, Equation (2.2.11) becomes

$$N - Ni = Ne^{-Ni/\rho}.$$

Hence, we get

$$\frac{N}{\rho} = -\frac{\log(1-i)}{i}.$$

On the other hand, when $t = 0$, $x_0 = \rho = Ne^{-\xi_1/\rho}$, and so

$$\frac{\xi_1}{\xi_1 + \xi_2} = \frac{\rho}{N} \log \frac{N}{\rho}.$$

This is the proportion of the total epidemic occurring before $t = 0$.

We also get the value of ξ_1 from

$$\rho = Ne^{-\xi_1/\rho}, \text{ which gives}$$

$$\log \frac{\rho}{N} = -\xi_1/\rho, \text{ and so}$$

$$\xi_1 = -\rho \log \frac{\rho}{N} = \rho \log \frac{N}{\rho}. \quad (2.2.12.)$$

Thus, the number of infectives at $t=0$, y_0 , is

$$y_0 = N - \rho - \xi_1 = N - \rho - \rho \log \frac{N}{\rho},$$

while the removal rate $\frac{dz}{dt}$ at the peak of the epidemic curve is y_0 .

Let a be a non-zero number of infectives which are introduced into a population of susceptibles at some finite time and we have an epidemic starting with $x = N'$, $y = a$. Then, from (2.2.11) and (2.2.12) we can take the value of z at the starting time to be

$$z' = -\xi_1 - \rho \log \frac{N'}{N} = \rho \log \frac{\rho}{N'}.$$

It is clear that with $a > 0$ we always have some kind of epidemic spread. If $\rho > N'$, then $z' > 0$ and we are already past the centre; the epidemic curve is J-shaped and falls away to zero. If $\rho < N'$, then $z' < 0$ and the curve is in a pre-central phase, so there will be a true epidemic with a peaked epidemic curve.

2.3. EQUILIBRIUM VALUES FOR THE BASIC DETERMINISTIC MODEL

Equilibrium values are obtained by assuming that the deaths of removed individuals are just balanced by the births of new susceptibles. In this case the simple differential equations for the deterministic model from the system (2.2.1) are

$$\left. \begin{aligned} \frac{dx}{dt} &= -\beta xy + \mu, \\ \frac{dy}{dt} &= \beta xy - \gamma y. \end{aligned} \right\} \quad (2.3.1)$$

where μ is a parameter describing the birth rate of susceptibles.

By letting the derivatives be equal to zero, the nontrivial equilibrium point (x_0, y_0) in (2.3.1) is given by,

$$(x_0, y_0) = \left(\frac{\gamma}{\beta}, \frac{\mu}{\gamma} \right). \quad (2.3.2)$$

The equations for small perturbations (u, v) from this equilibrium point are obtained by writing

$$x = x_0(1 + u), \quad y = y_0(1 + v). \quad (2.3.3)$$

Substituting (2.3.3) into (2.3.1) yields

$$\left. \begin{aligned} \sigma \frac{du}{dt} &= -(u + v + uv), \\ \tau \frac{dv}{dt} &= u(1 + v), \end{aligned} \right\} \quad (2.3.4)$$

where $\sigma = \frac{\gamma}{\beta\mu}, \quad \tau = \frac{1}{\gamma}$

We can neglect the product uv since uv is very small compared with u and v . So, we have

$$\left. \begin{aligned} \sigma \frac{du}{dt} &= -u - v, \\ \tau \frac{dv}{dt} &= u. \end{aligned} \right\} \quad (2.3.5)$$

In vector form, this reads $\frac{d}{dt} \begin{pmatrix} u \\ v \end{pmatrix} = A \begin{pmatrix} u \\ v \end{pmatrix}$, where A is the matrix,

$$A = \begin{bmatrix} -\frac{1}{\sigma} & -\frac{1}{\sigma} \\ \frac{1}{\tau} & 0 \end{bmatrix}.$$

This matrix is called *the community matrix* or *stability matrix*. The characteristic polynomial is

$$|A - \lambda I| = \begin{vmatrix} -\frac{1}{\sigma} - \lambda & -\frac{1}{\sigma} \\ \frac{1}{\tau} & -\lambda \end{vmatrix} = \lambda^2 + \frac{1}{\sigma}\lambda + \frac{1}{\sigma\tau} = 0. \quad (2.3.6.)$$

The epidemic models have either (i) **stable** steady states where small perturbations die out, or (ii) **unstable** steady states where perturbations from them grow unboundedly or result in limit cycle periodic solutions. The models which are said to exhibit a threshold effect have a non-zero stable state such that if the perturbation from it is sufficiently large or of the right kind, the population densities undergo large variations before returning to their steady states. The stability of an equilibrium in the epidemic model is determined by examining the eigenvalues of the community matrix. If the maximum value of the real parts of the eigenvalues is negative, it is stable. If the maximum value is positive, it is unstable.

From the characteristic polynomial (2.3.6), the eigenvalues are,

$$\lambda = -\frac{1}{2\sigma} \pm \sqrt{\left(\frac{1}{\sigma\tau} - \frac{1}{4\sigma^2}\right)}i.$$

Since the real parts of the eigenvalues are negative, the nontrivial equilibrium point (2.3.2) is stable. Furthermore, the general solution of the equations (2.3.5) with the initial condition, $(u(0), v(0)) = (u_0, v_0)$, is

$$u = u_0 e^{-\frac{1}{2\sigma}t} \cos \xi t + c_1 e^{-\frac{1}{2\sigma}t} \sin \xi t,$$

$$v = v_0 e^{-\frac{1}{2\sigma}t} \cos \xi t + c_2 e^{-\frac{1}{2\sigma}t} \sin \xi t,$$

$$\text{where } c_1 = \frac{-u_0 - 2v_0}{2\sigma\xi}, c_2 = \frac{1}{\xi} \left(\frac{u_0}{\tau} + \frac{v_0}{2\sigma} \right), \text{ and } \xi = \left(\frac{1}{\sigma\tau} - \frac{1}{4\sigma^2} \right)^{\frac{1}{2}}.$$

For a suitably chosen origin of time, we can choose

$$v(t) = ce^{-t/2\sigma} \cos \xi t, \text{ where } c = \sqrt{v_0^2 + c_2^2}.$$

We then obtain the solution for u from the second equation of (2.3.5),

$$u(t) = \left(\frac{\tau}{\sigma} \right)^{\frac{1}{2}} ce^{-\frac{1}{2\sigma}t} \sin(\xi t + \psi),$$

$$\text{where } \sin \psi = -\frac{1}{2} \left(\frac{\tau}{\sigma} \right)^{\frac{1}{2}}, \quad \frac{3}{2}\pi \leq \psi \leq 2\pi.$$

The solutions $u(t)$ and $v(t)$ involve damped harmonic trains of waves with period $2\pi/\xi$. It will be noticed that if τ/σ is small then the damping coefficient has relatively little influence on the period $2\pi/\xi$, which is roughly $2\pi(\sigma\tau)^{\frac{1}{2}} = 2\pi(\beta\mu)^{-\frac{1}{2}}$ for small τ/σ , and so largely depends on the birth rate for new susceptibles and the infection rate.

As outlined by Bailey (1975), the oscillatory behaviour of the process can also be represented by plotting the path traced by the point (x, y) . Doing this,

the deterministic solution can be compared with paths followed by actual realisations of the stochastic analogue. The deterministic curve found in this way can have the form of a spiral converging on the equilibrium point (x_0, y_0) . An argument due to Reuter (Bartlett, 1956) is as follows. Consider the function

$$f(u, v) = \{(1 + u) - \log(1 + u)\} + (\tau/\sigma)\{(1 + v) - \log(1 + v)\}.$$

Differentiating with respect to t and using (2.3.4) gives

$$\frac{df}{dt} = -\frac{u^2}{\sigma(1 + u)} \leq 0.$$

Thus f continually decreases when t increases. Since $f \geq 1 + \tau/\sigma$, the function f tends to a finite limit $f_0 \geq 1 + \tau/\sigma$, as t tends to infinity. Hence, the curves $f = c$ are closed, surround the point (x_0, y_0) , and converge as c tends to $1 + \tau/\sigma$. Considering the second differential coefficient $d^2 f/dt^2$, we can show that $f_0 = 1 + \tau/\sigma$. Consequently, the point (x, y) must tend to (x_0, y_0) .

The above discussion implies that when a constant influx of new susceptibles is sufficient to account for epidemic waves with a period of the right order of magnitude, the damping down to a steady endemic state entailed by the calculations is at variance with observed epidemiological facts.

2.4. HOST-VECTOR MODEL

This section introduces the basic deterministic epidemic model, which has a host-vector relationship. Diseases such as malaria and the RRV have hosts,

which can be humans or animals, and vectors, which are mosquitoes. These host-vector models can be considered as a special case of the two interacting groups models (Murray, 1993).

We suppose that there are two populations, one for the host and one for the vector. Let (x, y, z) be the population of human susceptibles, infectives and removals, (x', y', z') be the population of vector susceptibles, infectives and removals, $n = x + y + z$, the total human population, and $n' = x' + y' + z'$, the total vector population.

Then the basic system is given by :

$$\left. \begin{aligned} \frac{dx}{dt} &= -\beta xy', & \frac{dx'}{dt} &= -\beta' x' y, \\ \frac{dy}{dt} &= \beta xy' - \gamma y, & \frac{dy'}{dt} &= \beta' x' y - \gamma' y', \\ \frac{dz}{dt} &= \gamma y, & \frac{dz'}{dt} &= \gamma' y', \end{aligned} \right\} \quad (2.4.1.)$$

where β, β' are the infection rates for host and vector,

γ, γ' are the removal rates for host and vector, and

$\rho (= \gamma/\beta)$ and $\rho' (= \gamma'/\beta')$ are the relative removal rates.

The initial conditions for (x, y, z) and (x', y', z') when $t = 0$ are $(x_0, y_0, 0)$ and $(x'_0, y'_0, 0)$.

A diagram representing the model in (2.4.1) is given in Fig. 2.1

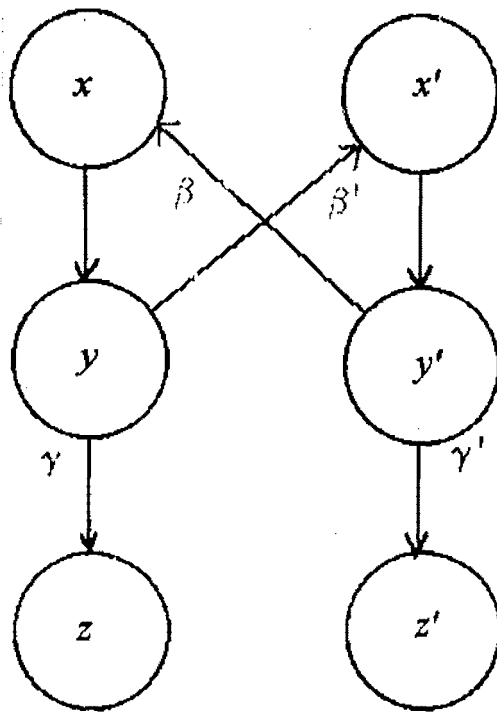


Fig. 2.1 A diagram for the host-vector model

From the differential equations given in (2.4.1), we obtain

$$-\log(x/x_0) = \beta z'/\gamma' \quad \text{and} \quad -\log(x'/x'_0) = \beta z/\gamma. \quad (2.4.2.)$$

Following the notation of Section 2.2 and writing the specifications of the two populations at $t = \infty$ as $(n - ni, 0, ni)$ and $(n' - n' i', 0, n' i')$, we have from the two equations (2.4.2)

$$\left. \begin{aligned} \beta n' i' / \gamma' &= -\log(1 - i), \\ \beta ni / \gamma &= -\log(1 - i'), \end{aligned} \right\} \quad (2.4.3.)$$

where we take y_0 and y'_0 to be negligibly small, so that x_0 and x'_0 are approximately equal to n and n' . By expanding the logarithmic terms in (2.4.3), we have

$$\frac{\beta\beta' nn' ii'}{\gamma\gamma'} = \left(i + \frac{1}{2}i^2\right) \left(i' + \frac{1}{2}i'^2\right).$$

After cancellation of the factor ii' and rearrangement we obtain

$$\frac{nn'}{\rho\rho'} - 1 = \frac{1}{2}(i + i'), \quad (2.4.4.)$$

where we have ignored the second-order term in ii' , and have written ρ and ρ' for the two relative removal-rates. From (2.4.4) it is obvious that $nn' > \rho\rho'$ for a true epidemic to occur. There are not in fact separate threshold conditions for man and vector, but there is a joint threshold condition related to the product of the relative removal-rates, $\rho\rho'$.

Let π be the product of the numbers of susceptibles in the two populations, so that $\pi = xx'$. Then we have $\pi_0 \approx nn'$, and therefore

$$\begin{aligned} \pi_\infty &= x_\infty x'_\infty \\ &\approx \pi_0(1 - i - i'). \end{aligned}$$

After cancellation of the factor ii' , substitution $i + i'$ from (2.4.4) and writing

$$\pi_0 = \rho\rho' + \varepsilon,$$

we obtain

$$\pi_0 - \pi_\infty \approx 2\varepsilon. \quad (2.4.5.)$$

As discussed in Bailey (1975), the result in (2.4.5) is a modified form of the Threshold Theorem and shows that if there is an epidemic, the product of the numbers of susceptibles is reduced to a point as far below the threshold as it originally was above it.

The exact values of the individual intensities, i and i' , can be obtained by the solutions of (2.4.3). We can get approximate values from the equations

$$i \approx \frac{2\varepsilon}{n\left(n' + \frac{\gamma'}{\beta}\right)}, \quad i' \approx \frac{2\varepsilon}{n'\left(n + \frac{\gamma}{\beta'}\right)},$$

where we have made use of the fact that $\rho\rho' \approx nn' - \varepsilon$.

If the parameters β , β' , γ and γ' are independent of n and n' , then public policy should act to ensure that $nn' < \rho\rho'$ or $nn' \ll \rho\rho'$. Thus, reducing the size of the vector population n' is a step in the direction of preventing the disease.

If they are dependent, as in the case of malaria, we may suppose that the mosquito vector exhibits a certain man-biting rate b' . Then in a unit time x' susceptible mosquitoes will bite $b'x'$ people, of whom $(b'x')\left(\frac{y}{n}\right)$ are affected by malaria. Let f be the proportion of the latter who are actually infectious. Then the rate at which newly infected mosquitoes appear is $b'fx'y/n$. In other words, $\beta' = b'f/n$. Similarly, in a unit time y' infected mosquitoes, of whom a proportion f' are infectious, will bite $b'y'$ people, of whom $(b'y')(x/n)$ are susceptibles. The rate at which newly infected people occur is thus $b'f'xy'/n$, so that $\beta = b'f'/n$. Thus for $nn' > \rho\rho'$ the condition for a true

epidemic to occur is that $nn' > \gamma\gamma' n^2 / b'^2 ff'$ or $n'/n > \gamma\gamma' / b'^2 ff'$. This threshold result, applicable to malaria, goes back to the original work of Ross(1911) and the studies of Kermack and McKendrick(1927).

2.5. THE EQUILIBRIUM VALUES FOR THE HOST-VECTOR MODEL

The host-vector model described by (2.4.1) can be modified by assuming that the deaths of removed individuals are just balanced by the births of new susceptibles of host and vector. Then

$$\left. \begin{aligned} \frac{dx}{dt} &= -\beta xy' + \mu, \quad \frac{dx'}{dt} = -\beta' x' y + \mu' \\ \frac{dy}{dt} &= \beta xy' - \gamma y, \quad \frac{dy'}{dt} = \beta' x' y - \gamma' y' \end{aligned} \right\} \quad (2.5.1.)$$

The equilibrium values for this system (x_0, y_0, x'_0, y'_0) are given by setting the expressions in (2.5.1) to zero. Thus the equilibrium point is

$$\left. \begin{aligned} x_0 &= \mu\gamma' / \beta\mu', \quad y_0 = \mu / \gamma, \\ x'_0 &= \mu' \gamma / \beta' \mu, \quad y'_0 = \mu' / \gamma'. \end{aligned} \right\} \quad (2.5.2.)$$

The equations for small departures from these equilibrium values are obtained by writing

$$\left. \begin{aligned} x &= x_0(1+u), \quad y = y_0(1+v), \\ x' &= x'_0(1+u'), \quad y' = y'_0(1+v'). \end{aligned} \right\} \quad (2.5.3.)$$

Substituting (2.5.3) and (2.5.2) in (2.5.1), we have

$$\left. \begin{aligned} \frac{du}{dt} &= -\frac{\beta\mu'}{\gamma'}(u+v+uv'), \\ \frac{dv}{dt} &= \gamma(u-v+v'+uv'), \\ \frac{du'}{dt} &= -\frac{\beta'\mu}{\gamma}(u'+v+u'v'), \\ \frac{dv'}{dt} &= \gamma'(u'+v-v'+u'v'). \end{aligned} \right\} \quad (2.5.4.)$$

We can eliminate the products $uv, u'v, uv'$, and $u'v'$ because they are small compared with u, v, u' , and v' .

Hence, we have the linearised community matrix

$$A = \begin{bmatrix} -\frac{\beta\mu'}{\gamma'} & 0 & 0 & -\frac{\beta\mu'}{\gamma'} \\ \gamma & -\gamma & 0 & \gamma \\ 0 & -\frac{\beta'\mu}{\gamma} & -\frac{\beta'\mu}{\gamma} & 0 \\ 0 & \gamma' & \gamma' & -\gamma' \end{bmatrix}$$

and the characteristic polynomial is

$$|A - \lambda I| = \begin{vmatrix} -\frac{\beta\mu'}{\gamma'} - \lambda & 0 & 0 & -\frac{\beta\mu'}{\gamma'} \\ \gamma & -\gamma - \lambda & 0 & \gamma \\ 0 & -\frac{\beta'\mu}{\gamma} & -\frac{\beta'\mu}{\gamma} - \lambda & 0 \\ 0 & \gamma' & \gamma' & -\gamma' - \lambda \end{vmatrix} = 0.$$

The eigenvalues of the community matrix can be obtained from the following polynomial

$$\lambda^4 + a\lambda^3 + b\lambda^2 + c\lambda + d = 0,$$

where $a = \gamma + \gamma' + \frac{\beta\mu'}{\gamma'} + \frac{\beta'\mu}{\gamma}$,

$$b = \beta\mu' + \beta'\mu + \frac{\beta\beta'\mu\mu'}{\gamma\gamma'} + \frac{\beta\mu'\gamma}{\gamma'} + \frac{\beta'\mu\gamma}{\gamma},$$

$$c = \beta\beta'\mu\mu' \left(\frac{1}{\gamma} + \frac{1}{\gamma'} \right) + \beta\mu'\gamma + \beta'\mu\gamma', \text{ and}$$

$$d = \beta\beta'\mu\mu'.$$

The condition for all of these eigenvalues of the community matrix to have negative real parts is too complex to consider here. However, if all of them are negative, then this equilibrium point is stable and small perturbations around the equilibrium point (2.5.2) will not have any marked effect. In other words, the disease will eventually die down to a steady epidemic level. On the other hand, if any of the eigenvalues is positive, then the equilibrium point is unstable.

2.6. SOME SPECIFIC MODELS FOR MALARIA

Human malaria is transmitted by mosquitoes such as *Plasmodium falciparum*, *Plasmodium vivax*, *Plasmodium ovale*, and *Plasmodium malariae*. *Plasmodium falciparum* causes the most fatal form of malaria due to its tendency to progress to a cerebral pathology. The parasite is transmitted by the female mosquito, in which the sexual cycle takes place. It is the asexual parasite stages in the blood and liver of humans that cause the disease in humans. Despite the differences between malaria and RRV, they are both mosquito-borne diseases. That means that both diseases have the same hosts and vector, which are humans and animals, and mosquitoes respectively.

As the RRV models introduced later are based on early malaria models we introduce in this chapter epidemic models for malarial transmission due to Kingsolver (1987), Moreira (1992), and Dye and Hasibeder (1988). Furthermore, some discussion of these models is given.

2.6.1. Kingsolver's model

Kingsolver constructed his model as a straightforward extension of the Ross-MacDonald model for the dynamics of malarial infection (Ross, 1911; MacDonald, 1952, 1957, 1973). He found that mosquitoes may preferentially choose hosts on the basis of host infection. From that he developed and analysed a simple model for the dynamics of malarial transmission that incorporates nonrandom feeding behaviour by the mosquito vector.

The simple general model given by Ross and MacDonald is

$$\begin{cases} \frac{dx}{dt} = ky\beta_v(x)M/N - rx, \\ \frac{dy}{dt} = \beta_i(x)(1-y) - \mu y, \end{cases} \quad (2.6.1)$$

where

x is the proportion of infectives in the human host population,

y is the proportion of infectives in the mosquito vector population,

k is the proportion of infected bites on the human hosts that produce an infection,

N is the size of the human population,

M is the size of the female mosquito population,

$m = M / N$ is the number of female mosquitoes per human host,

r is the per capita rate of recovery for the human host, and

μ is the per capita mortality rate for the mosquitoes.

The functions $\beta_u(x)$ and $\beta_i(x)$ are the rates of biting per female mosquito on uninfected and infected hosts, respectively. The total rate of biting per unit time is

$$B = \beta_u(x) + \beta_i(x).$$

Ross and MacDonald used a simple linear model for $\beta_u(x)$ and $\beta_i(x)$, namely,

$$\begin{cases} \beta_i(x) = Bx, \\ \beta_u(x) = B(1 - x) \end{cases},$$

for which the net reproductive rate of the parasite is $R = kmB^2 / \mu r$. If $R > 1$, an infection will continue and lead to a stable equilibrium at which an infection is maintained in both the host and vector populations. On the other hand, if $R < 1$ the disease will die out.

Kingsolver constructed and analysed three different models for the functions, $\beta_u(x)$ and $\beta_i(x)$, using nonrandom feeding behaviour by the mosquito vector. The three different models are as follows :

i) Consistent Host-Preference Model

$$\begin{cases} \beta_i(x) = B(1 - e^{-cx}), \\ \beta_u(x) = Be^{-cx}, \end{cases}$$

where c is a constant that reflects the intensity of the preference. In this model, Kingsolver assumed that the intensity of the preference is a constant.

ii) Increasing preference model

$$\begin{cases} \beta_i(x) = B \left[\frac{Px}{1 + (P-1)x} \right], \\ \beta_u(x) = B \left[1 - \frac{Px}{1 + (P-1)x} \right], \end{cases}$$

where P denotes the preference of the mosquitoes for infected hosts. When $P = 1$, the model is the same as the Ross-MacDonald model. The model assumes an increasing preference for infected hosts as the host population increases.

iii) Switching-Behaviour Model

$$\begin{cases} \beta_i(x) = \frac{B(1 - e^{-cx})}{1 + ae^{-cx}}, \\ \beta_u(x) = \frac{(1+a)B(1 - e^{-cx})}{1 + ae^{-cx}}, \end{cases}$$

where a and c are constants. Here he considered host-choice behaviour in which preference depends on the relative abundance of infected and uninfected hosts.

2.6.2. Moreira's model

Moreira (1992) applied the theory of Lienard equations and Liapunov's direct method (Van der Pol, 1928) in the dynamics of malarial transmission to guarantee a globally asymptotically stable positive equilibrium or a stable persistence of infection in terms of the rate of biting per female mosquito on uninfected hosts. His epidemic model for malaria is

$$\begin{cases} \frac{dx}{dt} = h(x)(kmy) - rx - \mu_1, \\ \frac{dy}{dt} = g(x)(1-y) - \mu_2 y + \mu_3, \end{cases} \quad (2.6.2)$$

where members of the human population, x , are harvested at a constant rate $\mu_1 > 0$ while the vector population, y , is stocked at a constant rate $\mu_3 > 0$;

$k > 0$ is the proportion of infected bites on the human hosts that produce an infection;

$m > 0$ is the number of female mosquitoes per human host;

$r > 0$ is the per capita rate of recovery for the human host; and

$\mu_2 > 0$ is the per capita mortality rate for the mosquitoes.

The functions $h(x)$ and $g(x)$ are the respective rates of biting per female mosquito on uninfected and infected hosts, and the total rate of biting, B , per unit time given by $B = h(x) + g(x)$ is assumed to be constant. For

convenience the host harvest rate μ_1 is replaced by $\frac{kmB\mu_3}{\mu_2}$. Moreira gave two applications involving different assumptions for $h(x)$ and $g(x)$.

The first application

$$\begin{cases} h(x) = \frac{B}{1+cx}, \\ g(x) = \frac{Bcx}{1+cx}, \end{cases} \quad (2.6.3)$$

where c is some positive constant. There will be a unique and globally asymptotically stable equilibrium of (2.6.2) if the net reproductive rate of the parasite R is greater than 1, where

$$R = \frac{ckmB^2(\mu_2 - \mu_3)}{\mu_3^2(r + \mu_1 c)}. \quad (2.6.4)$$

The second application

$$\begin{cases} h(x) = B \exp(-cx), \\ g(x) = B[1 - \exp(-cx)], \end{cases} \quad (2.6.5)$$

where c is a positive constant. As in the first application, (2.6.3) will have a unique stable equilibrium if the net reproduction rate (2.6.4) is greater than 1.

2.6.3. Dye and Hasibeder's model

Dye and Hasibeder (1988) investigated the persistence of a mosquito-borne disease (malaria) in a system where mosquitoes and hosts are grouped in patches containing any number of individuals.

In this model for the generation of malaria, S and I are the absolute numbers of infected (and infective) hosts and mosquitoes, and t denotes chronological time.

The equations are :

$$\begin{aligned}\frac{dS_i}{dt} &= \alpha \left(\sum_{j \in Q} \gamma_{ji} I_j \right) (1 - S_i / H_i) - \rho S_i \quad \text{for } i \in P, \\ \frac{dI_j}{dt} &= \beta (V_j - I_j) \left(\sum_{i \in P} \gamma_{ji} S_i / H_i \right) - \delta I_j \quad \text{for } j \in Q,\end{aligned}\tag{2.6.6}$$

where P and Q are finite sets containing all m hosts and all n mosquito patches ($|P|=m$, $|Q|=n$, $P \cap Q = \emptyset$). Patch i , for $i \in P$, has altogether H_i hosts (humans), S_i of whom are infected (but only a proportion of these people are sick, i.e. show disease symptoms). Patch j , for $j \in Q$, has a total of V_j vectors (mosquitoes) with I_j being infected (and infective).

α is the number of bites per mosquito per unit time multiplied by the proportion of bites by infected mosquitoes on uninfected hosts which result in human infection. β is the number of bites per mosquito per unit time multiplied by the proportion of bites by uninfected mosquitoes on infected hosts which result in mosquito infection.

So, α and β are the transmission rates of infection from vectors to hosts and vice versa.

ρ is the recovery rate of infected hosts,

δ is the death rate (equal to the birth rate) of the mosquitoes.

Finally, γ_{ji} , for $i \in P$ and $j \in Q$, is the per-bite probability that a mosquito from patch j bites a host in patch i (so that for each bite each mosquito chooses a host patch according to this set of probabilities).

This model assumes that immunity, latent periods, and seasonal variations in the parameters are negligible. The birth and death rates of the mosquitoes are assumed equal, while the births and deaths of the hosts are negligible since they are very small.

2.6.4. Discussion of Malaria Models

This section discusses in detail the models for malaria introduced in the previous sections 2.6.1, 2.6.2 and 2.6.3. Although malaria and the RRV diseases are different, studying models for malarial transmission is helpful in building an ecological model for the spread of RRV. Models for malarial transmission do however have some limitations. For example, the models introduced in this chapter do not divide the population into susceptibles and infectives, nor do they consider the age and sex distribution of the population. By considering these malaria models as simple RRV models, a more accurate RRV model may be developed by incorporating some or all of the RRV parameters such as age, sex, viraemia period, extrinsic incubation period, and seasonal variations. The nonrandom feeding behaviour by the mosquito vector in malaria models is, however, ignored since this behaviour is caused by the fever due to the malaria, whereas the RRV disease does not present the same symptoms.

Kingsolver's model (1987) considers host-vector interaction with nonrandom feeding behaviour, and applies it to the Ross-MacDonald model (Ross, 1911; MacDonald, 1952, 1957, 1973). However, because the Ross-MacDonald model is simple there are many limitations. For example, (a) human and mosquito population sizes and the mosquitoes' mortality rate are regarded as constants; (b) the model does not distinguish between different developmental stages of the mosquito, and (c) the immunity and mortality rates of the hosts are not considered.

However, Kingsolver did use the Ross-MacDonald model with three different types of nonrandom host choice to show that nonrandom host choice can have important quantitative and qualitative effects on the epidemiology of malarial transmission.

Moreira (1992) extended the Ross-MacDonald model with migration effects and applied Lienard's equation and Liapunov's direct method in his model for malarial transmission. His model has the same limitations as Kingsolver's, but the migration effects in his model can incorporate the immunity and mortality rates of the host.

Dye and Hasibeder's model (1988) considers the persistence of malaria in a system where mosquitoes and hosts are grouped in patches containing any number of individuals. This model confirms that nonhomogeneous host selection by mosquitoes leads to basic reproductive rates greater than or equal to those obtained under uniform host selection. Dye and Hasibeder found that

strong associations between particular groups of mosquitoes and hosts lead to higher basic reproductive rates.

A major flaw of this model is that it requires the precise values of the parameters in different patches to be estimated, a difficult process at best. However, by incorporating regional differences the model becomes more reliable and realistic. Overall, this model is quite generalised and gives us many applications where, for example, the patch parameters can be regarded as age parameters.

Having discussed the early models of Bailey (1975) and specific models of malaria in detail, we now move to develop and discuss several host-vector models for RRV transmission with varying complexity in Chapters 3 and 4.

CHAPTER 3.

THE HOST-VECTOR MODEL FOR THE RRV

The Ross River virus disease is transmitted between the hosts, humans and animals, and the vector, mosquitoes. The mechanism which maintains the infection in the mosquitoes is unknown. This thesis examines two possible hypotheses for the natural infection rate within the mosquito population. The first hypothesis is that there is only a single natural infection on mosquitoes prior to the outbreak. The second hypothesis is that the mosquitoes are exposed to continuous natural infection during the outbreak. In this chapter, the models are built on the first hypothesis, while Chapter 4 considers those models with the second hypothesis. Therefore, the natural infection within the mosquito population is included as an initial condition and neglected for the rest of the outbreak.

Since each mosquito and animal species has a different life cycle, the mosquito and animal populations will be divided into subpopulations by species for more accurate modelling. Similarly, the humans will be divided according to region, age, and sex, etc. However, the difficulty of obtaining parameter values for the simulation allows only a simple model to be constructed.

Sections 3.1. and 3.2. introduce the basic Ross River virus models including the mathematical analysis of the models, the threshold condition and a stability analysis of the equilibrium points. Section 3.3. introduces the general RRV

model which is a k -human and l -animal host and m -mosquito vector model, and examines the threshold condition.

3.1. THE BASIC MODEL WITH ONE HOST AND ONE VECTOR

In this section, the basic model for the Ross River virus has one host and one vector. Animal populations are neglected and their effects on the transmission will be included in the infection rates between the human host and the mosquito vector. An incubation period is the time elapsing between the receipt of RRV and the appearance of symptoms (Bailey, 1975). A viraemia period is the time elapsing between the receipt of RRV and grant of antibody, so that hosts can pass the virus to vectors during the period. Since the incubation and viraemia periods overlap, the incubation period for humans is neglected, while the viraemia period is used to calculate the recovery rate since after the viraemia period infected humans become immune. In the same fashion, the viraemia period for the animal population is used to calculate the animal recovery rate.

The host population is divided into three disjoint groups: The susceptible group, $x_1(t)$, consists of individuals who have not yet contracted the virus. The infective group, $y_1(t)$, consists of individuals who have contracted the virus and are infectious. Finally, the removed group, $z_1(t)$, consists of individuals who are removed from the infective group after the viraemia period. The vector population is divided into four disjoint groups. The susceptible group, $x_2(t)$, which have not yet contracted the disease. The latent group, $e(t)$, which are in the extrinsic incubation period (or latent period) and are not yet infectious. The

infectious group, $y_2(t)$, and the removed group, $z_2(t)$, who have been removed from the susceptible, latent and infective groups by natural mortality.

The following assumptions are made in this basic model :

1. Both populations are homogeneously mixing.
2. The total human population, $n_1(t)$, changes with a constant birth rate, α_1 , and a constant mortality rate, δ_1 . The new births into the host population during a time Δt , $\alpha_1 \Delta t$, are not infected. Therefore, the new births are put directly into the susceptible group.
3. The total mosquito population, $n_2(t)$, changes with a variable recruitment rate, $\alpha_2(t)$, and a variable mortality rate, $\delta_2(t)$. The new inputs into the vector population during a time Δt , $\alpha_2(t) \Delta t$, are not infected. Therefore, they go directly to the susceptible group.
4. The rate of occurrence of new infectious hosts is proportional to both the number of host-susceptibles and the number of infectious vectors. Thus, the number of infections in the host population in a time Δt is $\beta_1 x_1(t) y_2(t) \Delta t$, where β_1 is the constant infection rate from the vector to the host. Individuals are removed from the host-susceptible group, $x_1(t)$, with a constant death rate δ_1 . Hence, the number of removals from the host-susceptible group due to deaths in a time Δt is $\delta_1 x_1(t) \Delta t$.
5. The rate of occurrence of new latent vectors, which are infected but not infectious, is proportional to both the number of the vector-susceptibles and the number of the infectious hosts. Thus, the number of new infectious vectors in a

time Δt is $\beta_2 x_2(t) y_1(t) \Delta t$, where β_2 is the constant infection rate from the host to the vector.

6. The number of removals from the infectious host group, $y_1(t)$, due to deaths and immunity during a time Δt is $(\gamma + \delta_1) y_1(t) \Delta t$, where γ is a constant recovery rate. This rate is equal to $1/a_1$, where a_1 is a constant viraemia period.

7. Individuals in the latent vector population become infectious and are removed from the latent group, $e(t)$, at a rate proportional to the number of vector-latents. Hence, the number of new infectives in a time Δt is $\varepsilon(t) e(t) \Delta t$, where $\varepsilon(t)$ is a variable transfer rate between the latent group and the infective group. This rate is equal to $1/a_2(t)$, where $a_2(t)$ is a variable extrinsic incubation period.

Individuals in the vector population die and are removed from the susceptible, latent and infective groups, $x_2(t)$, $e_2(t)$ and $y_2(t)$, respectively, at a rate proportional to the number of each group. Hence, the number of removals due to deaths in a time Δt is $\delta_2(t)(x_2(t) + e_2(t) + y_2(t)) \Delta t$, where $\delta_2(t)$ is a variable mortality rate.

A diagram representing the simple model is given in Figure 3.1.

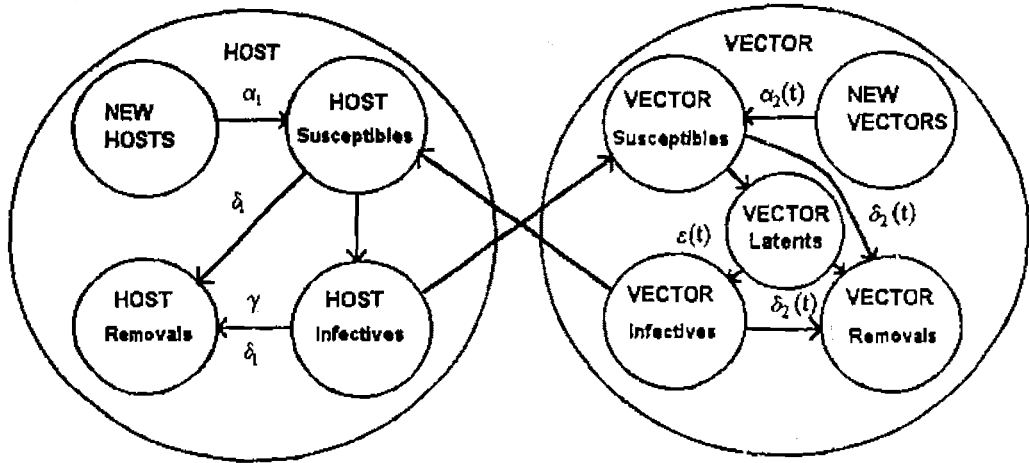


Figure 3.1 The flow diagram for the simple model for RRV transmission

With the given assumptions, the basic deterministic model for the Ross River virus which has one host and one vector is given by,

$$\begin{cases}
 \frac{dx_1(t)}{dt} = -\beta_1 x_1(t) y_2(t) - \delta_1 x_1(t) + \alpha_1, \\
 \frac{dy_1(t)}{dt} = \beta_1 x_1(t) y_2(t) - (\gamma + \delta_1) y_1(t), \\
 \frac{dz_1(t)}{dt} = \gamma y_1(t) - z_1(t), \\
 \frac{dx_2(t)}{dt} = -\beta_2 x_2(t) y_1(t) - \delta_2(t) x_2(t) + \alpha_2(t), \\
 \frac{de(t)}{dt} = \beta_2 x_2(t) y_1(t) - (\delta_2(t) + \epsilon(t)) e(t), \\
 \frac{dy_2(t)}{dt} = \epsilon(t) e(t) - \delta_2(t) y_2(t),
 \end{cases} \quad (3.1.1)$$

where the initial conditions when $t = 0$ are $(x_1(t), y_1(t), z_1(t)) = (x_{10}, y_{10}, 0)$ and

$$(x_2(t), e_2(t), y_2(t)) = (x_{20}, e_{20}, y_{20}).$$

All of the constant parameters in (3.1.1) are nonnegative, that is

$$\beta_1, \beta_2, \delta_1, \alpha_1, \gamma \geq 0,$$

and all of the variable parameters are positive, that is

$$\alpha_2(t) > 0 \text{ and } \delta_2(t), \varepsilon(t) \geq 0, \forall t \in \mathbb{R}^+.$$

From the dynamics given in (3.1.1), for a true epidemic to occur $\frac{dy_1(t)}{dt}, \frac{de(t)}{dt}$

and $\frac{dy_2(t)}{dt}$ must be positive :

$$\frac{dy_1(t)}{dt} = \beta_1 x_1(t) y_2(t) - (\gamma + \delta_1) y_1(t) > 0, \quad (3.1.2.)$$

$$\frac{de(t)}{dt} = \beta_2 x_2(t) y_1(t) - (\delta_2(t) + \varepsilon(t)) e(t) > 0, \quad (3.1.3.)$$

$$\text{and } \frac{dy_2(t)}{dt} = \varepsilon(t) e(t) - \delta_2(t) y_2(t) > 0. \quad (3.1.4.)$$

From those inequalities (3.1.2), (3.1.3) and (3.1.4), we obtain the three conditions

$$\frac{\beta_1 x_1(t) y_2(t)}{(\gamma + \delta_1) y_1(t)} > 1, \quad (3.1.5.)$$

$$\frac{\beta_2 x_2(t) y_1(t)}{(\delta_2(t) + \varepsilon(t)) e(t)} > 1, \quad (3.1.6.)$$

$$\text{and } \frac{\varepsilon(t) e(t)}{\delta_2(t) y_2(t)} > 1. \quad (3.1.7.)$$

By multiplying the three inequalities (3.1.5), (3.1.6) and (3.1.7), we get the threshold condition as the following inequality :

$$x_1(t) x_2(t) > \frac{(\gamma + \delta_1) \delta_2(t)}{\beta_1 \beta_2} \cdot \frac{\delta_2(t) + \varepsilon(t)}{\varepsilon(t)} = \rho_1 \rho_2(t) \cdot \frac{\delta_2(t) + \varepsilon(t)}{\varepsilon(t)}, \quad (3.1.8.)$$

where ρ_1 and $\rho_2(t)$ are the relative removal rates for host and vector at time t ,

$$\text{so that } \rho_1 = \frac{(\gamma + \delta_1)}{\beta_1} \text{ and } \rho_2(t) = \frac{\delta_2(t)}{\beta_2}.$$

When they are in the initial states, (3.1.8) can be replaced with the initial transfer rate, ϵ_0 , and the initial mortality rate, δ_{20} , so that

$$x_{10}x_{20} > \rho_1\rho_{20} \cdot \frac{\delta_{20} + \epsilon_0}{\epsilon_0}, \quad (3.1.9.)$$

where ρ_{20} is the initial relative removal rate of the vector.

Since $\frac{\delta_{20} + \epsilon_0}{\epsilon_0} > 1$, the above threshold condition (3.1.9) can be changed to,

$$x_{10}x_{20} > \rho_1\rho_{20}.$$

We now take y_{10} and y_{20} to be negligibly small, so that x_{10} and x_{20} are approximately equal to n_{10} and n_{20} . Thus, if an outbreak occurs, then the product of the two relative removal-rates is smaller than the products of two initial total populations, $\rho_1\rho_{20} < n_{10}n_{20}$. This result is the same as the threshold condition for the model (2.3.1) discussed in Section 2.3.

To examine the stability of the system of equations given in (3.1.1), the equations can be replaced with a new set of equations given in (3.1.10), in which the latent group in the vector population is neglected. The stability result for the new system given in (3.1.10) is exactly the same as for the system given in (3.1.1) since the latent group is dependent on the infective group in the vector population.

$$\begin{cases} \frac{dx_1}{dt} = -\beta_1 x_1 y_2 - \delta_1 x_1 + \alpha_1, \\ \frac{dy_1}{dt} = \beta_1 x_1 y_2 - (\gamma + \delta_1) y_1, \\ \frac{dx_2(t)}{dt} = -\beta_2 x_2 y_1 - \delta_2(t) x_2 + \alpha_2(t), \\ \frac{dy_2(t)}{dt} = \beta_2 x_2 y_1 - \delta_2(t) y_2. \end{cases} \quad (3.1.10.)$$

The equilibrium points of the system given in (3.1.10) are found by setting the derivatives in equations (3.1.10) equal to zero. The recruitment and mortality rates are changing with time t and they may be periodic but the exact functions are unknown currently. Hence, for examining the stability we shall assume that α_{20} and δ_{20} are the constant average values of the functions, $\alpha_2(t)$ and $\delta_2(t)$. However, this is only to analyse the stability conditions of the dynamics and correct only heuristically.

Since the mortality rates are not equal to zero, we have two equilibrium points:

$$i) (x_{10}, y_{10}, x_{20}, y_{20}) = \left(\frac{\alpha_1}{\delta_1}, 0, \frac{\alpha_{20}}{\delta_{20}}, 0 \right) \text{ and} \quad (3.1.11.)$$

$$ii) \text{ if } \alpha_1 \alpha_{20} \beta_1 \beta_2 - \delta_1 \delta_{20}^2 (\gamma + \delta_1) > 0,$$

$$\begin{aligned} x_{10} &= \frac{\delta_{20}(\alpha_1 \beta_2 + \delta_{20}(\gamma + \delta_1))}{\beta_2(\alpha_{20} \beta_1 + \delta_1 \delta_{20})}, x_{20} = \frac{(\gamma + \delta_1)(\alpha_{20} \beta_1 + \delta_1 \delta_{20})}{\beta_1(\alpha_1 \beta_2 + \delta_{20}(\gamma + \delta_1))}, \\ y_{10} &= \frac{\alpha_1 \alpha_{20} \beta_1 \beta_2 - \delta_1 \delta_{20}^2 (\gamma + \delta_1)}{\beta_2(\gamma + \delta_1)(\alpha_{20} \beta_1 + \delta_1 \delta_{20})}, y_{20} = \frac{\alpha_1 \alpha_{20} \beta_1 \beta_2 - \delta_1 \delta_{20}^2 (\gamma + \delta_1)}{\beta_1 \delta_{20}(\alpha_1 \beta_2 + \delta_{20}(\gamma + \delta_1))}. \end{aligned} \quad (3.1.12.)$$

Here we let the population growth rates of the host and vector be

$$\pi_1 = \frac{\alpha_1}{\delta_1} \text{ and } \pi_{20} = \frac{\alpha_{20}}{\delta_{20}}.$$

Therefore, if the product of the relative removal rates is larger than the product of the relative birth rates, the equilibrium point (3.1.12) exists for the system (3.1.10).

We consider the two equilibrium points in turn.

1) The first equilibrium point is given by

$$(x_{10}, y_{10}, x_{20}, y_{20}) = \left(\frac{\alpha_1}{\delta_1}, 0, \frac{\alpha_{20}}{\delta_{20}}, 0 \right).$$

The new differential equations for small perturbations from the equilibrium point can be obtained by letting

$$\begin{cases} x_1 = x_{10}(1 + u_1), y_1 = v_1, \\ x_2 = x_{20}(1 + u_2), y_2 = v_2, \\ \text{where } |u_1|, |v_1|, |u_2|, |v_2| \ll 1 \end{cases} \quad (3.1.13.)$$

and substituting (3.1.11) and (3.1.13) into (3.1.10). The products of the perturbations can be neglected since the products are very small compared to the perturbations. This gives the following linearised equations :

$$\begin{cases} \frac{du_1}{dt} = -\delta_1 u_1 - \beta_1 v_2, \\ \frac{dv_1}{dt} = -(\gamma + \delta_1) v_1 + \frac{\alpha_1 \beta_1}{\delta_1} v_2, \\ \frac{du_2}{dt} = -\beta_2 v_1 - \delta_{20} u_2, \\ \frac{dv_2}{dt} = \frac{\alpha_{20} \beta_2}{\delta_{20}} v_1 - \delta_{20} v_2. \end{cases} \quad (3.1.14.)$$

From the linearised system (3.1.14), we have the characteristic polynomial of the community matrix,

$$|A - \lambda I| = \begin{vmatrix} -\delta_1 - \lambda & 0 & 0 & -\beta_1 \\ 0 & -(\gamma + \delta_1) - \lambda & 0 & \frac{\alpha_1 \beta_1}{\delta_1} \\ 0 & -\beta_2 & -\delta_{20} - \lambda & 0 \\ 0 & \frac{\alpha_{20} \beta_2}{\delta_{20}} & 0 & -\delta_{20} - \lambda \end{vmatrix} = 0.$$

Two eigenvalues of the community matrix of the linearised equations are $-\delta_1$ and $-\delta_{20}$, and the rest will be determined by the quadratic equation :

$$\lambda^2 + (\delta_1 + \delta_{20} + \gamma)\lambda + (\delta_1 + \gamma)\delta_{20} - \beta_1 \beta_2 \frac{\alpha_1 \alpha_{20}}{\delta_1 \delta_{20}} = 0. \quad (3.1.15.)$$

The sum of roots, $\lambda_1 + \lambda_2 (= -(\delta_1 + \delta_{20} + \gamma))$, of (3.1.15) is negative. So the product of roots, $\lambda_1 \lambda_2$, will determine the stability of the equilibrium point.

We have,

$$\lambda_1 \lambda_2 = \beta_1 \beta_2 \left(\frac{\delta_{20}(\delta_1 + \gamma)}{\beta_1 \beta_2} - \frac{\alpha_1 \alpha_{20}}{\delta_1 \delta_{20}} \right) = \beta_1 \beta_2 (\rho_1 \rho_{20} - \pi_1 \pi_{20}).$$

We consider the two cases when the equation in (3.1.15) has complex roots or real roots.

1) Equation (3.1.15) has complex roots.

The eigenvalues will have negative real parts since the sum of the roots is negative. Therefore, the equilibrium point is asymptotically stable.

2) Equation (3.1.15) has real roots.

a) If the product of the relative removal rates is bigger than the product of population growth rates, i.e. $\rho_1 \rho_{20} > \pi_1 \pi_{20}$, then all of the eigenvalues are negative. Therefore, the equilibrium point is asymptotically stable (Hirsh and Smale, 1974).

b) If the product of the relative removal rates is smaller than the product of population growth rates, i.e. $\rho_1 \rho_{20} < \pi_1 \pi_{20}$, then there is a positive eigenvalue.

Therefore, the equilibrium point is unstable. (Hirsh and Smale, 1974)

2) The second equilibrium point is,

$$\begin{aligned} x_{10} &= \frac{\delta_{20}(\alpha_1 \beta_2 + \delta_{20}(\gamma + \delta_1))}{\beta_2(\alpha_{20} \beta_1 + \delta_1 \delta_{20})}, x_{20} = \frac{(\gamma + \delta_1)(\alpha_{20} \beta_1 + \delta_1 \delta_{20})}{\beta_1(\alpha_1 \beta_2 + \delta_{20}(\gamma + \delta_1))}, \\ y_{10} &= \frac{\alpha_1 \alpha_{20} \beta_1 \beta_2 - \delta_1 \delta_{20}^2 (\gamma + \delta_1)}{\beta_2 (\gamma + \delta_1) (\alpha_{20} \beta_1 + \delta_1 \delta_{20})}, y_{20} = \frac{\alpha_1 \alpha_{20} \beta_1 \beta_2 - \delta_1 \delta_{20}^2 (\gamma + \delta_1)}{\beta_1 \delta_{20} (\alpha_1 \beta_2 + \delta_{20}(\gamma + \delta_1))}, \end{aligned} \quad (3.1.16.)$$

with $\alpha_1 \alpha_{20} \beta_1 \beta_2 - \delta_1 \delta_{20}^2 (\gamma + \delta_1) > 0$.

We can examine the system for small perturbations from the equilibrium point (3.1.16) by letting

$$\begin{cases} x_1 = x_{10}(1 + u_1), y_1 = y_{10}(1 + v_1), \\ x_2 = x_{20}(1 + u_2), y_2 = y_{20}(1 + v_2), \\ \text{where } |u_1|, |v_1|, |u_2|, |v_2| \ll 1, \end{cases} \quad (3.1.17.)$$

and substituting (3.1.17) and (3.1.16) into (3.1.10). After neglecting the product of perturbations, we have the following linearised equations :

$$\begin{cases} \frac{du_1}{dt} = - \left(\frac{\alpha_1 \alpha_{20} \beta_1 \beta_2 - \delta_1 \delta_{20}^2 (\gamma + \delta_1)}{\delta_{20} (\alpha_1 \beta_2 + \delta_{20}(\gamma + \delta_1))} + \delta_1 \right) u_1 - \frac{\alpha_1 \alpha_{20} \beta_1 \beta_2 - \delta_1 \delta_{20}^2 (\gamma + \delta_1)}{\delta_{20} (\alpha_1 \beta_2 + \delta_{20}(\gamma + \delta_1))} v_2, \\ \frac{dv_1}{dt} = (\gamma + \delta_1)(u_1 - v_1 + v_2), \\ \frac{du_2}{dt} = - \left(\frac{\alpha_1 \alpha_{20} \beta_1 \beta_2 - \delta_1 \delta_{20}^2 (\gamma + \delta_1)}{(\gamma + \delta_1)(\alpha_{20} \beta_1 + \delta_1 \delta_{20})} + \delta_{20} \right) u_2 - \frac{\alpha_1 \alpha_{20} \beta_1 \beta_2 - \delta_1 \delta_{20}^2 (\gamma + \delta_1)}{(\gamma + \delta_1)(\alpha_{20} \beta_1 + \delta_1 \delta_{20})} v_1, \\ \frac{dv_2}{dt} = \delta_{20}(u_2 + v_1 - v_2). \end{cases} \quad (3.1.18.)$$

We can simplify (3.1.18) by letting

$$c_1 = \frac{\alpha_1 \alpha_{20} \beta_1 \beta_2 - \delta_1 \delta_{20}^2 (\gamma + \delta_1)}{\delta_{20} (\alpha_1 \beta_2 + \delta_{20} (\gamma + \delta_1))}, \text{ and } c_2 = \frac{\alpha_1 \alpha_{20} \beta_1 \beta_2 - \delta_1 \delta_{20}^2 (\gamma + \delta_1)}{(\gamma + \delta_1) (\alpha_{20} \beta_1 + \delta_1 \delta_{20})},$$

which are both positive since $\alpha_1 \alpha_{20} \beta_1 \beta_2 - \delta_1 \delta_{20}^2 (\gamma + \delta_1) > 0$. Hence, the simplified equations are :

$$\begin{cases} \frac{du_1}{dt} = -(c_1 + \delta_1)u_1 - c_1 v_2, \\ \frac{dv_1}{dt} = (\gamma + \delta_1)(u_1 - v_1 + v_2), \\ \frac{du_2}{dt} = -(c_2 + \delta_{20})u_2 - c_2 v_1, \\ \frac{dv_2}{dt} = \delta_{20}(u_2 + v_1 - v_2). \end{cases} \quad (3.1.19.)$$

From (3.1.19), we obtain the characteristic polynomial of the community matrix to be

$$|A - \lambda I| = \begin{vmatrix} -(c_1 + \delta_1) - \lambda & 0 & 0 & -c_1 \\ (\gamma + \delta_1) & -(\gamma + \delta_1) - \lambda & 0 & (\gamma + \delta_1) \\ 0 & -c_2 & -(c_2 + \delta_{20}) - \lambda & 0 \\ 0 & \delta_{20} & \delta_{20} & -\delta_{20} - \lambda \end{vmatrix} = 0. \quad (3.1.20.)$$

There is one negative root, $-\delta_{20}$, of the characteristic polynomial of the linearised system. Therefore, stability will be determined by the roots of the cubic equation,

$$\begin{aligned}
& \lambda^3 + \left(\frac{\alpha_1 \beta_2 (\alpha_{20} \beta_1 + \delta_1 \delta_{20})}{\delta_{20} (\alpha_1 \beta_2 + \delta_{20} (\gamma + \delta_1))} + \frac{\alpha_{20} \beta_1 (\alpha_1 \beta_2 + \delta_1 (\gamma + \delta_1))}{(\gamma + \delta_1) (\alpha_{20} \beta_1 + \delta_1 \delta_{20})} + \gamma + \delta_1 \right) \lambda^2 \\
& + \left(\frac{\alpha_1 \beta_2 (\gamma + \delta_1) (\alpha_{20} \beta_1 + \delta_1 \delta_{20})}{\delta_{20} (\alpha_1 \beta_2 + \delta_{20} (\gamma + \delta_1))} + \frac{\alpha_1 \alpha_{20} \beta_1 \beta_2 - \delta_1 \delta_{20}^2 (\gamma + \delta_1)}{(\alpha_{20} \beta_1 + \delta_1 \delta_{20})} + \frac{\alpha_1 \beta_2}{\delta_{20}} \frac{\alpha_{20} \beta_1}{(\gamma + \delta_1)} \right) \lambda \\
& + \frac{\alpha_1 \alpha_{20} \beta_1 \beta_2 - \delta_1 \delta_{20}^2 (\gamma + \delta_1)}{\delta_{20}} = 0
\end{aligned}$$

By the Routh-Hurwitz conditions (Murray, 1993), the necessary and sufficient condition for all roots of the cubic equation to have negative real parts is

$$\frac{\alpha_1 \beta_2 (\alpha_{20} \beta_1 + \delta_1 \delta_{20})}{\delta_{20} (\alpha_1 \beta_2 + \delta_{20} (\gamma + \delta_1))} + \frac{\alpha_{20} \beta_1 (\alpha_1 \beta_2 + \delta_1 (\gamma + \delta_1))}{(\gamma + \delta_1) (\alpha_{20} \beta_1 + \delta_1 \delta_{20})} + \gamma + \delta_1 > 0, \quad (3.1.21.)$$

$$\frac{\alpha_1 \alpha_{20} \beta_1 \beta_2 - \delta_1 \delta_{20}^2 (\gamma + \delta_1)}{\delta_{20}} > 0, \text{ and} \quad (3.1.22.)$$

$$\begin{aligned}
& \left(\frac{\alpha_1 \beta_2 (\alpha_{20} \beta_1 + \delta_1 \delta_{20})}{\delta_{20} (\alpha_1 \beta_2 + \delta_{20} (\gamma + \delta_1))} + \frac{\alpha_{20} \beta_1 (\alpha_1 \beta_2 + \delta_1 (\gamma + \delta_1))}{(\gamma + \delta_1) (\alpha_{20} \beta_1 + \delta_1 \delta_{20})} + \gamma + \delta_1 \right) \times \\
& \left(\frac{\alpha_1 \beta_2 (\gamma + \delta_1) (\alpha_{20} \beta_1 + \delta_1 \delta_{20})}{\delta_{20} (\alpha_1 \beta_2 + \delta_{20} (\gamma + \delta_1))} + \frac{\alpha_1 \alpha_{20} \beta_1 \beta_2 - \delta_1 \delta_{20}^2 (\gamma + \delta_1)}{(\alpha_{20} \beta_1 + \delta_1 \delta_{20})} + \frac{\alpha_1 \beta_2}{\delta_{20}} \frac{\alpha_{20} \beta_1}{(\gamma + \delta_1)} \right) \\
& > \frac{\alpha_1 \alpha_{20} \beta_1 \beta_2 - \delta_1 \delta_{20}^2 (\gamma + \delta_1)}{\delta_{20}}
\end{aligned} \quad (3.1.23.)$$

Since $\alpha_1 \alpha_{20} \beta_1 \beta_2 - \delta_1 \delta_{20}^2 (\gamma + \delta_1) > 0$ and all the parameters are positive, (3.1.21) and (3.1.22) are satisfied. Consequently, if (3.1.23) is satisfied then it is asymptotically stable. Otherwise it is not stable.

3.2. THE BASIC MODEL WITH TWO HOSTS AND ONE VECTOR.

In this section, the basic model for the Ross River virus which has two hosts and one vector is introduced and analysed.

The human host population is divided into three disjoint groups: The susceptible group, $x_1(t)$, consists of individuals who have not yet contracted the virus. The infective group, $y_1(t)$, consists of individuals who have contracted the virus and are infectious. Finally, the removal group, $z_1(t)$, consists of individuals who are removed from the susceptible and infective group due to death and the infective group due to immunity after the viraemia period.

The animal host population is also divided into three disjoint groups : The susceptible group, $x_2(t)$, consists of individuals who have not yet contracted the virus. The infective group, $y_2(t)$, consists of individuals who have contracted the virus and are infectious. Finally, the removal group, $z_2(t)$, consists of individuals who have been removed from the susceptible and infective group due to death at a variable mortality rate and the infective group after the viraemia period at the recovery rate.

The vector population is divided into four disjoint groups. The susceptible group, $x_3(t)$, consists of mosquitoes which have not yet contracted the disease. The latent group, $e(t)$, consists of mosquitoes which are in the extrinsic incubation period and not infectious yet. The infective group, $y_3(t)$, consists of mosquitoes which are infectious after the extrinsic incubation period, and the removal group, $z_3(t)$, consists of mosquitoes which have been removed from the susceptible, latent and infective groups by death.

The assumptions in this model are similar to the model (3.1.1). The following assumptions are made in this model :

1. All three populations are homogeneously mixing.
2. The total human, animal and mosquito populations, $n_1(t)$, $n_2(t)$ and $n_3(t)$, changes with constant and variable birth (or recruitment) rates, α_1 , $\alpha_2(t)$ and $\alpha_3(t)$ and constant and variable mortality rates, δ_1 , $\delta_2(t)$ and $\delta_3(t)$. The new births in all three populations are not infected and are put directly into the susceptible groups

These assumptions lead to the following simple model :

$$\begin{cases} \frac{dn_1(t)}{dt} = \alpha_1 - \delta_1 n_1(t), \\ \frac{dn_2(t)}{dt} = \alpha_2(t) - \delta_2(t) n_2(t), \\ \frac{dn_3(t)}{dt} = \alpha_3(t) - \delta_3(t) n_3(t). \end{cases}$$

3. The number of infections in the host populations in a time Δt are $\beta_1 x_1(t) y_3(t) \Delta t$ and $\beta_2 x_2(t) y_3(t) \Delta t$, where β_1 and β_2 are the constant infection rates from the vector to the human and animal, respectively. The number of removals in the host-susceptible groups due to deaths in a time Δt are $\delta_1 x_1(t) \Delta t$ and $\delta_2(t) x_2(t) \Delta t$.

4. The number of infections in the vector population in a time Δt is $\beta_3 x_3(t) (y_1(t) + y_2(t)) \Delta t$, where β_3 is the constant infection rate from the host to the vector. The infection rates from mosquitoes to humans and animals are assumed to be the same.

5. The number of removals due to death or immunity in a time Δt are $(\gamma_1 + \delta_1) y_1(t) \Delta t$ and $(\gamma_2 + \delta_2(t)) y_2(t) \Delta t$, where γ_1 and γ_2 are the constant

recovery rates and are equal to $1/a_1$ and $1/a_2$, where a_1 and a_2 are the viraemia periods for the human and animal hosts.

6. The number of new infectives during a time Δt is $\varepsilon(t)e(t)\Delta t$, where $\varepsilon(t)$ is a variable transfer rate between the latent group and the infective group and is equal to $1/a_3(t)$, where $a_3(t)$ is a variable extrinsic incubation period.

7. The number of removals due to deaths in a time Δt is $\delta_3(t)(x_3(t) + e(t) + y_3(t))\Delta t$, where $\delta_3(t)$ is a variable mortality rate.

A diagram representing this model is given in Figure 3.2.

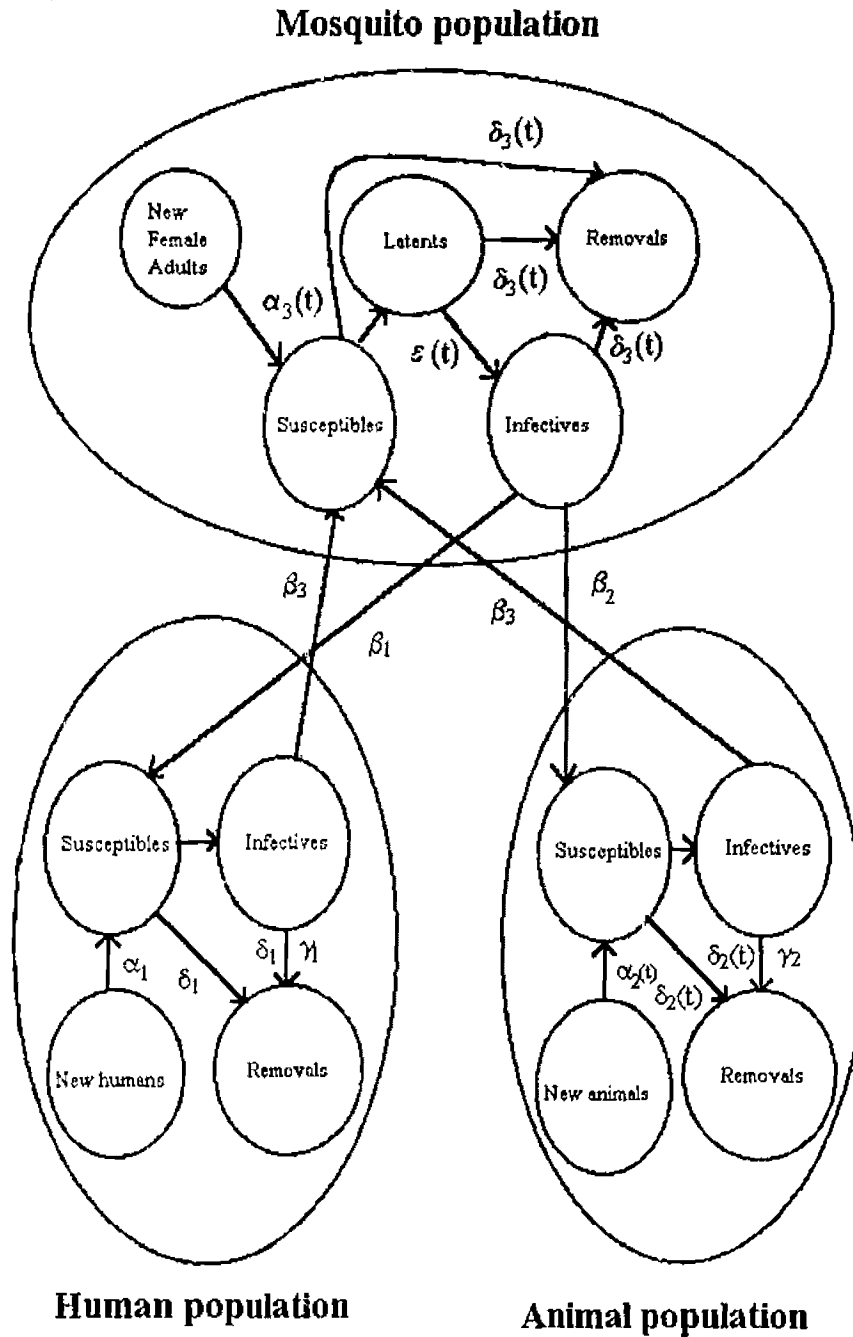


Figure 3.2 Flow diagram for RRV transmission between two hosts and one vector.

With the above assumptions, the basic deterministic model for the Ross River virus which has human and animal hosts and one vector is given by:

$$\begin{cases}
\frac{dx_1(t)}{dt} = -\beta_1 x_1(t) y_3(t) - \delta_1 x_1(t) + \alpha_1, \\
\frac{dy_1(t)}{dt} = \beta_1 x_1(t) y_3(t) - (\gamma_1 + \delta_1) y_1(t), \\
\frac{dz_1(t)}{dt} = \gamma_1 y_1(t) - \delta_1 z_1(t), \\
\frac{dx_2(t)}{dt} = -\beta_2 x_2(t) y_3(t) - \delta_2 x_2(t) + \alpha_2(t), \\
\frac{dy_2(t)}{dt} = \beta_2 x_2(t) y_3(t) - (\gamma_2 + \delta_2(t)) y_2(t), \\
\frac{dz_2(t)}{dt} = \gamma_2 y_2(t) - \delta_2(t) z_2(t), \\
\frac{dx_3(t)}{dt} = -\beta_3 x_3(t) (y_1(t) + y_2(t)) - \delta_3(t) x_3(t) + \alpha_3(t), \\
\frac{de(t)}{dt} = \beta_3 x_3(t) (y_1(t) + y_2(t)) - (\delta_3(t) + \varepsilon(t)) e(t), \\
\frac{dy_3(t)}{dt} = \varepsilon(t) e(t) - \delta_3(t) y_3(t),
\end{cases} \quad (3.2.1.)$$

where the initial conditions when $t = 0$ are: $(x_1(t), y_1(t), z_1(t)) = (x_{10}, y_{10}, 0)$,

$(x_2(t), y_2(t), z_2(t)) = (x_{20}, y_{20}, 0)$ and $(x_3(t), e(t), y_3(t)) = (x_{30}, e_0, y_{30})$.

All of the constant parameters in (3.2.1) are nonnegative:

$$\beta_1, \beta_2, \beta_3, \delta_1, \alpha_1, \gamma, \gamma_2 \geq 0,$$

and all of the variable parameters are nonnegative,

$$\alpha_2(t), \alpha_3(t) > 0 \text{ and } \delta_2(t), \delta_3(t), \varepsilon(t) \geq 0, \forall t \in \mathbb{R}^+.$$

From equations (3.2.1), for a true epidemic to occur $\frac{dy_1(t)}{dt}$, $\frac{dy_2(t)}{dt}$, $\frac{de(t)}{dt}$ and

$\frac{dy_3(t)}{dt}$ must be positive as in Section 3.1 so that

$$\frac{dy_1(t)}{dt} = \beta_1 x_1(t) y_3(t) - (\gamma_1 + \delta_1) y_1(t) > 0, \quad (3.2.2.)$$

$$\frac{dy_2(t)}{dt} = \beta_2 x_2(t) y_3(t) - (\gamma_2 + \delta_2(t)) y_2(t) > 0, \quad (3.2.3.)$$

$$\frac{de(t)}{dt} = \beta_3 x_3(t) (y_1(t) + y_2(t)) - (\delta_3(t) + \varepsilon(t)) e(t) > 0, \quad (3.2.4.)$$

$$\text{and } \frac{dy_3(t)}{dt} = \varepsilon(t) e(t) - \delta_3(t) y_3(t) > 0. \quad (3.2.5.)$$

From the inequalities (3.2.2), (3.2.3), (3.2.4) and (3.2.5), we obtain the following inequalities:

$$y_1(t) < \frac{\beta_1 x_1(t) y_3(t)}{(\gamma_1 + \delta_1)}, \quad (3.2.6.)$$

$$y_2(t) < \frac{\beta_2 x_2(t) y_3(t)}{(\gamma_2 + \delta_2(t))}, \quad (3.2.7.)$$

$$\text{and } \frac{\beta_3 \varepsilon(t) x_3(t) (y_1(t) + y_2(t))}{\delta_3(t) (\delta_3(t) + \varepsilon(t)) y_3(t)} < 1. \quad (3.2.8.)$$

From (3.2.6) and (3.2.7), we obtain the following condition:

$$y_1(t) + y_2(t) < \frac{\beta_1 x_1(t) y_3(t)}{(\gamma_1 + \delta_1)} + \frac{\beta_2 x_2(t) y_3(t)}{(\gamma_2 + \delta_2(t))}. \quad (3.2.9.)$$

Substituting (3.2.9) into (3.2.8), we obtain

$$\frac{\varepsilon(t)}{(\delta_3(t) + \varepsilon(t))} \frac{\beta_3 x_3(t)}{\delta_3(t)} \left\{ \frac{\beta_1 x_1(t)}{(\gamma_1 + \delta_1)} + \frac{\beta_2 x_2(t)}{(\gamma_2 + \delta_2(t))} \right\} > 1. \quad (3.2.10.)$$

Since $\frac{\varepsilon(t)}{(\delta_3(t) + \varepsilon(t))} < 1$, the threshold condition (3.2.10) can be changed to

$$\frac{x_3(t)}{\rho_3(t)} \left\{ \frac{x_1(t)}{\rho_1} + \frac{x_2(t)}{\rho_2(t)} \right\} > 1, \quad (3.2.11.)$$

where $\rho_1 = \frac{(\gamma_1 + \delta_1)}{\beta_1}$, $\rho_2(t) = \frac{(\gamma_2 + \delta_2(t))}{\beta_2}$, and $\rho_3(t) = \frac{\delta_3(t)}{\beta_3}$,

and ρ_1 , $\rho_2(t)$, and $\rho_3(t)$ are relative removal rates for the hosts and the vector at time t .

From the threshold condition (3.2.11), the following conditions can prevent a true outbreak from occurring.

1. Reducing the number of susceptibles in all the populations. Increased immunity or vaccination in the human and animal populations can reduce the number of possible susceptibles. A program of mosquito control can reduce the number of susceptibles in the vector population.
2. Reducing the infection rates between the hosts and vectors.
3. Shorter viraemia periods of host populations

To examine the stability of the system of equations given in (3.2.1), the equations can be replaced by a new set of equations given in (3.2.12) in which the latent group in the vector population is neglected. The stability result for the new system given in (3.2.12) is exactly the same as for the equations given in (3.2.1) since the latent group is dependent on the infective group in the vector population as in Section 3.1.

We have,

$$\begin{cases}
\frac{dx_1(t)}{dt} = -\beta_1 x_1(t) y_3(t) - \delta_1 x_1(t) + \alpha_1, \\
\frac{dy_1(t)}{dt} = \beta_1 x_1(t) y_3(t) - (\gamma_1 + \delta_1) y_1(t), \\
\frac{dx_2(t)}{dt} = -\beta_2 x_2(t) y_3(t) - \delta_2(t) x_2(t) + \alpha_2(t), \\
\frac{dy_2(t)}{dt} = \beta_2 x_2(t) y_3(t) - (\gamma_2 + \delta_2(t)) y_2(t), \\
\frac{dx_3(t)}{dt} = -\beta_3 x_3(t) (y_1(t) + y_2(t)) - \delta_3(t) x_3(t) + \alpha_3(t), \\
\frac{dy_3(t)}{dt} = \beta_3 x_3(t) (y_1(t) + y_2(t)) - \delta_3(t) y_3(t).
\end{cases} \quad (3.2.12.)$$

The equilibrium points of the equations (3.2.12) can be found by setting the derivatives in (3.2.12) to zero. Since the birth and mortality rates in the animal population and the recruitment and mortality rates in the mosquito population are changing with time t , for examining the stability we shall assume that α_{20} , δ_{20} , α_{30} , and δ_{30} are the constant average values of the functions, that $\alpha_2(t)$, $\delta_2(t)$, $\alpha_3(t)$, and $\delta_3(t)$, are as in Section 3.1. Hence, the equilibrium points lie in the domain contained by the following equations :

$$\begin{cases}
\delta_1 x_1(t) + (\gamma_1 + \delta_1) y_1(t) - \alpha_1 = 0, \\
\delta_{20} x_2(t) + (\gamma_2 + \delta_{20}) y_2(t) - \alpha_{20} = 0, \\
\delta_{30} x_3(t) + \delta_{30} y_3(t) - \alpha_{30} = 0.
\end{cases} \quad (3.2.13.)$$

At time $t = 0$ the equilibrium point is :

$$(x_{10}, y_{10}, x_{20}, y_{20}, x_{30}, y_{30}) = \left(\frac{a_1}{d_1}, 0, \frac{a_{20}}{d_{20}}, 0, \frac{a_{30}}{d_{30}}, 0 \right), \quad (3.2.14.)$$

After linearising in the departures u_1, v_1, u_2 , and v_2 , from the equilibrium point, we obtain the eigenvalues from the community matrix and its characteristic polynomial. Three eigenvalues of the community matrix are

$$\lambda = -\delta_1, -\delta_{20}, -\delta_{30}. \quad (3.2.15.)$$

Since the three eigenvalues in (3.2.15) are negative, stability will be determined by the rest of the eigenvalues, which are given by the following cubic equation:

$$\begin{aligned} & \lambda^3 + (\gamma_1 + \gamma_2 + \delta_1 + \delta_{20} + \delta_{30})\lambda^2 \\ & + \left[(\delta_1 + \gamma_1)(\delta_{20} + \gamma_2) + (\delta_{20} + \gamma_2)\delta_{30} + \delta_{30}(\delta_1 + \gamma_1) - \frac{\alpha_{30}\beta_3}{\delta_{30}} \left(\beta_2 \frac{\alpha_{20}}{\delta_{20}} + \beta_1 \frac{\alpha_1}{\delta_1} \right) \right] \lambda \\ & + (\delta_1 + \gamma_1)(\delta_{20} + \gamma_2)\delta_{30} - \frac{\alpha_{30}\beta_3}{\delta_{30}} \left(\beta_2 \frac{\alpha_{20}}{\delta_{20}} (\delta_1 + \gamma_1) + \beta_1 \frac{\alpha_1}{\delta_1} (\delta_{20} + \gamma_2) \right) \\ & = 0 \end{aligned} \quad (3.2.16.)$$

The Routh-Hurwitz conditions (Murray, 1993) for all the roots of the cubic equation to have negative real parts are

$$\begin{aligned} & \gamma_1 + \gamma_2 + \delta_1 + \delta_{20} + \delta_{30} > 0, \\ & (\delta_1 + \gamma_1)(\delta_{20} + \gamma_2)\delta_{30} - \frac{\alpha_{30}\beta_3}{\delta_{30}} \left(\beta_2 \frac{\alpha_{20}}{\delta_{20}} (\delta_1 + \gamma_1) + \beta_1 \frac{\alpha_1}{\delta_1} (\delta_{20} + \gamma_2) \right) > 0 \text{ and} \\ & (\delta_1 + \gamma_1)(\delta_{20} + \gamma_2)\delta_{30} - \frac{\alpha_{30}\beta_3}{\delta_{30}} \left(\beta_2 \frac{\alpha_{20}}{\delta_{20}} (\delta_1 + \gamma_1) + \beta_1 \frac{\alpha_1}{\delta_1} (\delta_{20} + \gamma_2) \right) > \\ & (\gamma_1 + \gamma_2 + \delta_1 + \delta_{20} + \delta_{30}) \times \\ & \left\{ (\delta_1 + \gamma_1)(\delta_{20} + \gamma_2) + (\delta_{20} + \gamma_2)\delta_{30} + \delta_{30}(\delta_1 + \gamma_1) - \frac{\alpha_{30}\beta_3}{\delta_{30}} \left(\beta_2 \frac{\alpha_{20}}{\delta_{20}} + \beta_1 \frac{\alpha_1}{\delta_1} \right) \right\}. \end{aligned}$$

Since the first condition above is automatically satisfied, stability will be determined by the second and third conditions. The complexity of the two

condition make it difficult to interpret. Additionally, the second condition is satisfied if the basic reproduction rate $R_0 < 1$ as

$$R_0 = \frac{\alpha_{30}\beta_3}{\delta_{30}^2} \left(\frac{\alpha_1\beta_1}{\delta_1(\delta_1 + \gamma_1)} + \frac{\alpha_{20}\beta_2}{\delta_{20}(\delta_{20} + \gamma_2)} \right) < 1.$$

3.3. THE GENERAL MODEL FOR RRV TRANSMISSION

Most of the parameters used in the deterministic models will have different parameter values for different patches describing different regions, species, sex, age, etc. However, it is difficult to estimate the values of these parameters. Therefore, most of the deterministic models are assumed to involve homogeneous mixing populations. In this section, the general model for Ross River virus transmission with heterogeneous mixing populations is considered. The general model assumes different parameters for different patches, which are described below. Humans and animals are the hosts of the Ross River virus in the general model and mosquitoes are the vectors.

The following assumptions are made in this general model :

1. All of the populations considered in the model are heterogeneously mixing.
2. There are l -human and m -animal population patches which can be defined according to region, sex, age, species, etc.
3. There are n - mosquito vector population patches which can be defined according to region, species, etc.
4. The incubation periods for humans are neglected, while the viraemia periods are used to calculate the recovery rates since the infected humans become

immune after the viraemia period. In the same fashion, the viraemia periods for the animal populations are used to calculate the recovery rates as in the human populations.

5. The human host populations are divided into three disjoint types of groups. The susceptible groups, $x_i^h(t)$, where $i = 1, 2, \dots, l$, are groups of individuals who have not yet contracted the virus. The infective groups, $y_i^h(t)$, where $i = 1, 2, \dots, l$, are groups of individuals who have contracted the virus and are infectious. Finally, the removal groups, $z_i^h(t)$, where $i = 1, 2, \dots, l$, are groups of individuals who have died or gained immunity and have been removed from the susceptible and infective groups.

6. The animal host populations are also divided into three disjoint types of groups similar to the human groups. The susceptible groups, $x_j^a(t)$, where $j = 1, 2, \dots, m$, are groups of individuals who have not yet contracted the virus. The infective groups, $y_j^a(t)$, where $j = 1, 2, \dots, m$, are groups of individuals who have contracted the virus and are infectious. Finally, the removal groups, $z_j^a(t)$, where $j = 1, 2, \dots, m$, are individuals who have died or gained immunity and have been removed from the susceptible and infective groups.

7. The vector populations are divided into four disjoint groups. The susceptible groups, $x_k^m(t)$, where $k = 1, 2, \dots, n$, consist of mosquitoes which have not contracted the disease. The latent groups, $e_k^m(t)$, where $k = 1, 2, \dots, n$, consist of mosquitoes which are in the extrinsic incubation period and are not infectious yet. The infective groups, $y_k^m(t)$, where $k = 1, 2, \dots, n$, consist of mosquitoes which

are infectious; and the removal groups, $z_k^m(t)$, where $k = 1, 2, \dots, n$, are mosquitoes which have died and have been removed from the susceptible, latent and infective groups.

8. The total human populations, $n_i^h(t)$, where $i = 1, 2, \dots, l$, have constant birth rates, α_i^h , where $i = 1, 2, \dots, l$, and constant mortality rates, δ_i^h , where $i = 1, 2, \dots, l$. New births occurring within a time Δt , $\alpha_i^h \Delta t$, in the human population are not infected. Therefore, the new births enter directly into the susceptible groups.

9. The total animal populations, $n_j^a(t)$, have variable birth rates, $\alpha_j^a(t)$, where $j = 1, 2, \dots, m$, and variable mortality rates, $\delta_j^a(t)$, where $j = 1, 2, \dots, m$. New births occurring within a time Δt , $\alpha_j^a(t) \Delta t$, in the animal populations are not infected. Therefore, the new births enter directly into the susceptible groups.

10. The total mosquito populations, $n_k^m(t)$, where $k = 1, 2, \dots, n$, have variable recruitment rates, $\alpha_k^m(t)$, and variable mortality rates, $\delta_k^m(t)$. The new inputs during a time Δt , $\alpha_k^m(t) \Delta t$, in the vector population are not infected. Therefore, they go directly into the susceptible groups.

11. Individual humans may migrate from one patch to another patch and so provide an extra route for transmission. Since humans are the major long-distance carriers of the RRV, the emigration and immigration rates in animal and mosquito populations are neglected. In the human populations, the emigration rates from the i th group to the j th group are $\varphi_{ij}^h(t)$, where $i, j = 1, 2, \dots, l$, and the immigration rates from the j th group to the i th group are $\theta_{ji}^h(t)$, where

$i, j = 1, 2, \dots, l$. If the emigration or immigration occurs in the same group or region, the rates will be equal to zero. Therefore, the rate of growth of the population of the i th susceptible group due to emigration and immigration will

be $\sum_{j=1}^l (\theta_{ji}^h(t) - \phi_{ij}^h(t)) x_j^h(t)$. Similarly, the rate of growth of the population of the

i th infective group due to the emigration and immigration will be

$$\sum_{j=1}^l (\theta_{ji}^h(t) - \phi_{ij}^h(t)) y_j^h(t).$$

12. The rate of occurrence of new infective hosts is proportional to both the number of the host-susceptibles and the number of the vector-infectives. Thus, the numbers of infections in the host populations during a time Δt are

$$\left(\sum_{k=1}^n \beta_{ik}^{mh} y_k^m(t) \right) x_i^h(t) \Delta t \text{ in humans and } \left(\sum_{k=1}^n \beta_{jk}^{ma} y_k^m(t) \right) x_j^a(t) \Delta t \text{ in animals, where}$$

β_{ik}^{mh} and β_{jk}^{ma} , $i = 1, 2, \dots, l$, $j = 1, 2, \dots, m$ and $k = 1, 2, \dots, n$, are the infection rates

from the vector populations to the human and animal populations, respectively.

Individuals in the host-susceptible groups die and are removed from the host-

susceptible groups, $x_i^h(t)$ and $x_j^a(t)$, at the mortality rates, δ_i^h and $\delta_j^a(t)$, where

$i = 1, 2, \dots, l$ and $j = 1, 2, \dots, m$, and rates proportional to the number of host-

infectives. Hence, the number of removals in the host-susceptible groups due to

death during a time Δt are $\delta_i^h x_i^h(t) \Delta t$ and $\delta_j^a(t) x_j^a(t) \Delta t$.

13. The rate of occurrence of new latent vectors, which are infected but not infectious, is proportional to both the populations of the susceptible groups of vectors and the populations of the infective groups of human and animal hosts.

Thus, the number of new infections in the vector population in a time Δt is

$$\left(\sum_{i=1}^l \beta_{ki}^{hm} y_i^h(t) + \sum_{j=1}^m \beta_{kj}^{ma} y_j^a(t) \right) x_k^m(t) \Delta t, \quad \text{where } \beta_{ki}^{hm} \text{ and } \beta_{kj}^{ma}, \quad i = 1, 2, \dots, l,$$

$j = 1, 2, \dots, m$ and $k = 1, 2, \dots, n$, are the infection rates from the humans and animals to the vectors, respectively.

14. Individuals in the host-infective populations which die or become immune after viraemia periods are removed from the host-infective groups, $y_i^h(t)$ and $y_j^a(t)$, at the mortality rates, δ_i^h and $\delta_j^a(t)$, where $i = 1, 2, \dots, l$ and $j = 1, 2, \dots, m$, and at the recovery rates, γ_i^h and γ_j^a and at rates proportional to the number of host-infectives. Hence, the numbers of removals due to death and immunity during a time Δt are $(\gamma_i^h + \delta_i^h) y_i^h(t) \Delta t$ and $(\gamma_j^a + \delta_j^a(t)) y_j^a(t) \Delta t$, where $i = 1, 2, \dots, l$ and $j = 1, 2, \dots, m$, where γ_i^h and γ_j^a are the recovery rates and are equal to $1/a_i^h$ and $1/a_j^a$, where a_i^h and a_j^a ($i = 1, 2, \dots, l$ and $j = 1, 2, \dots, m$) are the viraemia periods for human and animal hosts.

15. Individuals in the vector-latent population become infectious after the extrinsic incubation period, and are removed from the latent group, $e_k^m(t)$, at a rate proportional to the number of vector-latents. Hence, the number of new infectives in a time Δt is $\varepsilon_k^m(t) e_k^m(t) \Delta t$, $k = 1, 2, \dots, n$, where $\varepsilon_k^m(t)$ is the transfer rate between the latent group and the infective group and is equal to $1/a_k^m(t)$, $k = 1, 2, \dots, n$, where $a_k^m(t)$ is the variable extrinsic incubation period for the k th group.

16. Individuals in the vector population are removed due to death from the susceptible, latent and infective groups, $x_k^m(t)$, $e_k^m(t)$, $y_k^m(t)$, at the mortality rates, $\delta_k^m(t)$, where $k = 1, 2, \dots, n$, and at rates proportional to the number of each group. Hence, the number of removals due to death in a time Δt is $\delta_k^m(t)(x_k^m(t) + e_k^m(t) + y_k^m(t))\Delta t$, $k = 1, 2, \dots, n$, where $\delta_k^m(t)$ is the variable mortality rate for the k th group.

With the above assumptions, the general deterministic model for the RRV which has human and animal hosts and mosquito vectors is given in (3.3.1).

$$\begin{cases}
 \frac{dx_i^h(t)}{dt} = -\left(\sum_{k=1}^n \beta_{ik}^{mh} y_k^m(t)\right)x_i^h(t) - \delta_i^h x_i^h(t) + \alpha_i^h + \sum_{j=1}^l (\theta_{ji}^h(t) - \phi_{ij}^h(t))x_j^h(t), \\
 \frac{dy_i^h(t)}{dt} = \left(\sum_{k=1}^n \beta_{ik}^{mh} y_k^m(t)\right)x_i^h(t) - (\gamma_i^h + \delta_i^h)y_i^h(t) + \sum_{j=1}^l (\theta_{ji}^h(t) - \phi_{ij}^h(t))y_j^h(t), \\
 \frac{dz_i^h(t)}{dt} = \gamma_i^h y_i^h(t) - \delta_i^h z_i^h(t), \\
 \frac{dx_j^a(t)}{dt} = -\left(\sum_{k=1}^n \beta_{jk}^{ma} y_k^m(t)\right)x_j^a(t) - \delta_j^a x_j^a(t) + \alpha_j^a(t), \\
 \frac{dy_j^a(t)}{dt} = \left(\sum_{k=1}^n \beta_{jk}^{ma} y_k^m(t)\right)x_j^a(t) - (\gamma_j^a + \delta_j^a)y_j^a(t), \\
 \frac{dz_j^a(t)}{dt} = \gamma_j^a y_j^a(t) - \delta_j^a z_j^a(t), \\
 \frac{dx_k^m(t)}{dt} = -\left(\sum_{i=1}^l \beta_{ki}^{hm} y_i^h(t) + \sum_{j=1}^m \beta_{kj}^{am} y_j^a(t)\right)x_k^m(t) - \delta_k^m(t)x_k^m(t) + \alpha_k^m(t), \\
 \frac{de_k^m(t)}{dt} = \left(\sum_{i=1}^l \beta_{ki}^{hm} y_i^h(t) + \sum_{j=1}^m \beta_{kj}^{am} y_j^a(t)\right)x_k^m(t) - (\delta_k^m(t) + \varepsilon_k^m(t))e_k^m(t), \\
 \frac{dy_k^m(t)}{dt} = \varepsilon_k^m(t)e_k^m(t) - \delta_k^m(t)y_k^m(t),
 \end{cases}$$

where, $i = 1, 2, \dots, l$, $j = 1, 2, \dots, m$ and $k = 1, 2, \dots, n$.

(3.3.1.)

The emigration and immigration parameters for the human populations can be implemented in various ways. For example, the transfer between different age groups can be included in the migration parameters. The models (3.1.1) in Section 3.1 and (3.2.1) in Section 3.2 are simple cases of the general model (3.3.1) with l , m and k being 1. In both those models (3.1.1) and (3.2.1), the migration parameters are neglected since the populations are assumed to mix homogeneously.

In the general model (3.3.1), if we assume that

1. There is no migration.
2. The infection rates from specific hosts to vectors are same as follows;

$$\beta_{ik}^{mh} = \beta_i^{mh} \text{ and } \beta_{jk}^{ah} = \beta_j^{ah}, \text{ where } k = 1, 2, \dots, n.$$

Then, if an outbreak occurs, the following joint threshold condition calculated below in a manner similar to Sections 3.1 and 3.2 will be satisfied.

$$\left(\sum_{k=1}^n \frac{\varepsilon_k^m(t)}{(\delta_k^m(t) + \varepsilon_k^m(t))} \frac{x_k^m(t)}{\rho_k^{mh}(t)} \right) \left(\sum_{i=1}^l \frac{x_i^h(t)}{\rho_i^h(t)} \right) + \left(\sum_{k=1}^n \frac{\varepsilon_k^m(t)}{(\delta_k^m(t) + \varepsilon_k^m(t))} \frac{x_k^m(t)}{\rho_k^{ma}(t)} \right) \left(\sum_{j=1}^m \frac{x_j^a(t)}{\rho_j^a(t)} \right) > 1, \quad (3.3.2.)$$

where

$$\rho_i^h(t) = \frac{(\delta_i^h + \gamma_i^h)}{\beta_i^{hm}}, \rho_j^a(t) = \frac{(\delta_j^a + \gamma_j^a)}{\beta_j^{am}}, \rho_k^{mh}(t) = \frac{\delta_k^m(t)}{\beta_k^{mh}(t)} \text{ and } \rho_k^{ma}(t) = \frac{\delta_k^m(t)}{\beta_k^{ma}(t)},$$

$$i = 1, 2, \dots, l, \quad j = 1, 2, \dots, m \text{ and } k = 1, 2, \dots, n.$$

From the threshold condition (3.3.2), the following conditions similar to the conditions as in Section 3.2 can prevent a true outbreak from occurring.

1. Reducing the number of susceptibles in all host and vector populations involved in the transmission cycle.
2. Reducing the infection rates between the hosts and vectors.
3. Shorter viraemia periods of host populations

Further details of a mathematical analysis of this model is difficult due to the complexity of the interactions. We move now instead to Chapter 4 where we examine an RRV model with continuous natural infection.

CHAPTER 4.

THE HOST-VECTOR MODEL FOR THE RRV WITH CONTINUOUS

NATURAL INFECTION ON MOSQUITO POPULATION

In this chapter, the mathematical analysis of the host-vector model for the RRV transmission with continuous natural infection is presented. The natural infection rate can be defined as the rate which the virus is introduced into the vector population. An RRV isolation rate is defined as the proportion of the vector population which contains RRV. Laboratory results on the RRV isolation rates and *Aedes camptorhynchus* population during the 1995-96 outbreak in the Peel District as shown in Figure 4.1 indicate the time of onset of RRV in the vector population.

The vector population during the peak summer is very low but the isolation rate at the same time is very high. One of the reasons for this is the short period of the extrinsic incubation period in summer. On the other hand, during winter the isolation rate is zero because the mosquitoes are not infectious in winter and the virus persists at a very low level in the vector population. So, the mechanism of the virus introduction into the vector population could be a random function depending on the environmental conditions and is currently unknown.

In this thesis, two possible scenarios with a single and continuous natural infections are suggested and two types of models with these scenarios are analysed and computer-simulated.

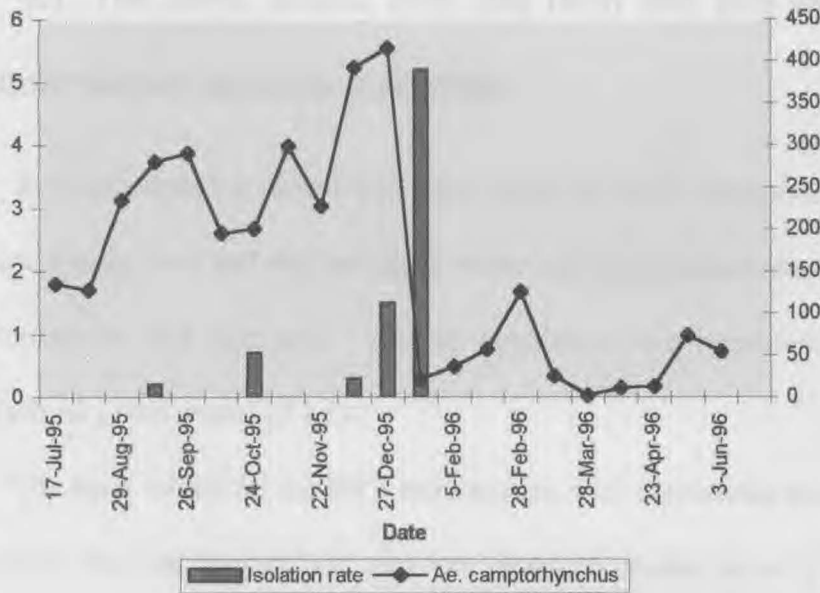


Figure 4.1 Ross River virus isolation rate per 1,000 *Aedes camptorhynchus* and the trapped *Aedes camptorhynchus* population during the 1995-96 outbreak in the Peel District

The previous Chapter 3 shows the analysis of the model with a single natural infection on the mosquito population. These models in Chapter 3 assume that there is only one single natural infection on the mosquito population prior to the outbreak. In this chapter, the host-vector models with continuous natural infections are introduced and analysed mathematically. Each model in this chapter has the same assumptions as in Chapter 3 and an additional assumption that the mosquitoes are exposed continuously to the environmental infection.

Section 4.1 and 4.2 introduces the basic RRV transmission models with a continuous natural infection and examines its threshold condition and stability. Section 4.3 introduces the general RRV model with continuous natural infection and examines its threshold condition.

4.1. THE BASIC MODEL WITH ONE HOST AND ONE VECTOR WITH CONTINUOUS NATURAL INFECTION

In this section, the basic host-vector model for RRV transmission, which has one human host and one mosquito vector and continuous natural infection, is introduced and discussed. Animal populations are neglected in the same fashion as the model (3.1.1).

The basic model for the RRV transmission with continuous natural infection which has one human host and one mosquito vector is as in (3.1.1), with

$$\frac{dx_1(t)}{dt}, \frac{dy_1(t)}{dt}, \frac{dz_1(t)}{dt}, \text{ and } \frac{dy_2(t)}{dt} \text{ as before and}$$

$$\begin{cases} \frac{dx_2(t)}{dt} = -\beta_2 x_2(t) y_1(t) - (\delta_2(t) + \psi) x_2(t) + \alpha_2(t), \\ \frac{de_2(t)}{dt} = \beta_2 x_2(t) y_1(t) + \psi x_2(t) - (\delta_2(t) + \epsilon(t)) e_2(t). \end{cases} \quad (4.1.1.)$$

All of the assumptions of the model (3.1.1) in section 3.1 hold for the basic model (4.1.1). The following assumption is added in the model (4.1.1).

The rate of occurrence of new latent vectors due to the continuous natural infection, which are infected but not infectious, is proportional to the number of the vector-susceptibles. Thus, the number of infections in the vector population in a time Δt is $\psi x_2(t) \Delta t$, where ψ is a nonnegative constant natural infection rate on the mosquito population.

From the dynamics given in (4.1.1), for a true epidemic to occur $\frac{dy_1(t)}{dt}$,

$\frac{de_2(t)}{dt}$ and $\frac{dy_2(t)}{dt}$ must be greater than zero. Hence, we obtain the three

conditions

$$\frac{\beta_1 x_1(t) y_2(t)}{(\gamma + \delta_1) y_1(t)} > 1, \quad (4.1.2.)$$

$$\frac{(\beta_2 y_1(t) + \psi) x_2(t)}{(\delta_2(t) + \varepsilon(t)) e_2(t)} > 1, \text{ and} \quad (4.1.3.)$$

$$\frac{\varepsilon(t) e_2(t)}{\delta_2(t) y_2(t)} > 1. \quad (4.1.4.)$$

By multiplying the three inequalities (4.1.2), (4.1.3) and (4.1.4), we get the joint threshold condition as the following inequality :

$$x_1(t) x_2(t) > \frac{(\gamma + \delta_1) \delta(t)}{\beta_1 \frac{(\beta_2 y_1(t) + \psi)}{y_1(t)}} \cdot \frac{\delta_2(t) + \varepsilon(t)}{\varepsilon(t)}. \quad (4.1.5.)$$

Since the natural infection rate ψ is very small compare to $\beta_2 y_1(t)$, the inequality can be expressed as,

$$x_1(t) x_2(t) > \frac{(\gamma + \delta_1) \delta(t)}{\beta_1 \beta_2} \cdot \frac{\delta_2(t) + \varepsilon(t)}{\varepsilon(t)} = \rho_1 \rho_2(t) \cdot \frac{\delta_2(t) + \varepsilon(t)}{\varepsilon(t)}, \quad (4.1.6.)$$

where ρ_1 and $\rho_2(t)$ are relative removal rates for host and vector at time t .

Thus, the basic model with continuous natural infection rate has the same threshold condition as the basic model with a single natural infection (3.1.1).

To examine the stability of the system of equations given in (4.1.1), the equations can be replaced with a new set of equations given in (4.1.7) as was done with the model (3.1.10) in Chapter 3.

$$\begin{cases} \frac{dx_1}{dt} = -\beta_1 x_1 y_2 - \delta_1 x_1 + \alpha_1, \\ \frac{dy_1}{dt} = \beta_1 x_1 y_2 - (\gamma + \delta_1) y_1, \\ \frac{dx_2(t)}{dt} = -\beta_2 x_2 y_1 - (\delta_2(t) + \psi) x_2 + \alpha_2(t), \\ \frac{dy_2(t)}{dt} = \beta_2 x_2 y_1 + \psi x_2 - \delta_2(t) y_2. \end{cases} \quad (4.1.7.)$$

The equilibrium points of the system given in (4.1.7) are found by setting the derivatives in equations (4.1.7) to zero. Since the recruitment and mortality rates in the vector population are changing with time t , for examining the stability we suppose that α_{20} and δ_{20} are the constant average values of the functions, $\alpha_2(t)$ and $\delta_2(t)$.

Setting the derivatives of the system (4.1.7) to zero and eliminating x_1 , x_2 and y_1 , in favour of y_2 , we have the following quadratic equation,

$$\begin{aligned} & \alpha_1 \alpha_2 \beta_1 \beta_2 y_2^2 + \{ \delta_1 \delta_2 (\gamma + \delta_1) (\delta_2(t) + \psi) - \alpha_1 \alpha_2 \beta_1 \beta_2 + \alpha_2 \beta_1 \psi (\gamma + \delta_1) \} y_2 \\ & - \alpha_2 \delta_1 \psi (\gamma + \delta_1) = 0. \end{aligned} \quad (4.1.8.)$$

From the quadratic equation, the necessary and sufficient condition for roots to be real is

$$\begin{aligned} & \{ \delta_1 \delta_2 (\gamma + \delta_1) (\delta_2(t) + \psi) - \alpha_1 \alpha_2 \beta_1 \beta_2 + \alpha_2 \beta_1 \psi (\gamma + \delta_1) \}^2 \\ & + 4 \alpha_1 \alpha_2 \beta_1 \beta_2 \cdot \alpha_2 \delta_1 \psi (\gamma + \delta_1) > 0. \end{aligned} \quad (4.1.9.)$$

Since all parameters in the model (4.1.7) are nonnegative, the condition (4.1.9) is satisfied. Furthermore, the product of the roots of the quadratic

equation (4.1.8), $-\frac{\alpha_2 \delta_1 \psi (\gamma + \delta_1)}{\alpha_1 \alpha_2 \beta_1 \beta_2}$, is negative, so there exists a unique

positive equilibrium point in the system (4.1.7).

Even though the only difference between the two basic models (3.1.1) and (4.1.1) is the assumption of continuous natural infection, the present model is much more complex.

After linearising of the system (4.1.7) by considering small perturbations from the equilibrium point, the eigenvalues of the community matrix can be obtained as in Chapter 3. If all of the eigenvalues are negative, then the equilibrium point is asymptotically stable. Otherwise, the equilibrium point is unstable.

4.2. THE BASIC MODEL WITH TWO HOSTS AND ONE VECTOR.

In this section, the basic host-vector model for the RRV which has two hosts and one vector and includes continuous natural infection is introduced and analysed. All assumptions used in the model (3.2.1) are applied in the model (4.2.1). Furthermore, the additional assumption of continuous natural infection is included :

- The number of infections in the vector population in a time Δt is $\psi x_3(t)\Delta t$, where ψ is a constant natural infection rate on the mosquito population.

With the above assumptions, the basic deterministic model for the RRV which has human and animal hosts and one vector and continuous natural infection is as in (3.2.1), with $\frac{dx_1(t)}{dt}$, $\frac{dy_1(t)}{dt}$, $\frac{dz_1(t)}{dt}$, $\frac{dx_2(t)}{dt}$, $\frac{dy_2(t)}{dt}$, $\frac{dz_2(t)}{dt}$, and $\frac{dy_3(t)}{dt}$ as before and

$$\begin{cases} \frac{dx_3(t)}{dt} = -\beta_3 x_3(t)(y_1(t) + y_2(t)) - (\delta_3(t) + \psi)x_3(t) + \alpha_3(t), \\ \frac{de(t)}{dt} = \beta_3 x_3(t)(y_1(t) + y_2(t)) + \psi \alpha_3(t) - (\delta_3(t) + \varepsilon(t))e(t). \end{cases} \quad (4.2.1.)$$

From the equations (4.2.1), if a true epidemic occurs, then we must have,

$$\frac{dy_1(t)}{dt} = \beta_1 x_1(t)y_3(t) - (\gamma_1 + \delta_1)y_1(t) > 0, \quad (4.2.2.)$$

$$\frac{dy_2(t)}{dt} = \beta_2 x_2(t)y_3(t) - (\gamma_2 + \delta_2(t))y_2(t) > 0, \quad (4.2.3.)$$

$$\frac{de(t)}{dt} = \beta_3 x_3(t)(y_1(t) + y_2(t)) + \psi \alpha_3(t) - (\delta_3(t) + \varepsilon(t))e(t) > 0, \text{ and } (4.2.4.)$$

$$\frac{dy_3(t)}{dt} = \varepsilon(t)e(t) - \delta_3(t)y_3(t) > 0. \quad (4.2.5.)$$

From the inequalities (4.2.2), (4.2.3), (4.2.4) and (4.2.5), we obtain the following inequalities,

$$y_1(t) < \frac{\beta_1 x_1(t)y_3(t)}{(\gamma_1 + \delta_1)}, \quad (4.2.6.)$$

$$y_2(t) < \frac{\beta_2 x_2(t)y_3(t)}{(\gamma_2 + \delta_2(t))}, \text{ and } (4.2.7.)$$

$$\frac{\varepsilon(t)}{(\delta_3(t) + \varepsilon(t))} \frac{\{\beta_3(y_1(t) + y_2(t)) + \psi\}}{\delta_3(t)y_3(t)} x_3(t) < 1. \quad (4.2.8.)$$

From (4.2.6) and (4.2.7), we obtain the following condition,

$$y_1(t) + y_2(t) < \frac{\beta_1 x_1(t)y_3(t)}{(\gamma_1 + \delta_1)} + \frac{\beta_2 x_2(t)y_3(t)}{(\gamma_2 + \delta_2(t))}. \quad (4.2.9.)$$

Substituting (4.2.9) into (4.2.8), we obtain

$$\frac{\varepsilon(t)}{(\delta_3(t) + \varepsilon(t))} \frac{\{\beta_3(y_1(t) + y_2(t)) + \psi\}}{\delta_3(t)(y_1(t) + y_2(t))} x_3(t) \left\{ \frac{\beta_1 x_1(t)}{(\gamma_1 + \delta_1)} + \frac{\beta_2 x_2(t)}{(\gamma_2 + \delta_2(t))} \right\} > 1. \quad (4.2.10.)$$

Since the natural infection rate ψ is small compared to $\beta_2 y_1(t)$, the inequality (4.2.10) can be expressed as,

$$\frac{\beta_3 \varepsilon(t) x_3(t)}{\delta_3(t)(\delta_3(t) + \varepsilon(t))} \left\{ \frac{\beta_1 x_1(t)}{(\gamma_1 + \delta_1)} + \frac{\beta_2 x_2(t)}{(\gamma_2 + \delta_2(t))} \right\} > 1. \quad (4.2.11.)$$

Thus, the basic host-vector model (4.2.1) has the same threshold condition (4.2.11) as the threshold condition of the basic model with a single natural infection (3.2.1).

The equilibrium points of the equations (4.2.1) can be found by setting the derivatives in (4.2.1) to zero. The stability condition can be obtained by examining the eigenvalues of the linearised system near the equilibrium points as in Section 4.1.

4.3. THE GENERAL MODEL FOR THE RRV TRANSMISSION

In this section, the general host-vector model for RRV transmission with heterogeneous mixing populations is considered in the same way as the general model (3.3.1). The only additional assumption is that all mosquito species are exposed to continuous natural infection.

The rate of occurrence of new latent vectors due to the continuous natural infection, which are infected but not infectious, is proportional to the number of vector-susceptibles. Thus, the number of new infections in the vector population in a time Δt is $\psi^m x_k^m(t) \Delta t$, where ψ^m , $i = 1, 2, \dots, l$, is the constant natural infection rate on the m th mosquito species population.

With the given assumptions the general deterministic model for the RRV transmission, which has human and animal hosts and mosquito vectors, is as

in (3.3.1), with $\frac{dx_i^h(t)}{dt}$, $\frac{dy_i^h(t)}{dt}$, $\frac{dz_i^h(t)}{dt}$, $\frac{dx_j^a(t)}{dt}$, $\frac{dy_j^a(t)}{dt}$, $\frac{dz_j^a(t)}{dt}$, and

$\frac{dy_k^m(t)}{dt}$ as before and

$$\begin{cases} \frac{dx_k^m(t)}{dt} = - \left(\sum_{i=1}^l \beta_{ki}^{hm} y_i^h(t) + \sum_{j=1}^m \beta_{kj}^{am} y_j^a(t) \right) x_k^m(t) - (\delta_k^m(t) + \psi^m) x_k^m(t) + \alpha_k^m(t), \\ \frac{de_k^m(t)}{dt} = \left(\sum_{i=1}^l \beta_{ki}^{hm} y_i^h(t) + \sum_{j=1}^m \beta_{kj}^{am} y_j^a(t) \right) x_k^m(t) + \psi^m x_k^m(t) - (\delta_k^m(t) + \varepsilon_k^m(t)) e_k^m(t), \end{cases} \quad (4.3.1.)$$

where, $k = 1, 2, \dots, n$.

The general model (4.3.1) can incorporate the emigration and immigration parameters for the human populations in various ways. For example, the transfer between different age groups can be included in the migration parameters. The groups in the model (4.3.1) can be regarded as heterogeneous mixing populations. The models (4.1.1) in Section 4.1 and (4.2.1) in Section 4.2 are special cases of the general model (4.3.1). In both those models (4.1.1) and (4.2.1), the migration parameters are neglected.

The threshold condition for the general model (4.3.1) without migration for a true outbreak to occur is calculated in a manner similar to Sections 3.3 and 4.1, and can be shown to be :

$$\left(\sum_{k=1}^n \frac{\varepsilon_k^m(t)}{(\delta_k^m(t) + \varepsilon_k^m(t))} \frac{x_k^m(t)}{\rho_k^{mh}(t)} \right) \left(\sum_{i=1}^l \frac{x_i^h(t)}{\rho_i^h(t)} \right) + \left(\sum_{k=1}^n \frac{\varepsilon_k^m(t)}{(\delta_k^m(t) + \varepsilon_k^m(t))} \frac{x_k^m(t)}{\rho_k^{ma}(t)} \right) \left(\sum_{j=1}^m \frac{x_j^a(t)}{\rho_j^a(t)} \right) > 1, \quad (4.3.2.)$$

where

$$\rho_i^h(t) = \frac{(\delta_i^h + \gamma_i^h)}{\beta_i^{hm}}, \rho_j^a(t) = \frac{(\delta_j^a + \gamma_j^a)}{\beta_j^{am}}, \rho_k^{mh}(t) = \frac{\delta_k^m(t)}{\beta_k^{mh}(t)} \text{ and } \rho_k^{ma}(t) = \frac{\delta_k^m(t)}{\beta_k^{ma}(t)},$$

for $i = 1, 2, \dots, l$, $j = 1, 2, \dots, m$ and $k = 1, 2, \dots, n$.

Having completed a detailed analysis of all of our models we now move on to Chapter 5. In Chapter 5, the simulation models and the estimation methods for the parameters used in the simulation models are discussed.

CHAPTER 5.

PARAMETER ESTIMATION FOR THE SIMULATION

As was mentioned in Chapters 3 and 4, many parameter values used in the general models of RRV transmission (3.3.1) and (4.3.1) are unknown. Our present knowledge of the parameters only allows us to use the simple models (3.1.1) and (4.1.1) with one human-host and one mosquito-vector. Even though the animal population is neglected in these models, the influence of the animal interaction on the transmission cycle is incorporated by assuming that the mosquito feeding rate on animals is a fraction of the feeding rate on humans. The regions considered in the simulation are the South Coastal districts of Western Australia since most serologically confirmed cases of the RRV disease have been reported in the south-west of Western Australia. In this thesis, the models are used to simulate two big outbreaks of 1991/92 and 1995/96 in the Peel district and one outbreak of 1995/96 in the Leschenault district in the south-west of Western Australia. The geographical location of the regions is given in Figure 5.1.

In the following sections, the methods used to estimate the parameters appearing in simulation models (3.1.1) and (4.1.1) for RRV transmission are discussed. Section 5.1 introduces the two simulation models, one with a single natural infection in the mosquito population, the other with continuous natural infection. Section 5.2 estimates the parameter values for the human population

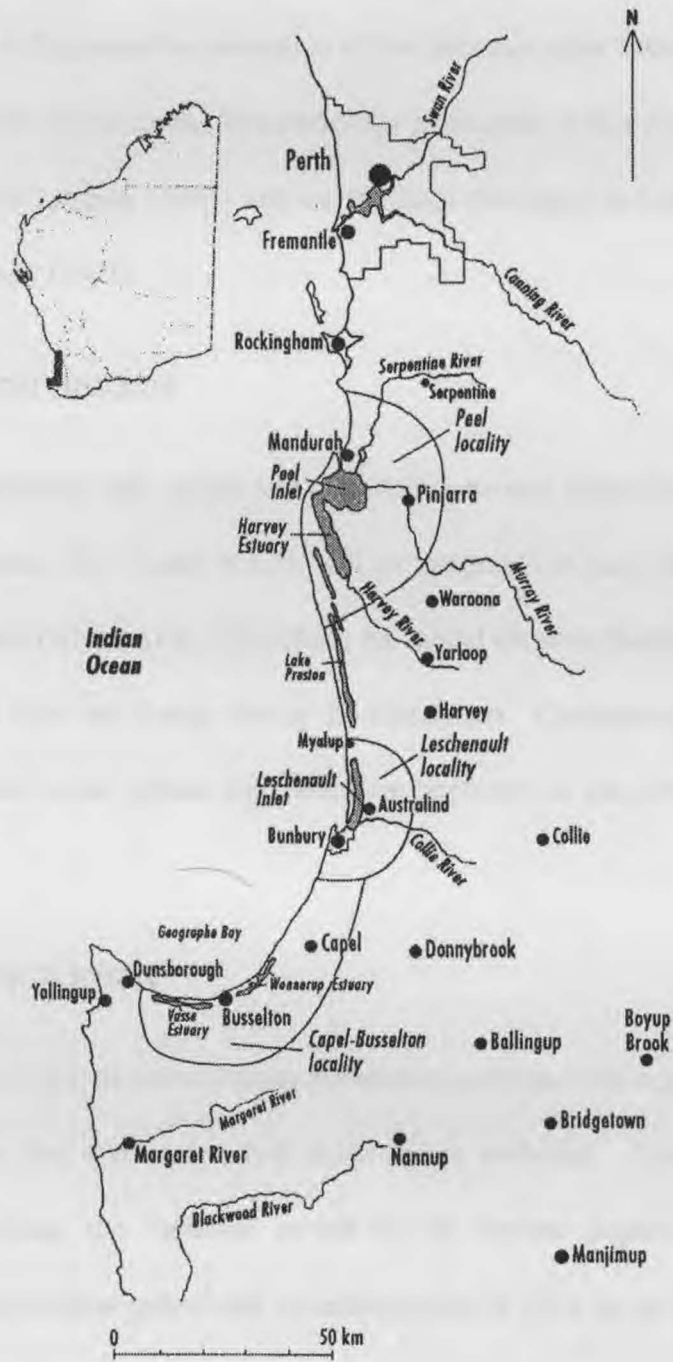


Figure 5.1 Map showing the study areas, south-west of WA, used in this simulation models. Figure provided by Dr Michael Lindsay, Department of Microbiology, The University of WA.

prior to the outbreaks. Section 5.3 introduces the methods used to estimate the parameters relating to the mosquito population during the outbreak. Finally, Section 5.4 discusses the estimation of the infection rates between the human and mosquito populations. The parameter estimation in this chapter is based on data from Lindsay (1995) and on methods discussed in Comiskey (1988) and Comiskey (1991).

5.1. Simulation models

The simulation models with single and continuous natural infection in the mosquito populations, (3.1.1) and (4.1.1), will be integrated at daily intervals for a simulated period of one year. Therefore, the model assumes that the total human population does not change during the simulation. Consequently, the birth and death rates in the human population are neglected in the simulation models.

5.2. HUMAN POPULATION

The initial value of the removed human population indicates the size of the human population that was immunised prior to the outbreak. Later, the method for estimating the viraemia period in the human population is introduced. The incubation period and viraemia period of RRV in the human population overlap during transmission. Since the simulation focuses on the ratio of clinical to subclinical human infections, the incubation period is neglected in the simulation model. The simulation models given in (5.1.1) and (5.1.2) assume that the total human population does not change during the outbreak, hence the size of the total human population is a constant given by,

$$n_i = x_i(t) + y_i(t) + z_i(t).$$

The regions considered in the simulation are the Peel and the Leschenault districts in Western Australia. The Peel district is located between 70 and 130 km south of Perth and extends from the coast to the base of the Darling Scarp approximately 25 km inland. The Peel district has an approximate area of 770km². The Leschenault district is between 165 and 190 km south of Perth, also on the Swan Coastal Plain and extends inland approximately 30 km. The total area of the Leschenault district is 230 km² (Lindsay, 1995). The approximate total human populations in these districts during big outbreaks are listed in Table 5.2.

Table 5.2 The approximate human populations during the outbreaks of 1991/92 and 1995/96 (Lindsay, 1995).

Region \ period	1991-1992	1995-1996
The Peel district	38,049	56,000
The Leschenault district	25,657	35,000

There is currently no information about the prevalence of antibodies to RRV in south-western Australia. Hence, the proportion of immunised humans was extrapolated from work done in regions of eastern Australia with a similar geography to the Peel study district. Furthermore, the chosen area has a similar environmental conditions as the study areas have. Serosurveys prior to a big outbreak of RRV disease in 1988-89 suggested that 25% of the population were sero-positive in the Gippsland region, Victoria (Wolstenholme, 1991). This region has a similar latitude to the south-west region of Western Australia and the major vector mosquito species was thought to be *Aedes (Ochelerotatus) camptorhynchus*. A sero-positive value

(proportion of immunised humans) of 25% prior to the 1995/96 outbreak in the Peel district was therefore assumed for the simulation. Therefore, as an initial condition we set the number of removed hosts equal to this value. The population of humans that are actually viraemic (infectious) was assumed to be initially zero.

Hence, the initial number of susceptibles, infectives and removals in the human population prior to the outbreaks are assumed to be :

$$\text{Human susceptible population} : x_{10} = (1 - 0.25) \times n_1,$$

$$\text{Human infective population} : y_{10} = 0,$$

$$\text{Human removal population} : z_{10} = 0.25 \times n_1.$$

The viraemia period is the length of time the virus persists in the host, that is, the amount of time required for the formation of antibodies. In reality this period is between 1 and 6 days. For simulation purposes we assume that the viraemia period, a_1 , is exactly 4 days. The recovery rate for the human population is taken to be the inverse of the mean viraemia period :

$$\gamma = 1/a_1 = 1/4.$$

5.3. Mosquito population

In this section, the major dominant mosquito species in the study areas are introduced. Then, the methods by which samples of the female mosquito population in the study areas were trapped and the resulting data used to calculate an interpolated daily population are described. Following this, the methods used to estimate the variable mortality rate and the variable

recruitment rate for the mosquito population are discussed. Finally, the method used to estimate the variable extrinsic incubation period is introduced.

As mentioned in Chapter 3, the main vector of the RRV in the south-west of Western Australia is *Aedes camptorhynchus*. In the two areas being simulated, the Peel district and the Leschenault district in Western Australia, *Aedes camptorhynchus* is the major dominant species during big outbreaks. Furthermore, *Aedes vigilax* is the second dominant species and *Culex globocoxitus* is the third dominant species in the Peel and Leschenault areas. The percentage contributions of the major dominant mosquito species in those regions are listed in Table 5.3.

Table 5.3 The percentage contributions of the major dominant mosquitoes in the Peel district and Leschenault district (Lindsay, 1995).

Region \ mosquito species	<i>Aedes camptorhynchus</i>	<i>Aedes vigilax</i>	<i>Culex globocoxitus</i>
The Peel district	73.4 %	11.2 %	3.1 %
The Leschenault district	60 %	17 %	5.4 %

Since *Aedes camptorhynchus* is the major dominant mosquito species in the two districts, the *Aedes camptorhynchus* species will be used for the simulation.

The total vector population $n_2(t)$ can be determined by trapping samples of the female *Aedes camptorhynchus* population. Several non-overlapping circular sites (each of 50 m radius) were chosen within the case study area. Once or twice per month *Aedes camptorhynchus* were trapped at each site over the course of a single day. This irregular data is then used to estimate the

daily number of *Aedes camptorhynchus* trapped per site. From these values, we then determined the daily average number of *Aedes camptorhynchus*, $n_d(t)$, trapped per site. Given that we know the size of the case study area we can determine the number of traps, wt , required to cover this area. Thus we can now estimate the number of *Aedes camptorhynchus* that would be caught if we were to trap over the entire case study area, viz. $n_d(t) \times wt$.

By using the Natural Cubic Spline method, we can interpolate the monthly data to give a daily estimate of the *Aedes camptorhynchus* population. There is a problem that the interpolated data can predict a negative population. To avoid this, we let the negative population to be zero.

To determine the mosquito mortality rate, $\tilde{\delta}_2(t)$, the *Aedes camptorhynchus* life expectancy will be used. The *Aedes camptorhynchus* mortality rate, $\tilde{\delta}_2(t)$, varies between $1/56$ and $1/5$, based on the fact that the minimum mosquito life expectancy is 5 days in summer and the maximum is 56 days in winter. Mortality rates for *Aedes camptorhynchus* were extrapolated from studies of *Aedes aegypti* and *Aedes taeniorhynchus* (Turell, 1990). Using a cosine function we can construct a smoothed estimate for the mortality rate function

$$\tilde{\delta}_2(t) = \frac{1}{2} \left(\frac{1}{5} + \frac{1}{56} \right) - \frac{1}{2} \left(\frac{1}{5} - \frac{1}{56} \right) \cos \left(\frac{2\pi t}{T} \right),$$

where T is a total simulation period.

The basic mortality rate curve obtained here will be used for the whole simulation. After calculating the recruitment rate, the mortality rate for each simulation will be modified to account for environmental effects.

The models (3.1.1) and (4.1.1) include only the adult female *Aedes camptorhynchus* population since only female mosquitoes consume blood meals from hosts. Therefore, the variable recruitment rate for the new adult female *Aedes camptorhynchus* is not proportional to the *Aedes camptorhynchus* population during the simulation. The recruitment rate during the outbreak is calculated by using the simple differential equation :

$$\frac{dn_2(t)}{dt} = \tilde{\alpha}_2(t) - \tilde{\delta}_2(t)n_2(t), \quad (5.3.1)$$

where $n_2(t)$ is the daily interpolated average number of *Aedes camptorhynchus* trapped per site (i.e. $n_a(t)$) and $\tilde{\alpha}_2(t)$ is the recruitment rate.

Since the recruitment rate must be positive, if the recruitment rate implied by equation (5.3.1) is negative then we assume that there was some environmental changes which resulted in additional deaths in the vector population. Hence, we subtract the negative recruitment rate from the basic mortality rate. So, whenever the recruitment rate, $\tilde{\alpha}_2(t)$, is negative we modify the mortality rate, $\tilde{\delta}_2(t)$ by choosing :

$$\tilde{\delta}_{2\text{mod}}(t) = \tilde{\delta}_2(t) + \tilde{\alpha}_2(t) / n_2(t) \text{ so that } \tilde{\alpha}_2(t) = 0.$$

Therefore, we have both a positive mortality rate and a reasonable recruitment rate. Since we use the real *Aedes camptorhynchus* population, the mortality rate and recruitment rate will contain environmental factors which are not at the moment understood.

The extrinsic incubation period of *Aedes camptorhynchus*, a_2 , varies according to the temperature and humidity. The period is less than 3 days in summer and 3 weeks in winter. The parameter values for the extrinsic

incubation periods of the *Aedes camptorhynchus* population were extrapolated from studies of another alphavirus (Rift Valley fever virus) and *Aedes taeniorhynchus* (Turell, 1985).

Hence, the extrinsic incubation period will be modelled as a cosine curve :

$$a_2(t) = \frac{1}{2}(21 + 3) - \frac{1}{2}(21 - 3)\cos\left(\frac{2\pi t}{T}\right), \text{ where } T \text{ is the period of oscillation.}$$

The simulation assumes that the smoothed extrinsic incubation period is periodic with period of one year. In the simulation, the date of the maximum life expectancy and extrinsic incubation period of *Aedes camptorhynchus* is assumed to be the first of July. As an initial condition for the *Aedes camptorhynchus* population, the susceptible population can be found by subtracting the initial infective population from the initial value of the total population. The removal population is equal to zero since the *Aedes camptorhynchus* life cycle is short and there is no immunity in the *Aedes camptorhynchus* population. There has been no reported literature on studies of natural infection in *Aedes camptorhynchus*. This simulation assumes that prior to the outbreak the minimum proportion of infected *Aedes camptorhynchus* is $1/15,617$ which is the minimum proportion of the RRV isolation among *Aedes camptorhynchus* (Lindsay, 1995). The simulation model (5.1.2) assumes that the natural infection rate in the *Aedes camptorhynchus* population is $1/15,617 \times 30$. Here it is assumed that it takes 30 days to reach the minimum infection rate during an outbreak.

Hence, the initial numbers of the susceptible, infective and removal groups in the mosquito population are :

- Vector susceptible population : $x_{20} = n_{20} - y_{20}$,
- Vector latent population : $e_0 = 0$,
- Vector infective population : $y_{20} = (1/15,617) \times n_{20}$,
- and Vector removal population : $z_{20} = 0$.

5.4. Infection rates β_1, β_2

Most mathematical simulations choose the infection rate as the probability of transmission of the disease. In the RRV simulation, the infection rate is determined by the *Aedes camptorhynchus* feeding preference, transmission rate, and the VIR rate. The transmission rate is the chance that one *Aedes camptorhynchus* bite causes the transmission of the RRV. Among all hosts the *Aedes camptorhynchus* has a biting preference for humans. The preference is, also, used to include the other hosts in the transmission cycle. As the populations of other hosts are unknown, by using the inverse of the human feeding rate and multiplying by the infected human population other hosts will be included. Here, the simulation assumes that there are (1 / human feeding rate) times more infectives including animal infectives than human infectives.

The simulation model includes two further assumptions :

1. It is likely that only a proportion of infected humans can pass the virus on to mosquito vectors. This proportion is not known. Therefore, the simulation assumes that only 50 per cent of the infective humans can pass the virus on to mosquito vectors. This is referred to as the VIR rate in the simulation.

2. The human population is distributed in only 60 percent of the study region where *Aedes camptorhynchus* can bite the human population. This is referred to as the distribution rate in the simulation.

The infection rate from the vector to host can be calculated as :

$$\beta_1 = \frac{\text{Human feeding rate} \times \text{Distribution rate} \times \text{Transmission rate}}{\text{Total human population}}$$

Entomological studies from various parts of Australia indicate that human feeding by *Aedes camptorhynchus* is usually no greater than 5 per cent (0.05) (Kay *et al.*, 1987). The simulation will examine the sensitivity of the model to the vector-host transmission rate which will be varied from 0.25 to 0.75. These values have been used for Murray Valley encephalitis (Kay *et al.*, 1987).

The infection rate from the host to the vector can be obtained by multiplying the human feeding rate, VIR rate, and transmission rate, and dividing by the total human population as :

$$\beta_2 = \frac{\text{VIR rate} \times \text{Distribution rate} \times \text{Transmission rate}}{\text{Human feeding rate} \times \text{Total } Ae. \text{ camptorhynchus population at the time } t}$$

The simulation will also examine the sensitivity of the model to the host-vector transmission rate which will be varied from 0.25 to 0.75 in steps of 0.05.

Having discussed the parameter estimation we now move on to Chapter 6 where the simulation results are described for two outbreaks in the Peel district and one outbreak in the Leschenault district in Southwestern Australia.

CHAPTER 6.

SIMULATION RESULTS

As mentioned in the previous chapters, the RRV transmission models are divided into two types according to whether the natural infection in the *Aedes camptorhynchus* population is single or continuous. The simulations of RRV transmission presented in this chapter consider two big outbreaks in the Peel district and one outbreak in the Leschenault district in Southwestern Australia.

Section 6.1 presents simulation results using a variety of methods suitable for determining the spread of the disease. Section 6.1 is based on the outbreak of 1991/92 in the Peel district. Sections 6.2 and 6.3 describe the simulation results for the outbreak of 1995/96 in the Peel and Leschenault districts. Finally, Section 6.4 presents a discussion of the ecological implications of the simulation results. The algorithms for the simulation were written by the author using computer programs written in the C language.

6.1. SIMULATION RESULTS FOR THE 1991/92 OUTBREAK IN THE PEEL DISTRICT

The Peel district is located between 70 and 130 km south of Perth and extends from the coast to the base of Darling Scarp approximately 25 km inland. The study area is defined according to mosquito breeding sites by Lindsay (1995). The total area of the Peel district is approximately 770 km².

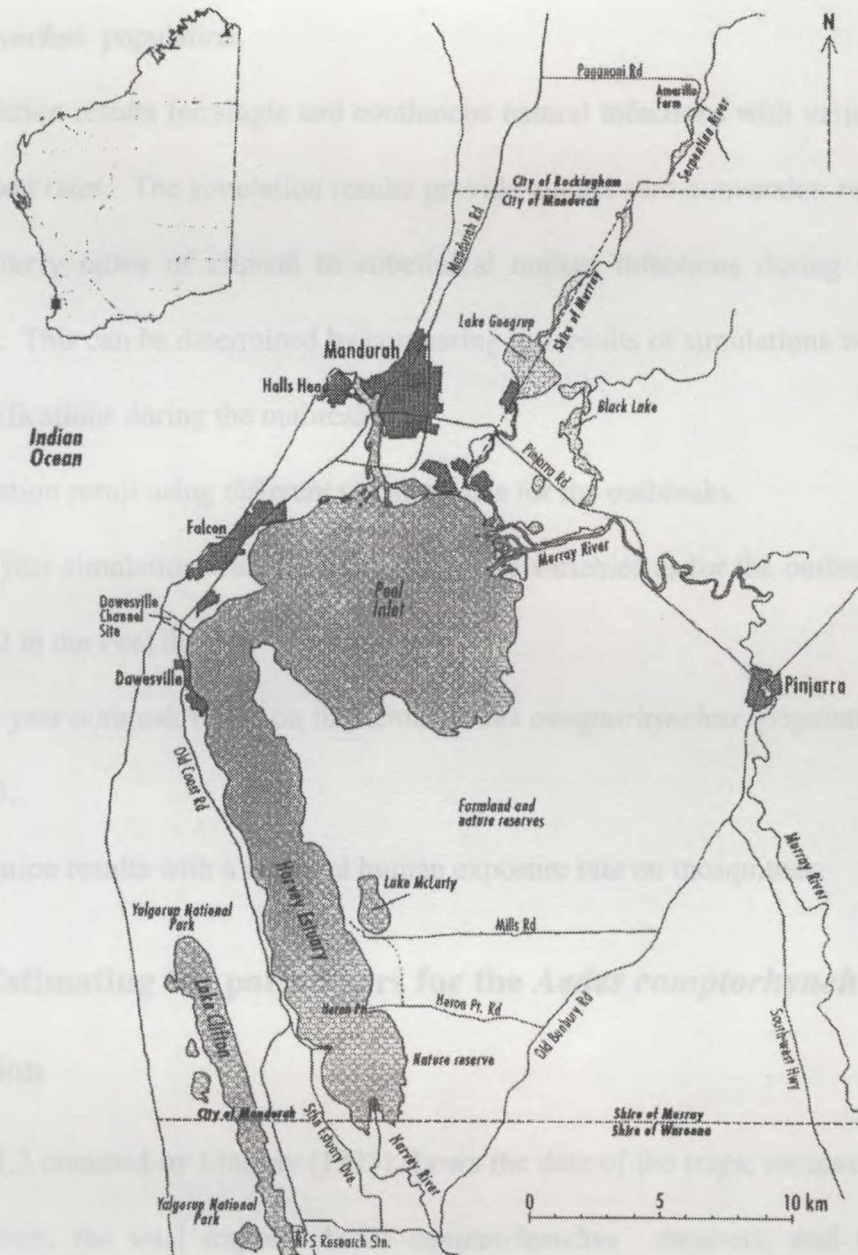


Figure 6.1.1 Map showing the Peel district, south-west of WA. Figure provided by Dr Michael Lindsay, Department of Microbiology, The University of Western Australia.

The simulation results in this section include the following :

1. Interpolated daily *Aedes camptorhynchus* population.

2. Recruitment and mortality rates and extrinsic incubation period of the *Aedes camptorhynchus* population.
3. Simulation results for single and continuous natural infections with various transmission rates. The simulation results provide annual sero-conversion rates and the likely ratios of clinical to subclinical human infections during the outbreaks. This can be determined by comparing the results of simulations with actual notifications during the outbreaks.
4. Simulation result using different starting dates for the outbreaks.
5. A ten year simulation with the same parameter variables as for the outbreak of 1991/92 in the Peel district.
6. A two year outbreak based on the actual *Aedes camptorhynchus* population in 1991/93.
7. Simulation results with a seasonal human exposure rate on mosquitoes.

6.1.1. Estimating the parameters for the *Aedes camptorhynchus* population

Table 6.1.2 obtained by Lindsay (1995) shows the date of the traps, successful trap numbers, the total trapped *Aedes camptorhynchus* numbers, and the average number of trapped *Aedes camptorhynchus* per trap in the Peel district during 1991/92. Since the trapped *Aedes camptorhynchus* population is fortnightly data, the daily *Aedes camptorhynchus* population can be estimated by a suitable numerical method. The interpolated daily *Aedes camptorhynchus* population in the Peel district during 1991/92, which was obtained by applying the Natural Cubic Spline interpolation method to the data for the trapped *Aedes camptorhynchus* population, is shown in Figure 6.1.3.

Table 6.1.2 The date of the traps, successful trap numbers, the total trapped *Aedes camptorhynchus* numbers from successful traps, and the mean number of trapped *Aedes camptorhynchus* per trap in the Peel district during 1991/92 (Lindsay, 1995).

Date	traps	Sum (from traps) <i>Aedes camptorhynchus</i>	Mean <i>Aedes camptorhynchus</i>
4-Jul-91	9	7404	822.67
6-Aug-91	9	4245	471.67
28-Aug-91	10	21352	2135.20
17-Sep-91	9	7141	793.44
3-Oct-91	9	2924	324.89
16-Oct-91	7	7592	1084.57
4-Nov-91	2	1823	911.50
7-Nov-91	11	2240	203.64
19-Nov-91	6	2298	383.00
9-Dec-91	9	690	76.67
17-Dec-91	7	107	15.29
3-Jan-92	8	481	60.13
20-Jan-92	8	5	0.63
29-Jan-92	2	1	0.50
30-Jan-92	6	0	0.00
20-Feb-92	9	1319	146.56
26-Feb-92	10	1898	189.80
4-Mar-92	9	327	36.33
25-Mar-92	8	21	2.63
1-Apr-92	8	44	5.50
23-Apr-92	9	446	49.56
27-May-92	7	939	134.14
24-Jun-92	7	339	48.43
29-Jul-92	5	1965	393.00
10-Sep-92	9	3940	437.78
12-Oct-92	11	5317	483.36

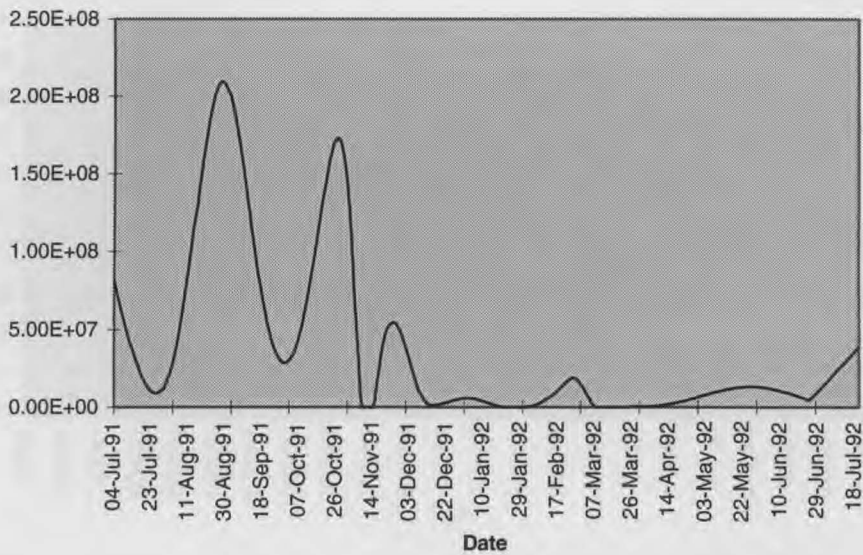


Figure 6.1.3 Interpolated daily *Aedes camptorhynchus* population during the outbreak of 1991/92 in the Peel District

The basic daily mortality rate is assumed to be a normalised cosine curve which has a minimum of $1/56$ and a maximum of $1/5$ based on the *Aedes camptorhynchus* life expectancy of 5 days in summer and 8 weeks in winter. The daily recruitment rate is obtained by inserting the daily interpolated *Aedes camptorhynchus* population and the basic mortality rate into a simple population dynamics model. The recruitment rate can not have negative values, hence, if the recruitment rate obtained from the population dynamics is negative then the negative part is subtracted from the basic mortality rate as explained in Chapter 5.

The modified daily mortality and recruitment rates are displayed in Figures 6.1.4 and 6.1.5.

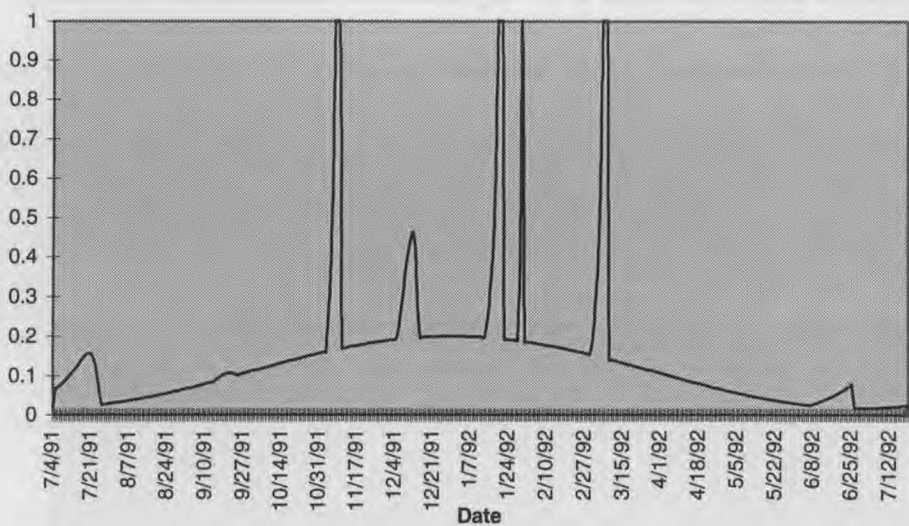


Figure 6.1.4 Modified daily mortality rate during the outbreak of 1991/92 in the Peel District.

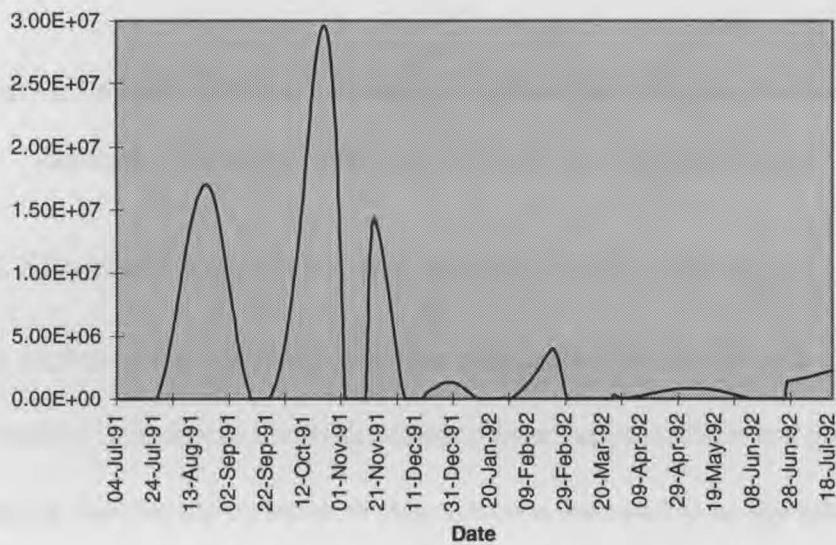


Figure 6.1.5 Modified daily recruitment rate during the outbreak of 1991/92 in the Peel District.

In Figure 6.1.6, the extrinsic incubation period is assumed to be a cosine curve which has a minimum of 3 days in summer and a maximum of 21 days in winter.

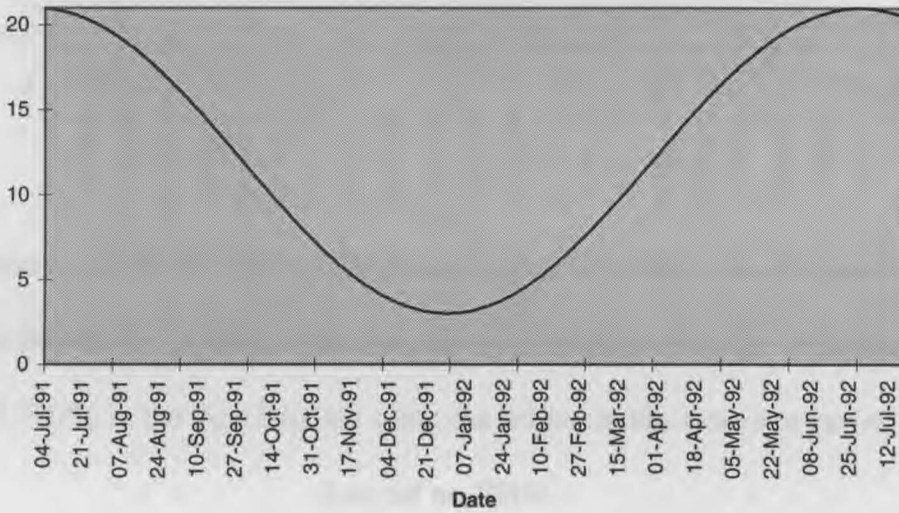


Figure 6.1.6 Daily extrinsic incubation period of the *Aedes camptorhynchus* population during the outbreak of 1991/92 in the Peel District.

6.1.2. Simulation result for the models (3.1.1) and (4.1.1)

In this section, the simulation results for the models (3.1.1) and (4.1.1) with a single natural infection in the *Aedes camptorhynchus* population are presented. The starting date for the outbreak in this section is assumed to be the 4th of July 1991. The simulation results in Figures 6.1.7, 6.1.8 and 6.1.9 for the model (3.1.1) show the daily changes of the susceptible and the infectious human populations and infectious *Aedes camptorhynchus* population in the Peel district in 1991/92. The results are based on transmission rates varying from 25 % to 75 % with 5 % increments.

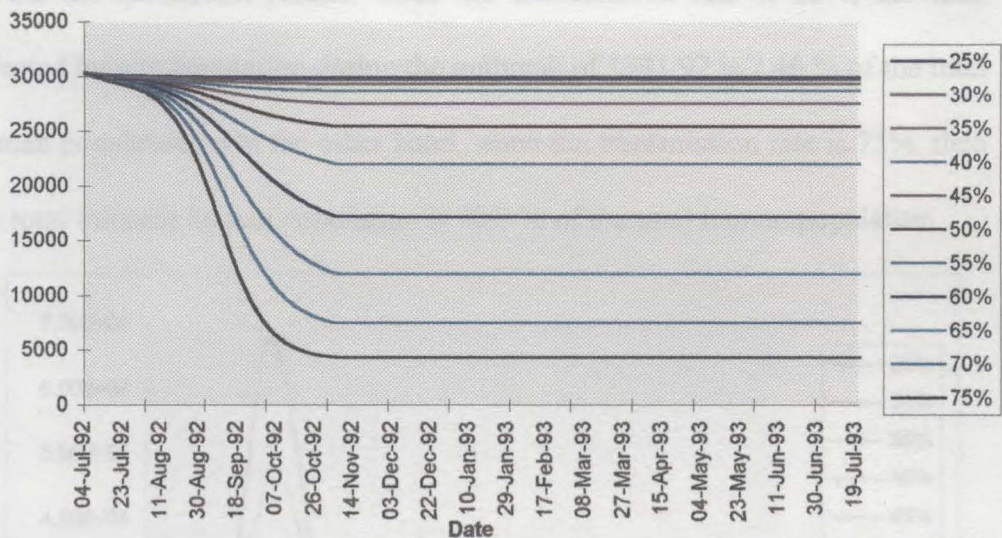


Figure 6.1.7 Daily susceptible human population with a single natural infection in the *Aedes camptorhynchus* population during the outbreak of 1991/92 in the Peel District when the transmission rates are varied (Legend on RHS).

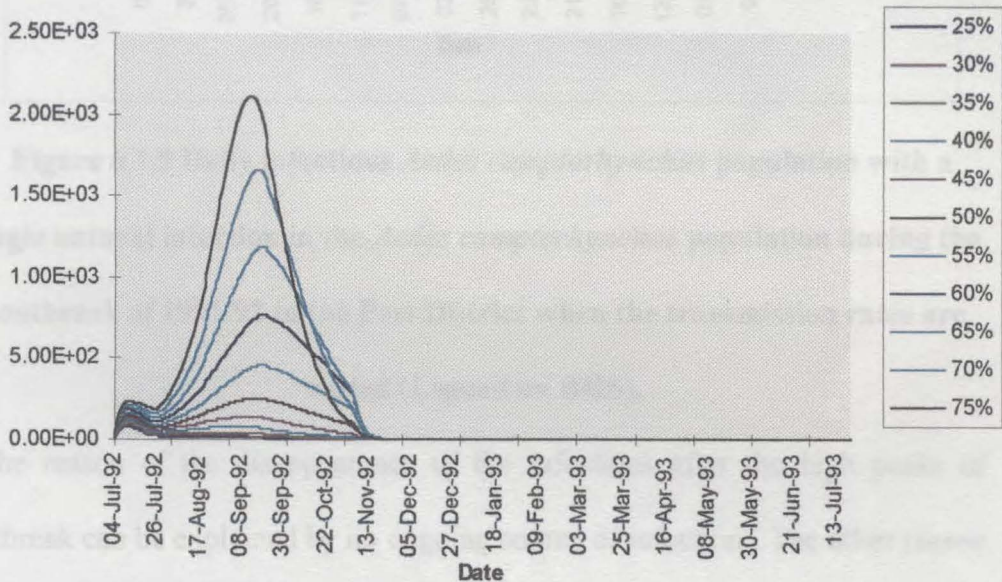


Figure 6.1.8 Daily infectious human population with a single natural infection in the *Aedes camptorhynchus* population during the outbreak of 1991/92 in the Peel District when the transmission rates are varied (Legend on RHS).

From the simulation results, when the transmission rate is 25%, the total infected human population during the outbreak of 1991/92 is 2.46 % of the total human population. On the other hand, when the transmission rate is 75%, then the total infected human population is 70.9 % of the total human population.

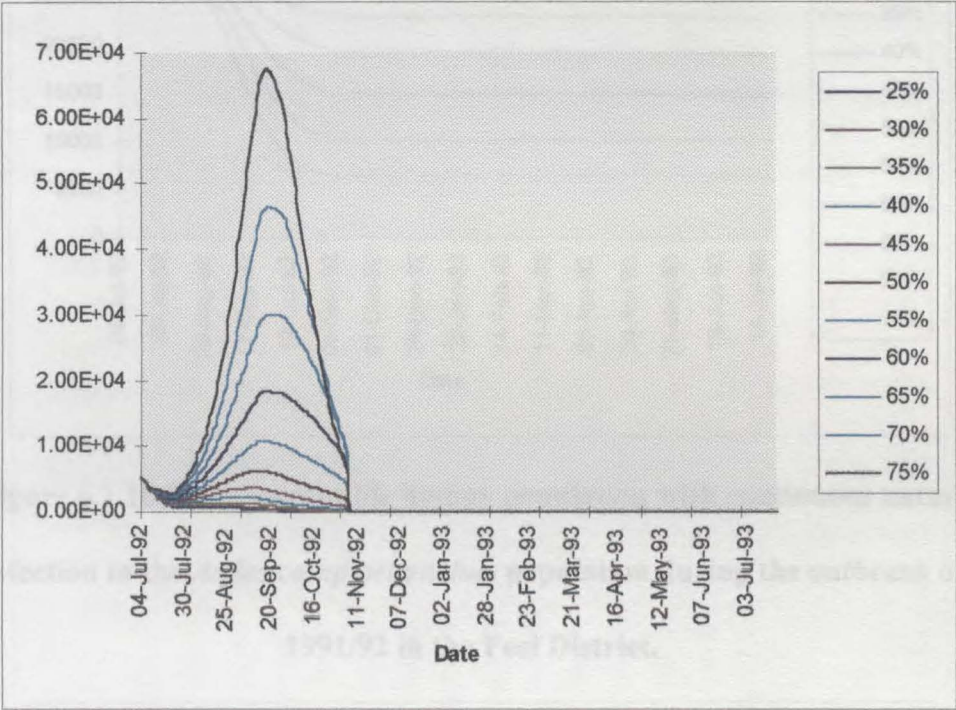


Figure 6.1.9 Daily infectious *Aedes camptorhynchus* population with a single natural infection in the *Aedes camptorhynchus* population during the outbreak of 1991/92 in the Peel District when the transmission rates are varied (Legend on RHS).

The reason of the disappearance of the infections after the high peaks of outbreak can be explained by no ongoing source of infection. The other reason of this is that the vector population after the peak of the outbreak is very small compared with the earlier population as shown in Figure 6.1.3. The simulation results below in Figures 6.1.10, 6.1.11 and 6.1.12 for the model with continuous natural infection in the mosquito population (4.1.1) show the daily changes in the susceptible and infectious human populations and infectious *Aedes*

camptorhynchus population in the Peel district in 1991/92. The results are based on transmission rates varying from 25 % to 75 % with a 5 % increment.

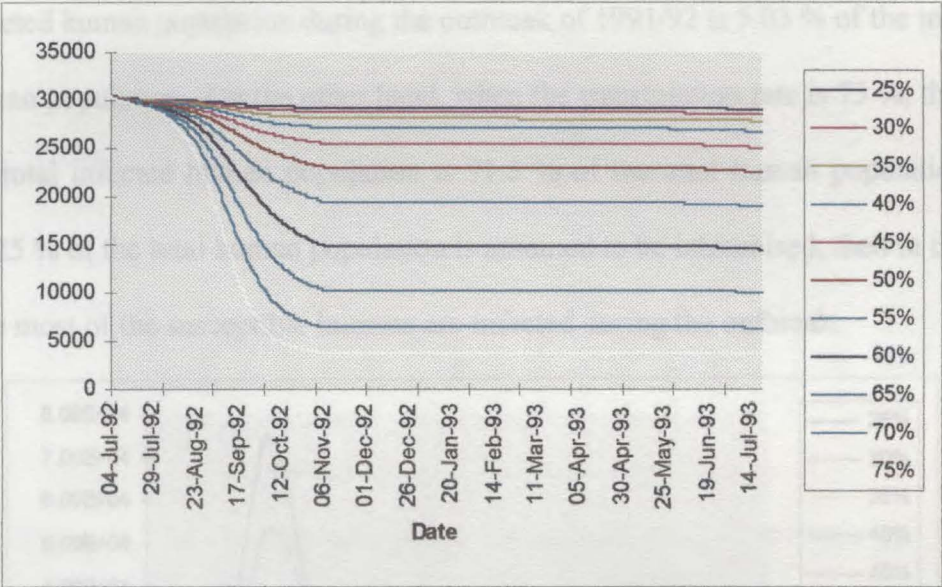


Figure 6.1.10 Daily susceptible human population with continuous natural infection in the *Aedes camptorhynchus* population during the outbreak of 1991/92 in the Peel District.

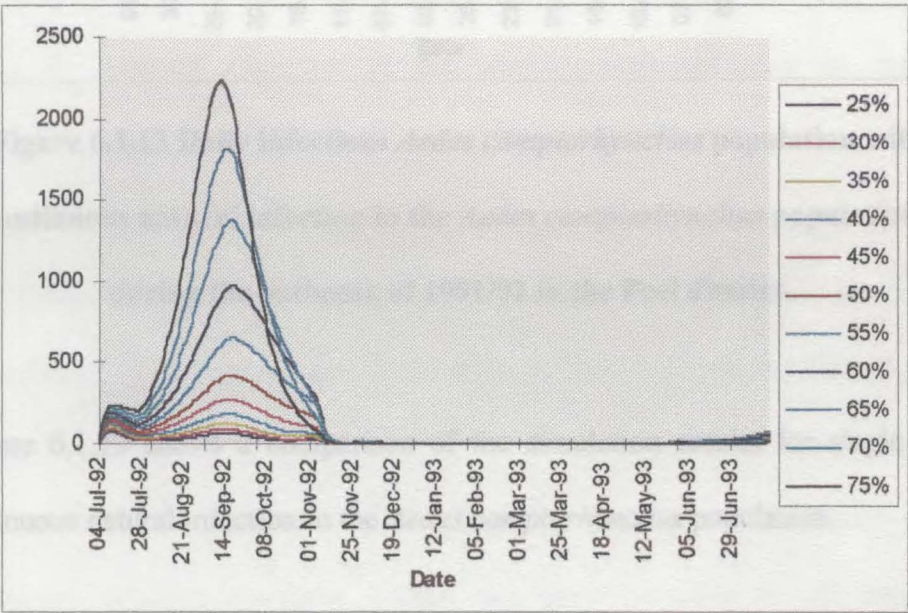


Figure 6.1.11 Daily infectious human population with continuous natural infection in the *Aedes camptorhynchus* population during the outbreak of 1991/92 in The Peel District.

From the simulation results, when the transmission rate is 25 %, the total infected human population during the outbreak of 1991/92 is 5.03 % of the total human population. On the other hand, when the transmission rate is 75 %, then the total infected human population is 71.5 % of the total human population. As 25 % of the total human population is assumed to be immunised, then in this case most of the susceptible humans are infected during the outbreak.

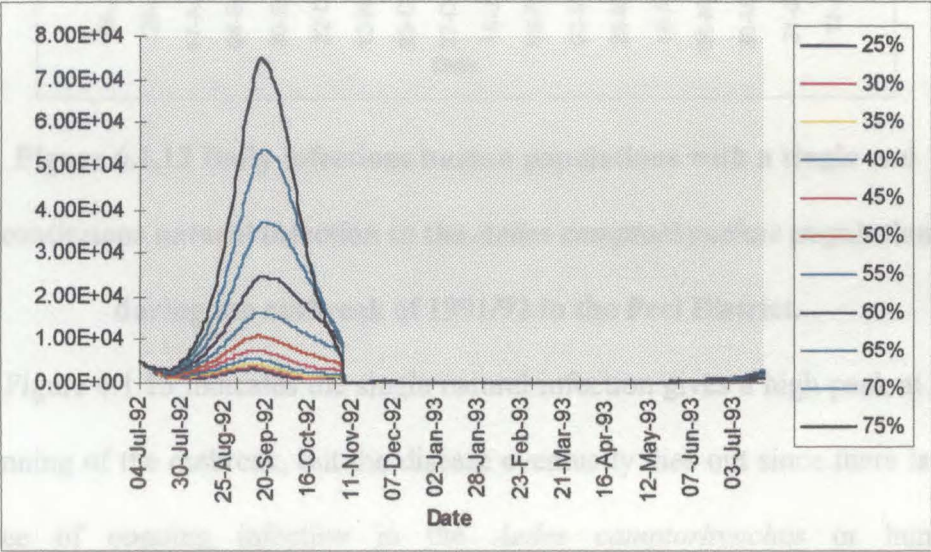


Figure 6.1.12 Daily infectious *Aedes camptorhynchus* population with continuous natural infection in the *Aedes camptorhynchus* population during the outbreak of 1991/92 in the Peel district.

Figure 6.1.13 shows a comparison of the simulation results for single and continuous natural infection in the *Aedes camptorhynchus* population.

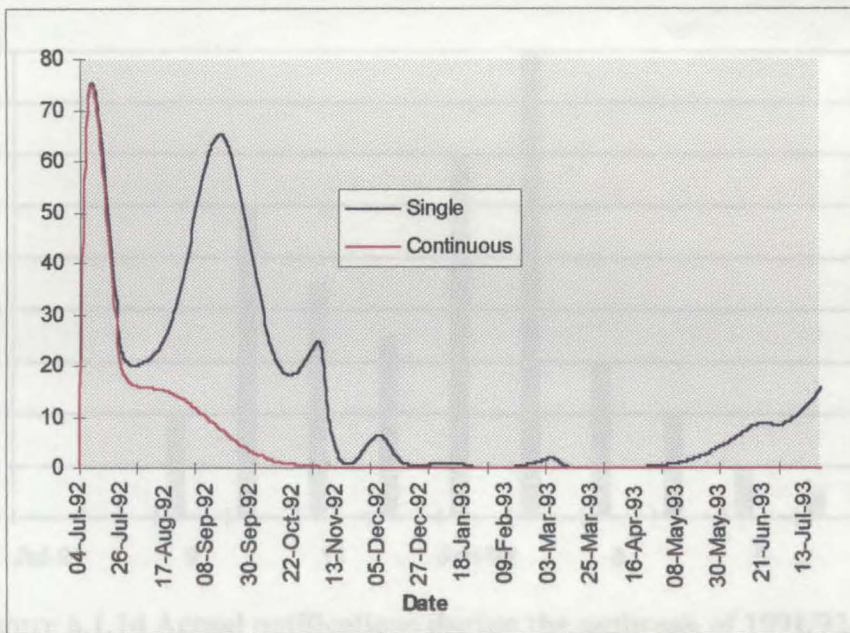


Figure 6.1.13 Daily infectious human populations with a single and continuous natural infection in the *Aedes camptorhynchus* population during the outbreak of 1991/92 in the Peel District.

As Figure 6.1.13 indicates the single natural infection gives a high peak at the beginning of the outbreak, but the disease eventually dies out since there is no source of ongoing infection in the *Aedes camptorhynchus* or human populations. On the other hand, Figure 6.1.13 indicates that continuous natural infection allows the disease to persist in the host and vector populations.

The following Figure 6.1.14 shows the actual number of notifications during the outbreak. The reported incidence of Ross River virus in the Peel district during the outbreak of 1991/92 was 77. A database has been constructed to record the incidence, timing and place of exposure of cases of Ross River virus disease in Western Australia. Data has been provided by all medical practitioners throughout the south-west of Western Australia who were registered with the Medical Board of Western Australia on the 29th July 1986.

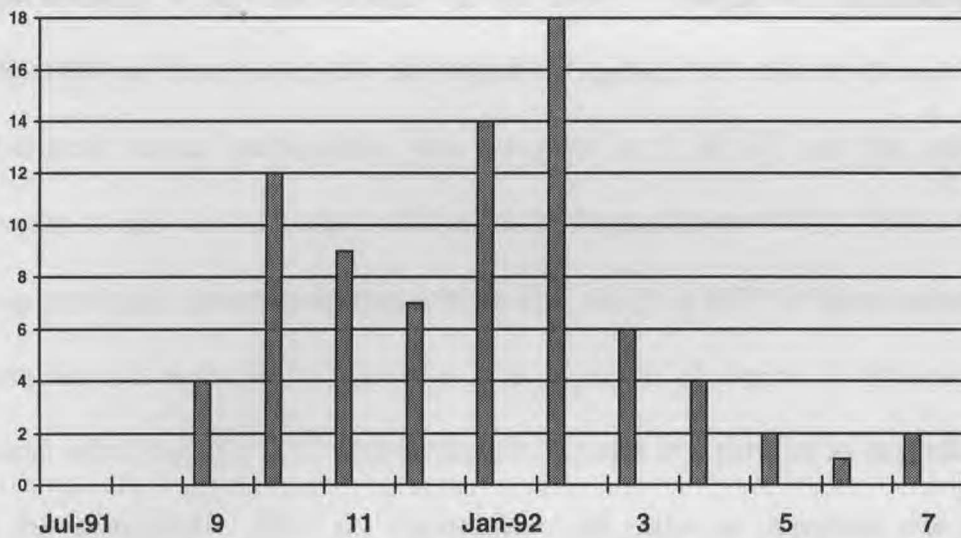


Figure 6.1.14 Actual notifications during the outbreak of 1991/92 in the Peel District

The simulation results with transmission rates varied and a single natural infection predict a minimum of 475 people (about 1.17 % of the total human population) with 25% transmission rate and a maximum of 26,021 people (about 64.2 % of the total human population) with 75% transmission rate were infected. The result suggests that the ratio of clinical to subclinical human cases during the outbreak was 1 clinical case to between 6 and 337 subclinical human infections since there were only 77 clinical notifications. On the other hand, the simulation results with continuous natural infection predict that between 1,375 (with 25% transmission rate) and 26,669 (with 75% transmission rate) people were infected (about 3 ~ 66 % of the total human population). In this case, the likely ratios of clinical to subclinical human cases during the outbreak were 1 : 17 ~ 346. During the major outbreak of 1983/1984 in the Griffith region of New South Wales, most RRV infections were thought to have resulted in illness (Hawkes et al., 1985). In Queensland, the annual ratio of clinical to subclinical cases has been estimated as 1 to 80 and the annual seroconversion rate is

approximately 4 per cent (Asakov et al., 1981). During the outbreak of 1988/1989 in Victoria (mostly the Gippsland region), the ratio of clinical to subclinical human notifications was estimated at 1 to 3.3 and the seroconversion rate was estimated at 0.4 per cent (Wolstenholme, 1991). Based on these previously determined ratios and the endemicity of RRV in Southwestern Australia, it is plausible to expect the minimum ratio of clinical to subclinical human infections of 1 : 17 and a seroconversion rate of 3 per cent as suggested by this simulation. Since the transmission rate plays an important role of predicting the ratios of clinical to subclinical human infections and the seroconversion rates, the transmission rate should be obtained to get more realistic results.

Since the RRV disease is endemic in Western Australia, continuous natural infection in the *Aedes camptorhynchus* population is a more reasonable explanation of the transmission cycle. There could be a question on the persistence of the virus during winter since this simulation treats *Aedes camptorhynchus* as the only mosquito species. However, there is no evidence to prove that Ross River virus persists in another mosquito species during winter. The time difference between the simulation results and the actual notifications could be explained by the reason that it takes some time for the *Aedes camptorhynchus* to reach the human residential area. Also, the starting date of the outbreak could be later than assumed. The following section presents results of simulations using different starting dates for the outbreak.

6.1.3. Simulation results using different starting dates for the outbreak

There has been no research undertaken on the environmental infection causes of RRV in the *Aedes camptorhynchus* population. Even when environmental infection takes place is not known. Here, the simulation examines different starting dates for the outbreak and compares the results with those obtained when starting in mid-winter. Since the RRV disease is endemic in the study area and the host-vector model with continuous natural infection provides a more plausible mechanism for the outbreak, the simulation model (4.1.1) is used in this section. To inspect the trend of the epidemic curves, the transmission rate is assumed to be 25 % through the simulations in this section. Since the onset of the outbreak is currently not known, this section presents results of simulations of the 1991/92 outbreak in the Peel district with four other starting dates : 6th and 28th August, 17th September, and 3rd of October, 1991.

The following Figures 6.1.15 and 6.1.16 present the infectious human population and infectious *Aedes camptorhynchus* populations during the outbreak of 1991/92 in the Peel region with the five starting dates of 4th July, 6th and 28th August, 17th September, and 3rd October, 1991.

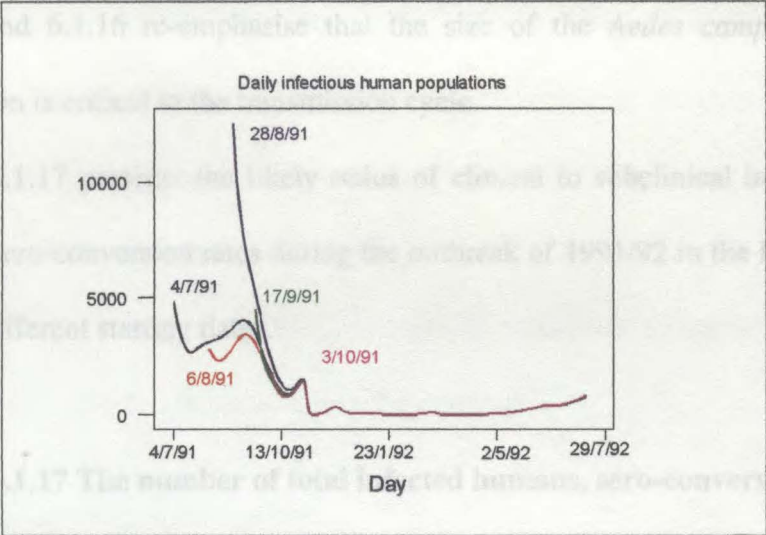


Figure 6.1.15 Daily infectious human populations during the outbreak of 1991/92 in the Peel district using different starting dates for the outbreak.

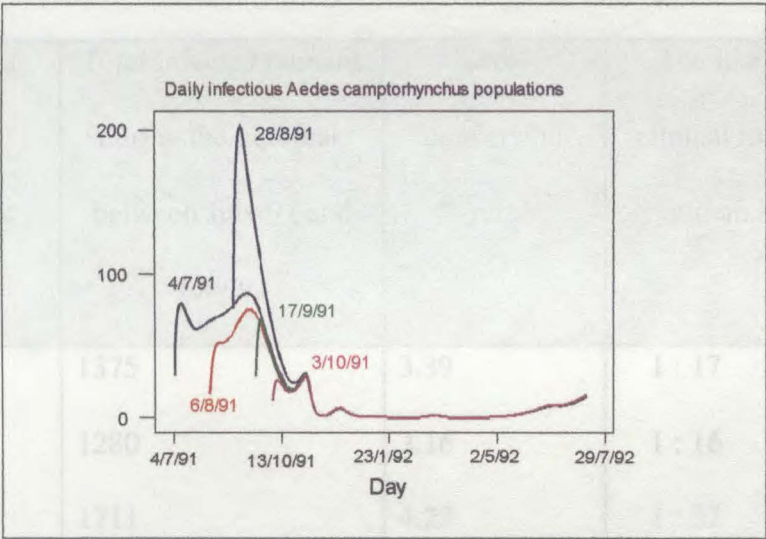


Figure 6.1.16 Daily infectious *Aedes camptorhynchus* population during the outbreak of 1991/92 in the Peel district using different starting dates for the outbreak.

Figures 6.1.15 and 6.1.16 show surprising peaks when the starting date is 28/8/91. Since the initial condition for the infective *Aedes camptorhynchus* population is proportional to the total *Aedes camptorhynchus* population at the time, the large size of the trapped *Aedes camptorhynchus* population on August 28th in Table 6.1.2, 2135, caused the peaks. Hence, the results of Figures

6.1.15 and 6.1.16 re-emphasise that the size of the *Aedes camptorhynchus* population is critical to the transmission cycle.

Table 6.1.17 presents the likely ratios of clinical to subclinical human cases and the sero-conversion rates during the outbreak of 1991/92 in the Peel district for the different starting dates.

Table 6.1.17 The number of total infected humans, sero-conversion rates, and the likely ratios of clinical to subclinical human infections during the outbreak of 1991/92 in the Peel district according to the starting date of the outbreak.

Starting date of the outbreak	Total infected humans during the outbreak between July/91 and July/92	Sero- conversion rate	The likely ratio of clinical to subclinical human infections
4/7/91	1375	3.39	1 : 17
6/8/91	1280	3.16	1 : 16
28/8/91	1711	4.22	1 : 22
17/9/91	641	1.6	1 : 8
3/10/91	390	0.96	1 : 5

Results with later starting dates of the outbreak were expected to yield fewer human infections after the outbreak since the reduction is caused by the shorter outbreak period and the mosquito population on the starting date. However, the more vector population at the beginning of the outbreak caused more human infections. For example, the total infected humans of 1,280 from the result with

the starting date, 6/8/91, is less than 1,711 infected humans from the result with the starting date, 28/8/1991. The mosquito population at the starting dates of the outbreak on 6th and 28th of August, 1991, are 37,129,066 and 167,946,096 and the infectious mosquitoes assumed in the simulation are 2,377 and 10,754, respectively. Consequently, the larger initial infectious mosquito population yielded more infected humans during the outbreak.

6.1.4. Ten year simulation

In this section, simulation results are presented for a ten year outbreak based on the outbreak of 1991/92 in the Peel district are given.

The simulation is based on the following assumptions :

1. The human population does not change during the entire outbreak.
2. All of the parameters for the *Aedes camptorhynchus* population are obtained from the one year outbreak of 1991/92 in the Peel district. The changes in the *Aedes camptorhynchus* population each year are assumed to be the same as in the previous year.

Figures 6.1.18 and 6.1.19 show the changes in the infectious human and *Aedes camptorhynchus* populations during the ten year outbreak.

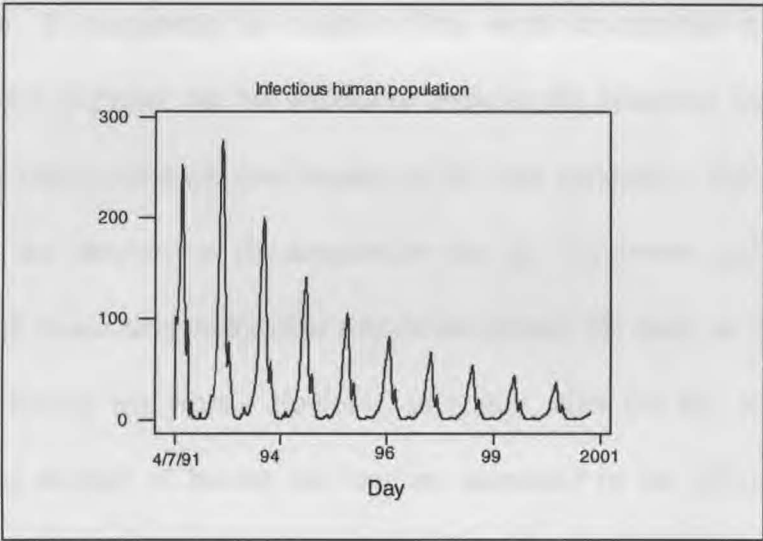


Figure 6.1.18 Daily infectious human population during the ten year outbreak based on the outbreak of 1991/92 in the Peel district.

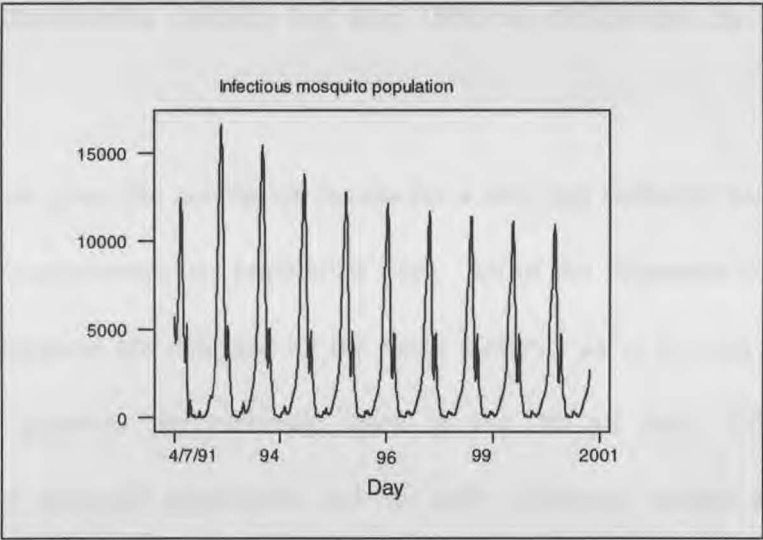


Figure 6.1.19 Daily infectious *Aedes camptorhynchus* population during the ten year outbreak based on the outbreak of 1991/92 in the Peel district.

As observed in Figures 6.1.18 and 6.1.19, more infections occurred in the second outbreak because the first outbreak started later in the yearly cycle. The decline in the vector infections is not as rapid as the decline in the human infections because the birth rate in the human population is assumed to be zero while the susceptible vector population is continually being renewed by

recruitment. Consequently, the number of the vector susceptibles remains the same for each outbreak, but the interaction between the infectious humans and susceptible vectors becomes less frequent in the later outbreaks. Figures 6.1.18 and 6.1.19 are obtained on the assumption that the recruitment and mortality rates for the *Aedes camptorhynchus* population remain the same as in 1991/92 for the following ten years. However, in reality, after the big outbreak of 1991/92 the number of human notifications decreased in the following year. The results of the ten year simulation indicate that if the *Aedes camptorhynchus* population is seasonal, then the outbreak will also be seasonal.

6.1.5. Simulation results for the 1991/93 outbreak in the Peel district

This section gives the simulation results for a two year outbreak based on the real *Aedes camptorhynchus* population data. All of the parameter estimations for the simulation are obtained by the same methods as in Section 6.1. The simulation assumes the outbreak starts at the 4th of July, 1991. The interpolated mosquito population and the daily infectious human and *Aedes camptorhynchus* populations for the outbreak of 1991/93 in the Peel district are presented in Figures 6.1.20, 6.1.21 and 6.1.22, respectively.

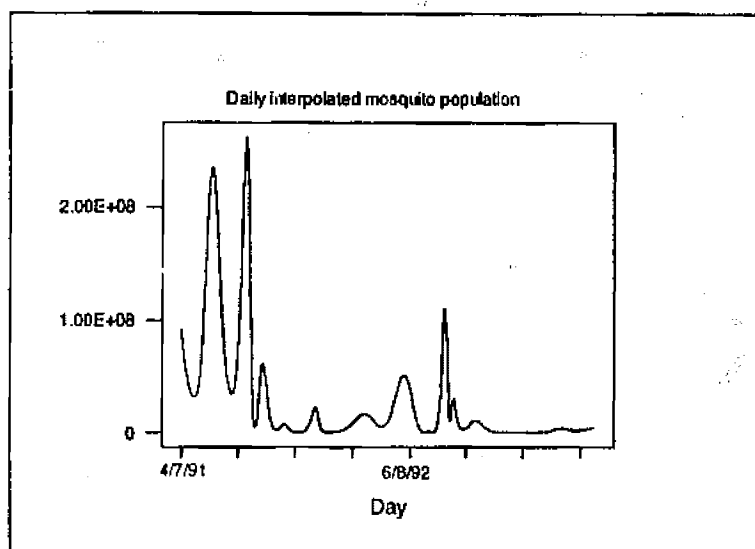


Figure 6.1.20 Interpolated daily *Aedes camptorhynchus* population during the outbreak of 1991/93 in the Peel district.

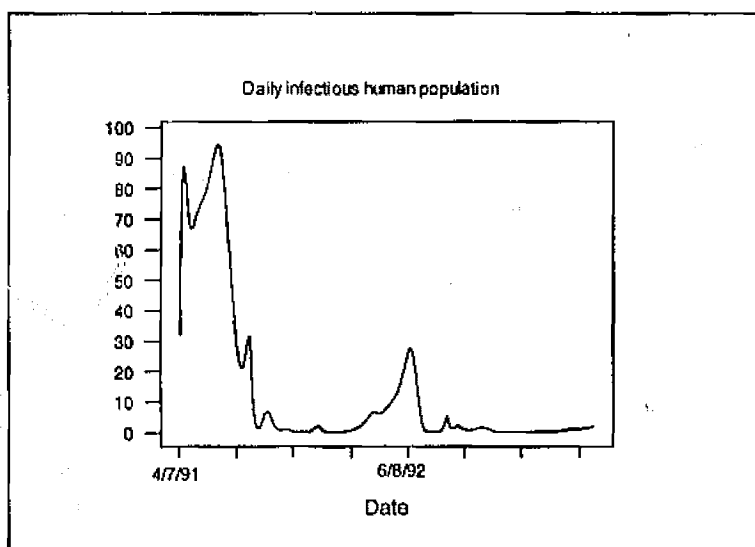


Figure 6.1.21 Daily infectious human population during the outbreak of 1991/93 in the Peel district.

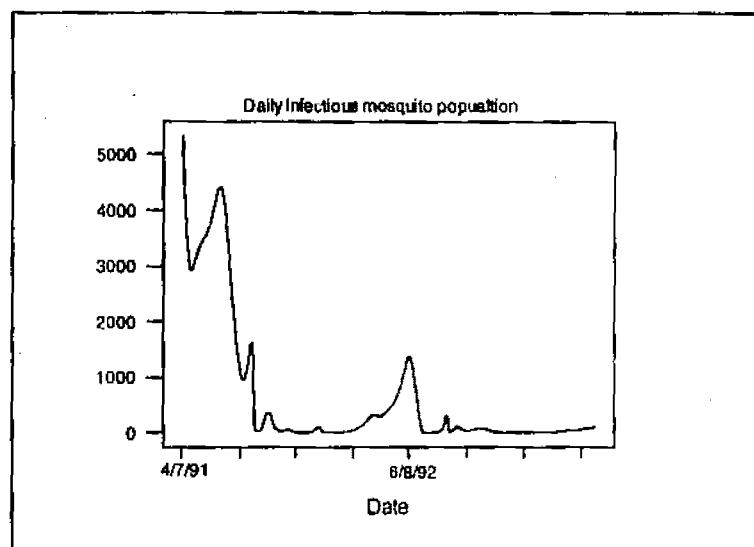


Figure 6.1.22 Daily infectious *Aedes camptorhynchus* population during the outbreak of 1991/93 in the Peel district.

As can be seen on Figure 6.1.20, the *Aedes camptorhynchus* population was substantially smaller in the second year (1992/93). The decline of the *Aedes camptorhynchus* population results in a reduction in the number of human and *Aedes camptorhynchus* infections as shown in Figures 6.1.21 and 6.1.22.

6.1.6. Simulation results with a variable human exposure rate

In this section, the simulation examines the host-vector model with a variable human exposure rate. Since people spend more time outside, and are more exposed to mosquitoes in summer than in winter, seasonal changes in human behaviour can influence the infection rate between humans and *Aedes camptorhynchus*. Hence, the simulation model assumes that the human exposure rate changes annually with 0.5 as the minimum rate on 1st July (mid-winter) and 1 as the maximum rate on 1st January (mid-summer).

Therefore, the infection rates between humans and *Aedes camptorhynchus* are

$$\beta_1 = \frac{\text{Human feeding rate} \times \text{Distribution rate} \times \text{Transmission rate} \times \text{Human Exposure rate}}{\text{Total human population}},$$

and

$$\beta_2 = \frac{\text{VIR rate} \times \text{Distribution rate} \times \text{Transmission rate} \times \text{Human Exposure rate}}{\text{Human feeding rate} \times \text{Total } Aedes \text{ camptorhynchus population at the time } t},$$

where β_1 is the infection rate from *Aedes camptorhynchus* to humans and β_2 is the infection rate from humans to *Aedes camptorhynchus*.

The following Figures 6.1.23 and 6.1.24 give a comparison of the simulation results with and without a variable human exposure rate during the outbreak of 1991/92 in the Peel district.

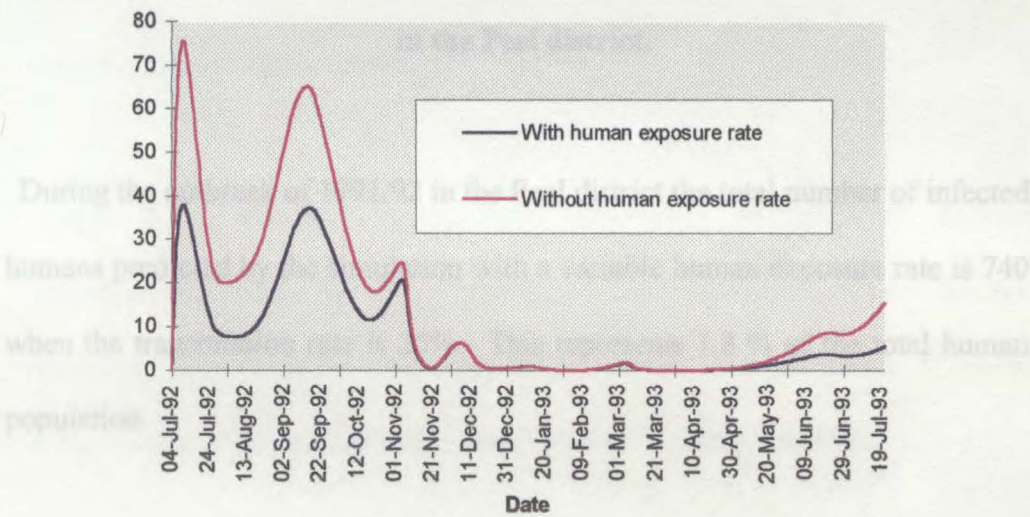


Figure 6.1.23 Daily infectious human population with and without a variable human exposure rate during the outbreak of 1991/92 in the Peel district.

In this section, simulation results for the RRV outbreak of 1991/92 in the Peel district are presented. Since the RRV outbreak is endemic in Southwestern Australia and the model with a single natural infection can not bring ongoing infection after the peak of outbreak, the continuous natural infection is more

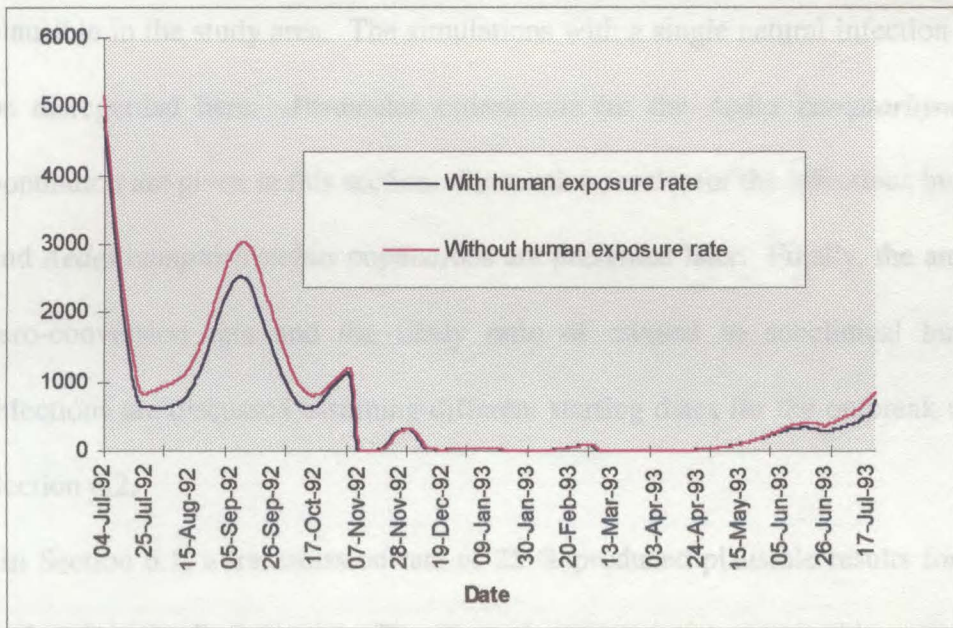


Figure 6.1.24 Daily infectious *Aedes camptorhynchus* population with and without a variable human exposure rate during the outbreak of 1991/92 in the Peel district.

During the outbreak of 1991/92 in the Peel district the total number of infected humans predicted by the simulation with a variable human exposure rate is 740 when the transmission rate is 25%. This represents 1.8 % of the total human population.

6.2. SIMULATION RESULTS FOR THE 1995/96 OUTBREAK IN THE PEEL DISTRICT

In this section, simulation results for the RRV outbreak of 1995/96 in the Peel district are presented. Since the RRV outbreak is endemic in Southwestern Australia and the model with a single natural infection can not bring ongoing infection after the peak of outbreak, the continuous natural infection is more

plausible in the study area. The simulations with a single natural infection will be disregarded here. Parameter estimations for the *Aedes camptorhynchus* population are given in this section. Simulation results for the infectious human and *Aedes camptorhynchus* populations are presented later. Finally, the annual sero-conversion rate and the likely ratio of clinical to subclinical human infections are discussed assuming different starting dates for the outbreak as in Section 6.2.

In Section 6.1, a transmission rate of 25 % produced plausible results for the outbreak in the Peel district. Therefore, the transmission rate in this section is assumed to be 25 %. The variable human exposure rate examined in Subsection 6.1.6 is not included in this simulation model as the range of the human exposure rate is still unknown.

Table 6.2.1 obtained by Lindsay, University of Western Australia (unpublished), shows the date of the traps, successful trap numbers, the total number of trapped *Aedes camptorhynchus*, and the average number of trapped *Aedes camptorhynchus* per trap in the Peel district during 1995/96.

Table 6.2.1 The date of the traps, successful trap numbers, the total trapped mosquito numbers from successful traps, and the average number of the trapped mosquitoes per trap in the Peel district during 1995/96.

Date	traps	Sum (from traps) <i>Aedes camptorhynchus</i>	Mean <i>Aedes camptorhynchus</i>
17-Jul-95	20	2704	135.200
14-Aug-95	19	2438	128.316
29-Aug-95	20	4686	234.300
14-Sep-95	21	5891	280.524
26-Sep-95	20	5809	290.450
11-Oct-95	20	3904	195.200
24-Oct-95	20	4000	200.000
6-Nov-95	19	5676	298.737
22-Nov-95	20	4550	227.500
7-Dec-95	19	7452	392.211
27-Dec-95	18	7486	415.889
15-Jan-96	19	407	21.421
5-Feb-96	18	661	36.722
15-Feb-96	18	1018	56.556
28-Feb-96	18	2256	125.333
11-Mar-96	19	473	24.895
28-Mar-96	19	50	2.632
10-Apr-96	19	207	10.895
23-Apr-96	19	247	13.000
14-May-96	19	1389	73.105
3-Jun-96	19	1037	54.579
18-Jul-96	19	5158	271.474

As in Section 6.2, the interpolated daily *Aedes camptorhynchus* population, the parameter estimations of the mortality and recruitment rates, and the extrinsic incubation period are shown in the following Figures 6.2.2, 6.2.3, 6.2.4, and 6.2.5, respectively.

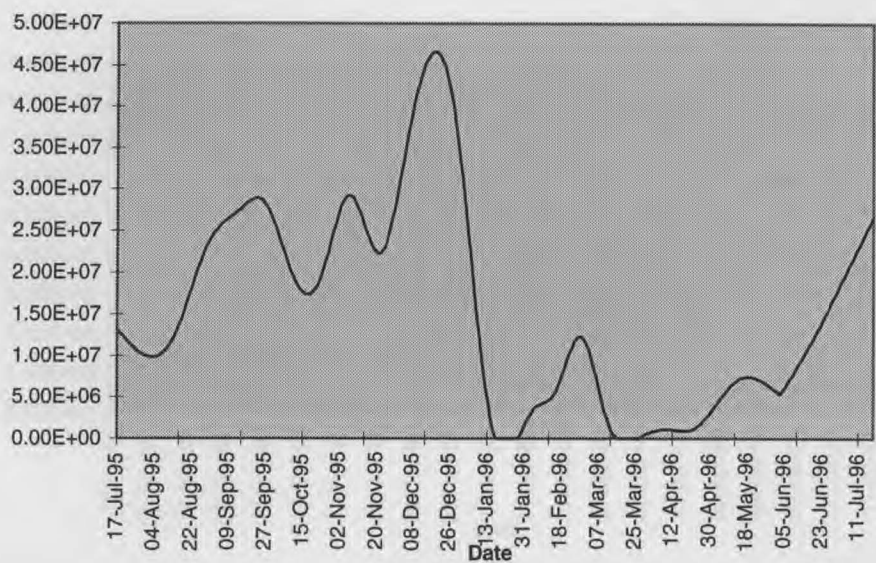


Figure 6.2.2 Interpolated daily *Aedes camptorhynchus* population during the outbreak of 1995/96 in the Peel district.

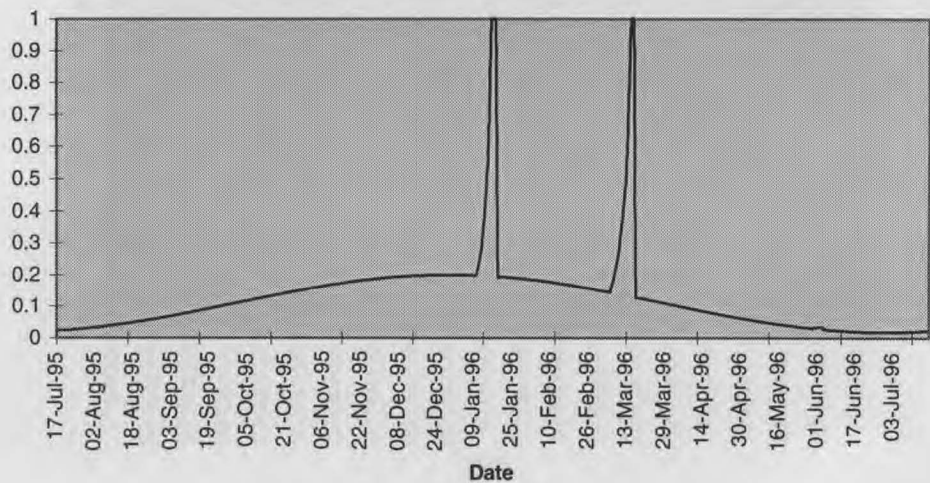


Figure 6.2.3 Modified daily mortality rate during the outbreak of 1995/96 in the Peel district.

Two peaks in Figure 6.2.3 are found after generating the daily recruitment rate on *Aedes camptorhynchus* population given in Figure 6.2.4. This implies that during the period of two peaks some environmental changes occurred and caused more death on *Aedes camptorhynchus* population.

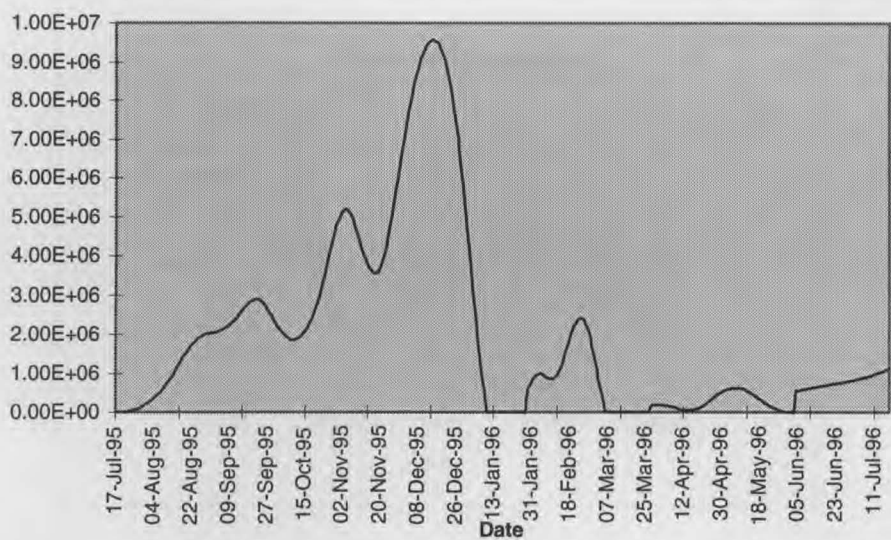


Figure 6.2.4 Modified daily recruitment rate during the outbreak of 1995/96 in the Peel district.

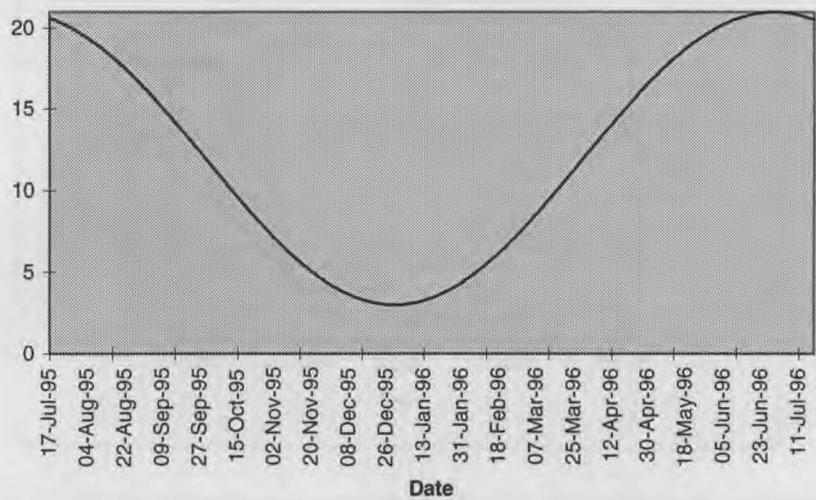


Figure 6.2.5 Daily extrinsic incubation period during the outbreak of 1995/96 in the Peel district.

The following Figures 6.2.6 and 6.2.7 present the infectious human population and infectious mosquito population during the outbreak of 1995/96 in the Peel region with five different starting dates: 4th July, 14th and 29th August, 14th and 26th September, 1995. Starting dates of the outbreak are selected according to the mosquito trap dates given in Table 6.2.1.

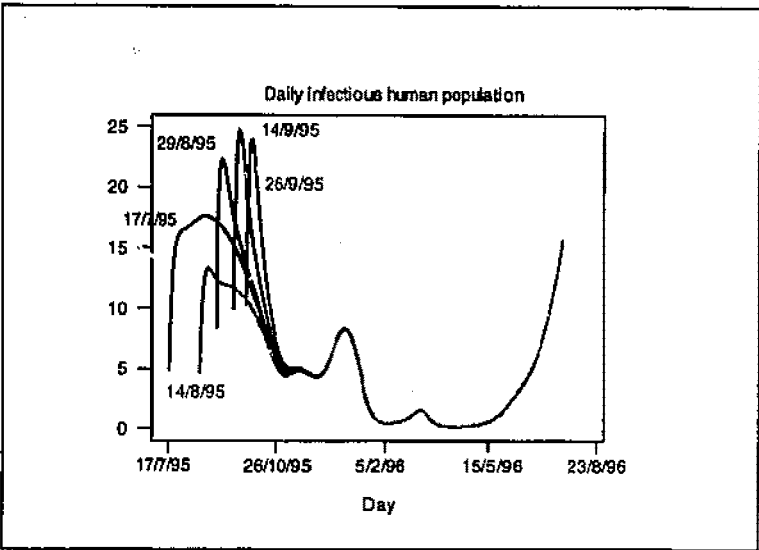


Figure 6.2.6 Daily infectious humans during the outbreak of 1995/96 in the Peel district using different starting dates for the outbreak

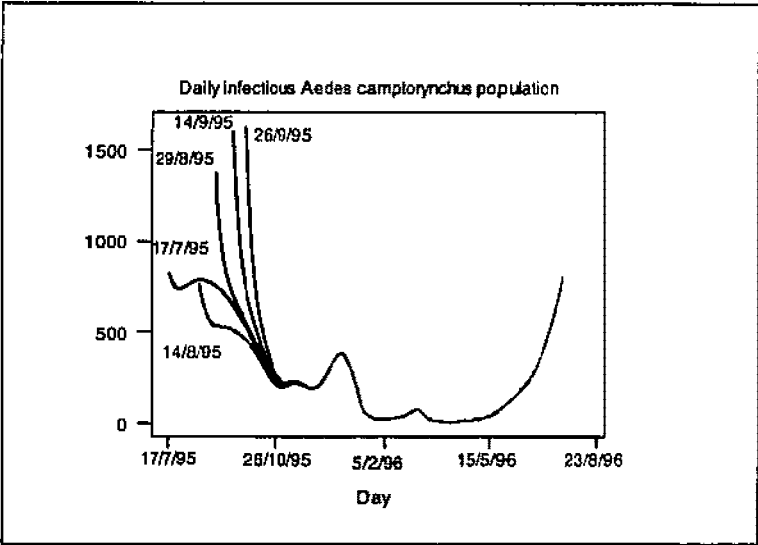
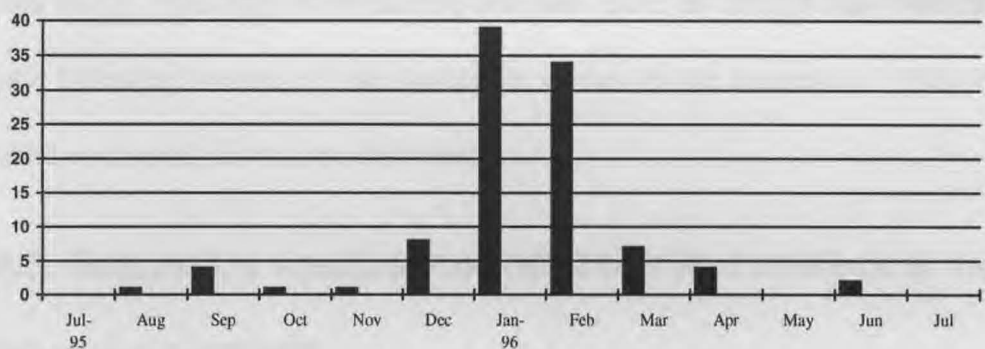


Figure 6.2.7 Daily infectious mosquitoes during the outbreak of 1995/96 in the Peel district using different starting dates for the outbreak

Figure 6.2.7 shows the starting sizes of the infectious *Aedes camptorhynchus* population for the different starting dates. Figure 6.2.8 shows the actual number of notifications during the outbreak. The table 6.2.9 presents the likely ratios of clinical to subclinical human cases and the annual sero-conversion rates during the outbreak of 1995/96 in the Peel district for the different starting dates. The number of total human notifications during the outbreak of 1995/96 was 101.



**Figure 6.2.8 Human notifications during the outbreak of 1995/96
in the Peel district**

Table 6.2.9 The number of the total infected humans, sero-conversion rates, and the likely ratios of clinical to subclinical human infections during the outbreak of 1995/96 in the Peel district according to the starting date of the outbreak when the transmission rate is 25%.

Starting date of the outbreak	Total infected humans during the outbreak between July/95 and July/96	Sero- conversion rate	The likely ratio of clinical to subclinical human infections
17/7/95	585	1.04	1 : 5.8
14/8/95	423	0.75	1 : 4.19
29/8/95	430	0.77	1 : 4.26
14/9/95	389	0.7	1 : 4.85
26/9/95	353	0.63	1 : 3.5

Compared to the results for the outbreak of 1991/92 given in Section 6.1, the number of human infections for 1995/96 is small. The reason for the reduction is the small size of the mosquito population. However, the fewer human infections staring from 14/8/95 than from 29/8/95 can be explained by that the

initial vector population at the starting time was more on 29/8/95 than 14/8/95. In the following section 6.3, the simulation results for the outbreak of 1995/96 in the Leschenault district are described.

6.3. SIMULATION RESULTS FOR THE 1995/96 OUTBREAK IN THE LESCHENAULT DISTRICT

The Leschenault district is between 165 and 190 km south of Perth, also on the Swan Coastal Plain and extending inland approximately 30 km. The total area of the Leschenault district is 214 km² (Lindsay, 1995). The location of the Leschenault district is given in Figure 6.3.1.

Simulation results in this section are presented in the following order :

1. Parameter estimations for the daily *Aedes camptorhynchus* population, recruitment and mortality rates and extrinsic incubation period of the *Aedes camptorhynchus* population.
2. Simulation results with different transmission rates.
3. Sero-conversion rates and the likely ratios of clinical to subclinical human infections.

6.3.1. Estimating the parameters for the *Aedes camptorhynchus* population

Table 6.3.2 obtained by Lindsay (1995) shows the date of the traps, successful trap numbers, the total trapped *Aedes camptorhynchus* numbers, and the average number of trapped *Aedes camptorhynchus* per trap in the Leschenault district during 1995/96. Using the same method as in Section 6.1, the interpolated daily

Aedes camptorhynchus population in the Leschenault district during 1995/96 is calculated and shown in Figure 6.3.3.

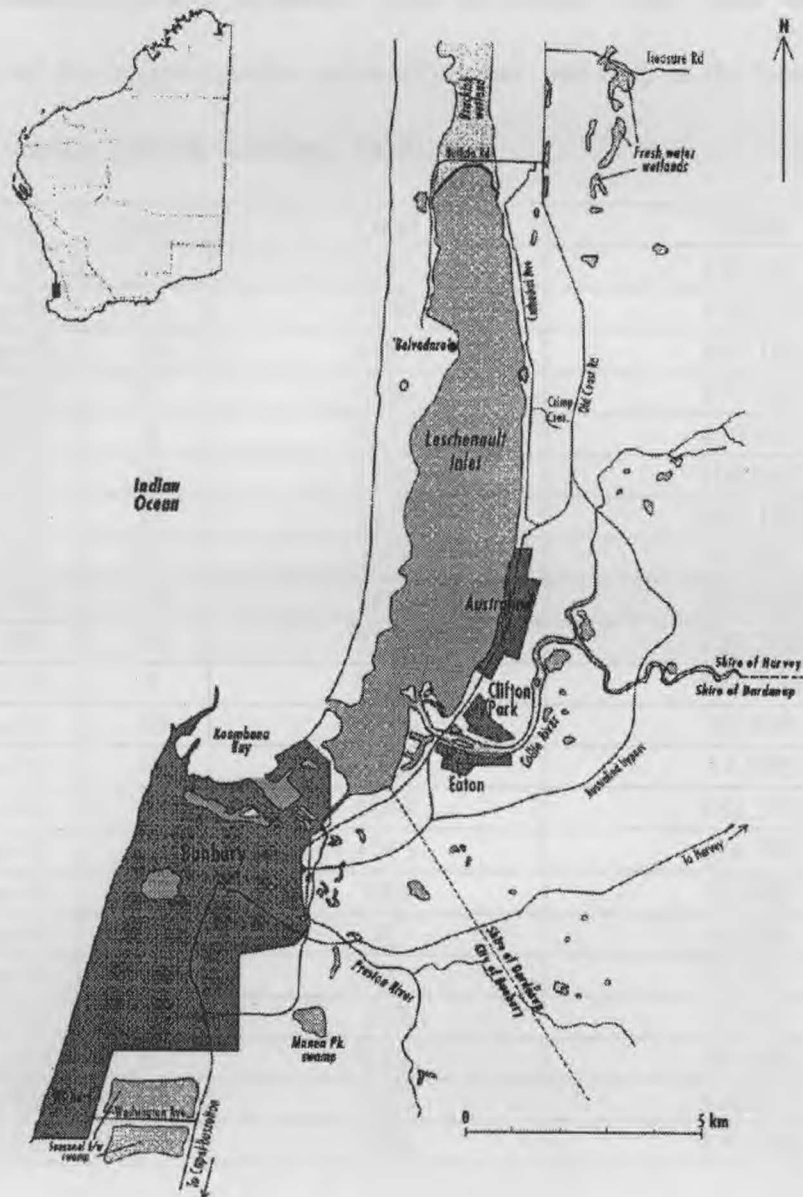


Table 6.3.1 Map showing the Leschenault district, south-west of WA.

**Figure provided by Dr Michael Lindsay, Department of Microbiology,
The University of WA.**

Table 6.3.2 The trap date, successful trap numbers, the total trapped *Aedes camptorhynchus* numbers from successful traps, and the mean number of the trapped *Aedes camptorhynchus* per trap in the Leschenault district during 1995/96 (Lindsay, 1995).

Trap date	traps	Total	Mean
20-Jul-95	11	1523	138.455
14-Aug-95	11	1880	170.909
29-Aug-95	10	1481	148.100
13-Sep-95	11	4104	373.091
27-Sep-95	9	4137	459.667
11-Oct-95	11	1198	108.909
24-Oct-95	11	1839	167.182
6-Nov-95	11	853	77.545
22-Nov-95	10	3855	385.500
7-Dec-95	10	1292	129.200
27-Dec-95	9	4901	544.556
15-Jan-96	10	864	86.400
31-Jan-96	10	140	14.000
15-Feb-96	9	1643	182.556
28-Feb-96	10	1943	194.300
11-Mar-96	10	289	28.900
28-Mar-96	7	28	4.000
10-Apr-96	7	21	3.000
23-Apr-96	7	157	22.429
14-May-96	6	528	88.000
3-Jun-96	7	2232	318.857
18-Jul-96	9	1589	176.556

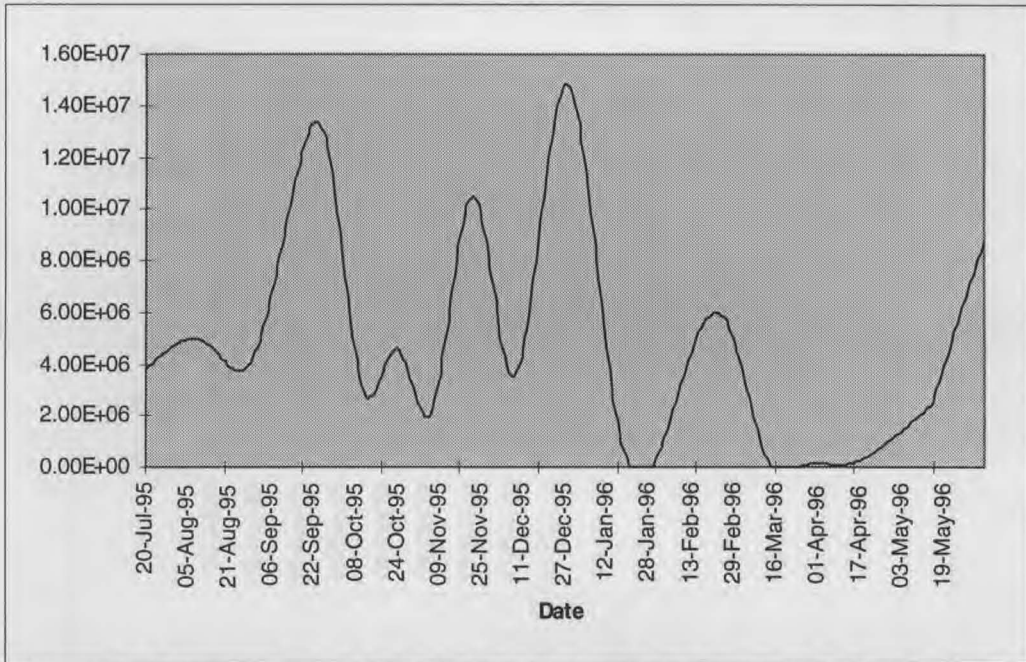


Figure 6.3.3 Interpolated daily *Aedes camptorhynchus* population during the outbreak of 1995/96 in the Leschenault District

The modified mortality and recruitment rates and extrinsic incubation period of the *Aedes camptorhynchus* population are obtained by the same methods as in Section 6.1 and displayed in Figures 6.3.4, 6.3.5, and 6.3.6.

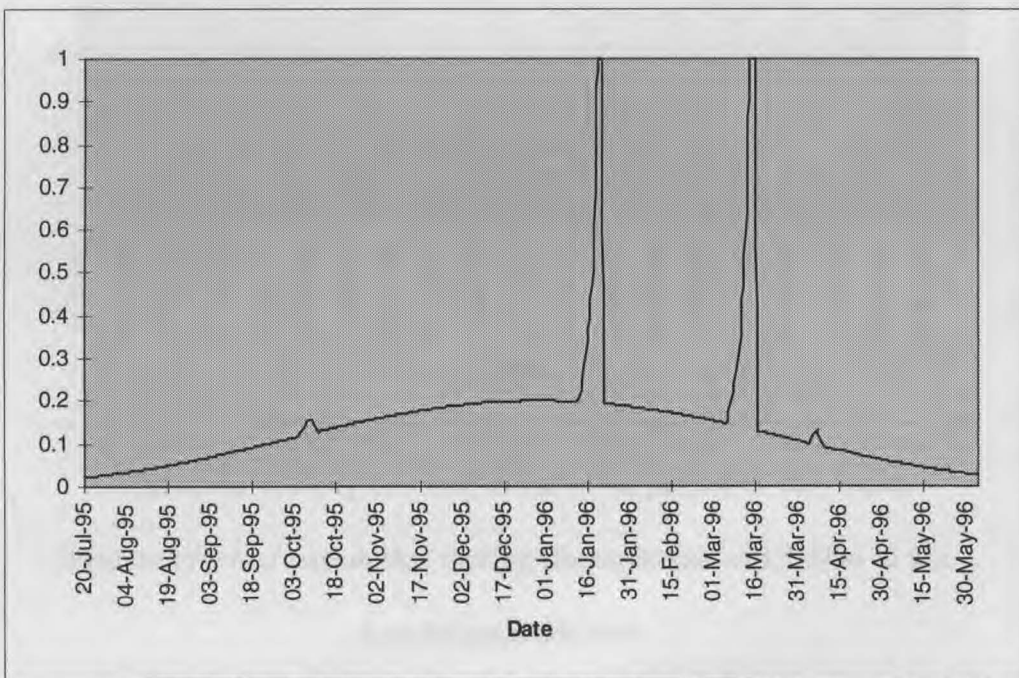


Figure 6.3.4 Modified daily mortality rate during the outbreak of 1995/96 in the Leschenault District.

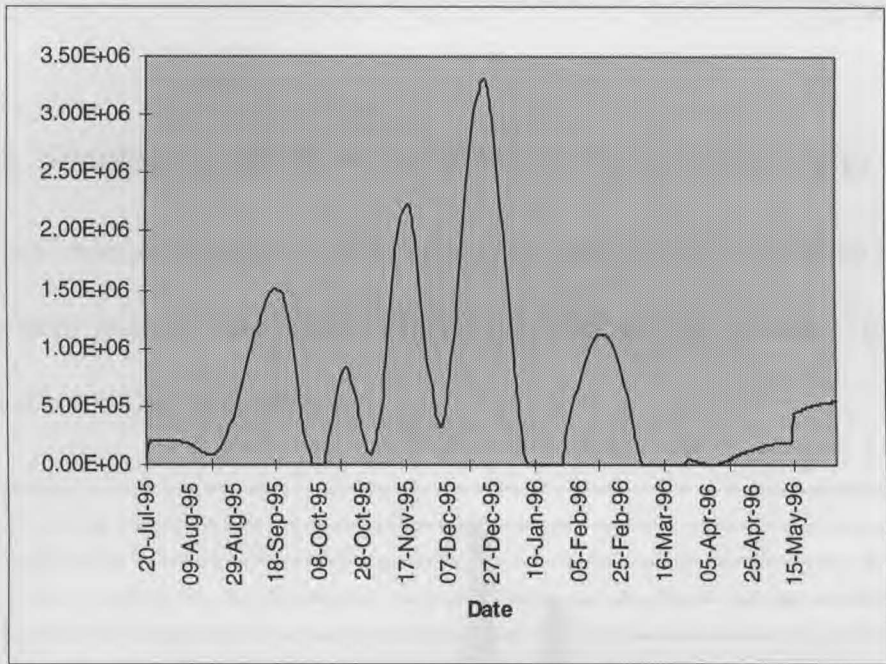


Figure 6.3.5 Modified daily recruitment rate during the outbreak of 1995/96 in the Leschenault District.

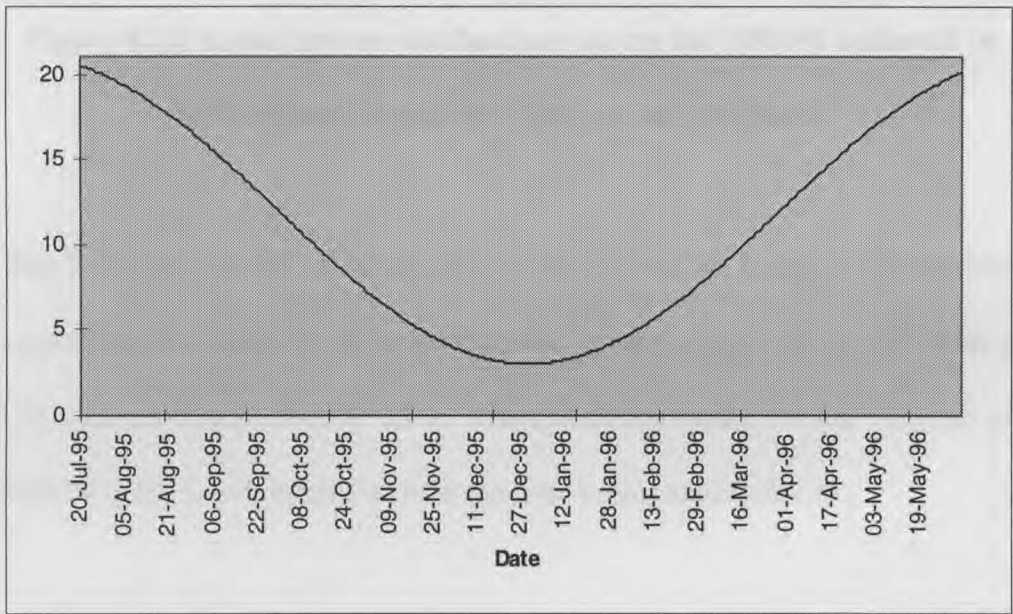


Figure 6.3.6 Daily extrinsic incubation period of the *Aedes camptorhynchus* population during the outbreak of 1995/96 in the Leschenault District.

6.3.2. Simulation results of the different transmission rates

The total number of human notifications during the outbreak of 1995/96 in the Leschenault district was 304. Figure 6.3.7 shows the monthly human notifications during the outbreak.

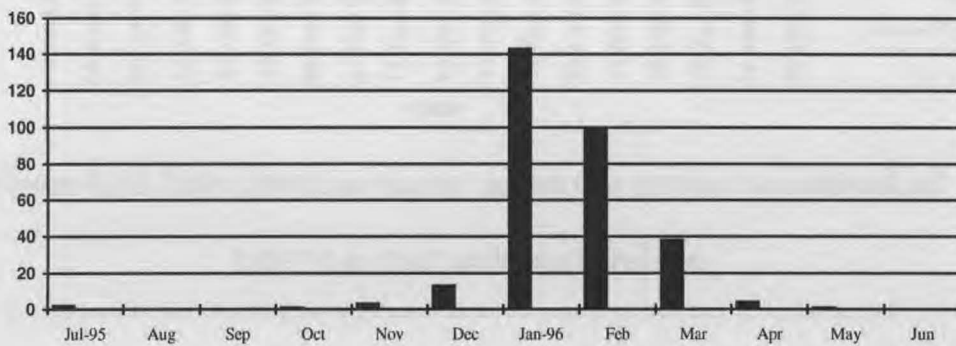


Figure 6.3.7 Actual human notifications during the 1995/96 outbreak in the Leschenault district (Lindsay, unpublished).

The following simulation results for the daily infectious human and mosquito populations are based on transmission rates varying from 0.25 to 0.75 with a 0.05 increment as in Section 6.1.2. The simulation model for the outbreak of 1995/96 in the Leschenault district is the host-vector model (4.1.1).

The following Figures 6.3.8 and 6.3.9 present the infectious human population and infectious *Aedes camptorhynchus* population during the outbreak of 1995/96 in the Leschenault district.

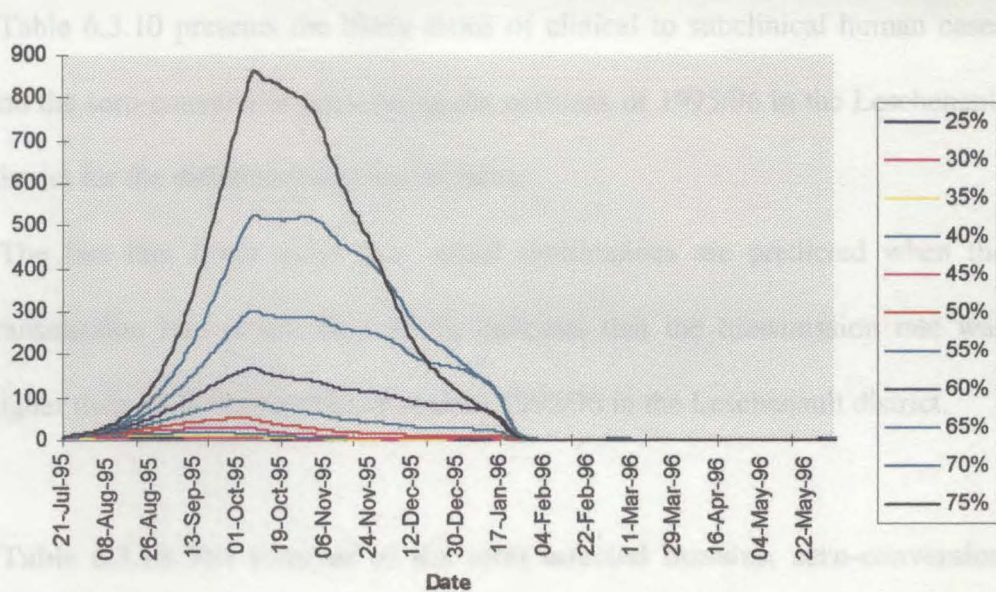


Figure 6.3.8 Daily infectious human population during the outbreak of 1995/96 in the Leschenault district.

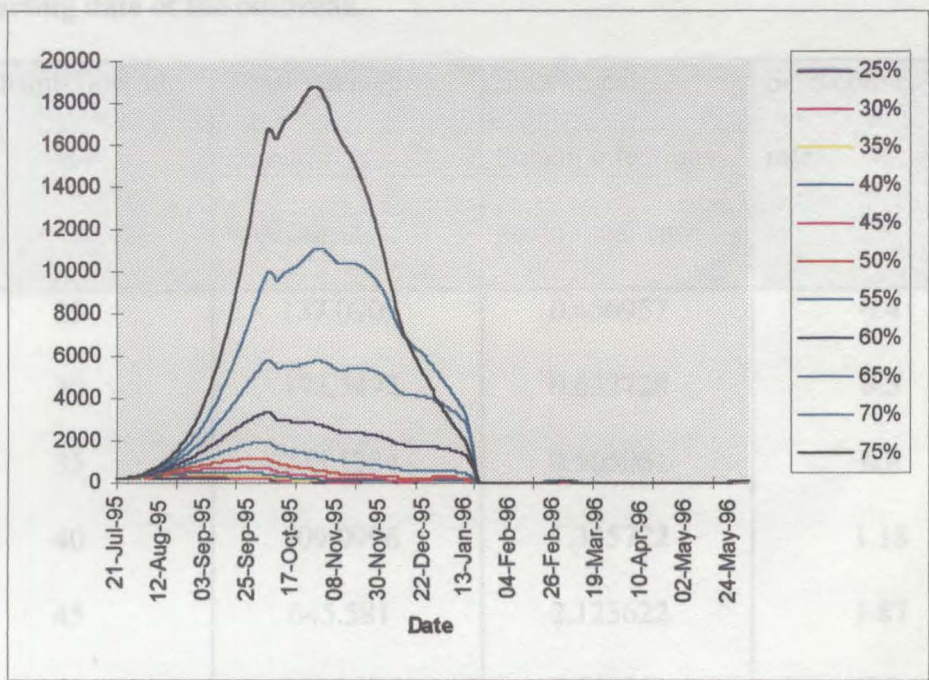


Figure 6.3.9 Daily infectious *Aedes camptorhynchus* population during the outbreak of 1995/96 in the Leschenault district.

Table 6.3.10 presents the likely ratios of clinical to subclinical human cases and the sero-conversion rates during the outbreak of 1995/96 in the Leschenault district for the different transmission rates.

The fact that fewer cases than actual notifications are predicted when the transmission rate is less than 35 % indicates that the transmission rate was higher than 35 % during the outbreak of 1995/96 in the Leschenault district.

Table 6.3.10 The number of the total infected humans, sero-conversion rates, and the likely ratios of clinical to subclinical human infections during the outbreak of 1995/96 in the Leschenault district according to the starting date of the outbreak.

Transmission rate (%)	Total infected human population	Subclinical human infections per clinical case	Sero conversion rate
25	137.0909	0.450957	0.4
30	192.3492	0.632728	0.5
35	275.1384	0.905061	0.8
40	409.0996	1.345722	1.18
45	645.581	2.123622	1.87
50	1106.776	3.640711	3.2
55	2096.367	6.895943	6.07
60	4251.681	13.98579	12.3
65	8102.263	26.65218	23.48
70	12658.13	41.63859	36.69
75	16419.4	54.01118	47.6

6.4. DISCUSSION OF SIMULATION RESULTS

The previous Sections 6.1, 6.2, and 6.3 have presented simulation results based on the outbreaks of 1991/92 and 1995/96 which occurred in the Peel and the Leschenault districts.

Parameters relating to the *Aedes camptorhynchus* population during the outbreak were estimated for the outbreaks; these parameters include the daily interpolated mosquito population, the recruitment and mortality rates and extrinsic incubation period.

The modified mortality rate for the *Aedes camptorhynchus* population in 1991/92, (6.1.4), has a different shape to these for the two outbreaks of 1995/96, (6.2.3) and (6.3.4). The different mortality rates are likely to indicate that the environmental effects modulating the *Aedes camptorhynchus* population were changing more rapidly during the outbreak of 1991/92 in the Peel district than the other two outbreaks. The similarity of the modified mortality rates in (6.2.3) and (6.3.4) during the outbreaks of 1995/96 in the Peel and Leschenault districts indicate that the weather patterns in the two districts during the outbreaks were similar. The reason for this may be that these regions are very close, lying only 100 km apart.

In section 6.1, various types of methods were used to determine the spread of the disease during the outbreak of 1991/92 in the Peel district.

Subsection 6.1.2 presented the results of using two different hypotheses : a single and continuous natural infection in the *Aedes camptorhynchus* population

with different transmission rates. According to the simulation results given in Figure 6.1.13, in the case of a single natural infection the disease eventually dies out as there is no source of ongoing infection in the *Aedes camptorhynchus* or human populations. In the case of continuous natural infection, the disease persists in the host and vector populations during the rest of the outbreak. Since the RRV disease is endemic in Southwestern Australia, continuous natural infection in the *Aedes camptorhynchus* population is a more plausible mechanism of RRV transmission than single natural infection.

The results of using different transmission rates showed that higher transmission rates result in more human infections, which is to be expected.

Since the date of the introduction of the RRV into the *Aedes camptorhynchus* population is currently not known, different starting dates for the outbreak are simulated in Subsection 6.1.3. Later starting dates and the total number of the mosquito population on the starting dates for the outbreak produce different results of human infections as seen in Table 6.1.17.

In Subsection 6.1.4, Figures 6.1.18 and 6.1.19 presented the results of a ten year simulation based on the assumption that the *Aedes camptorhynchus* population changes for ten years with the same parameter variables as during the outbreak of 1991/92 in the Peel district. The results indicate that if the *Aedes camptorhynchus* population fluctuated in the same way as in 1991/92 for ten years then there would be an outbreak of similar magnitude each year. Since this did not happen, the next Subsection 6.1.5 examines a simulation of consecutive outbreaks in the Peel district based on the actual trapped *Aedes camptorhynchus* population. Figures 6.1.20 and 6.1.21 are consistent with the

trend in actual notifications, which indicated an outbreak of RRV in 1991/92 followed by a recess of two or three years.

In Subsection 6.1.5, the simulation examined the human exposure rate during the outbreak of 1991/92 in the Peel district. Since humans are more exposed to mosquitoes in summer than in winter, a variable human exposure could influence the infection rate. Since there was very little discussion in the literature on human exposure, the model assumed the human exposure rate is 0.5 in winter and 1 in summer, and modelled it as a cosine curve in the same way as the extrinsic incubation period of the mosquito population. With the assumption of a variable human exposure rate, the results as given in Figures 6.1.23 and 6.1.24 showed a significant reduction in human infections as compared with the results obtained without a variable human exposure rate. Since the range of variation in the human exposure rate is not yet known, a variable exposure rate was not included in the simulations of the other two outbreaks. As a future research of this study, the sensitivity analysis of this rate shall be followed later.

Section 6.2 presented results from models of the 1995/96 outbreak in the Peel district with continuous natural infection. Compared to the results for the same transmission rate (25 %) in Section 6.1, the number of human infections occurring the 1995/96 outbreak given in Table 6.2.9 is approximately 2.8 times less than that of the 1991/92 outbreak in the same area. The smaller size of the mosquito population during the 1995/96 outbreak resulted in the reduction of the human infections. However, the actual number of notifications during the outbreak of 1995/96 was 101, which is more than in 1991/92. One of the possible explanations for this is that the public is now more aware of the disease

than it was in 1991/92. Also, it is possible that the transmission rate during the outbreak of 1995/96 was higher than that of 1991/92.

Section 6.3 presented results from models with continuous natural infection for the outbreak of 1995/96 in the Leschenault district. The results given in Table 6.3.9 indicate that during the outbreak the transmission rate was at least higher than 35 % since if the transmission rate was less than 35 % the number of human infections predicted by the simulation are less than the actual number of notifications.

The seroconversion rates and ratios of clinical to subclinical human infections during the outbreaks were obtained for each outbreak. From the simulation results, the transmission rate varied show the range of the results according to its different value and implied that the transmission rate must be determined to gain the realistic result.

CHAPTER 7.

CONCLUSION

This chapter presents a brief summary and conclusion of the previous chapters, and suggests future directions for the research.

7.1. Summary

The host-vector models for the RRV were presented and their mathematical analyses were discussed in Chapters 3 and 4. The threshold conditions for a true outbreak to occur were obtained for each model and its ecological implications were discussed.

Some of the parameters included in the models are time-dependent and their exact functional forms are unknown, so the stability analysis of the host vector models has been undertaken by replacing these parameters with their constant average values. Even though the general models (3.3.1) and (4.3.1) are more realistic, it is difficult to estimate many of the parameter values involved in the simulation. For this reason, only the simple models (3.1.1) and (4.1.1), with one human host and one mosquito species vector, *Aedes camptorhynchus*, were simulated in this thesis.

The methods used to estimate parameters relating to the host and vector populations were introduced and discussed in Chapter 5. The limited literature on the parameters of the mosquito population compelled us to extrapolate some parameter values from published studies of other arboviruses

and to use numerical methods to estimate other parameter values. For example, it is believed that the recruitment and mortality rates of the mosquito population are dependent on environmental factors such as temperature, humidity, tidal phase, etc. Research on the impact of these factors has not yet been completed. Hence, in this thesis a cosine curve was chosen to fit the daily mortality rate and used to extract the daily recruitment rate from the daily interpolated mosquito population.

The lack of knowledge about the mechanism of the mosquito population led us to consider a host-vector model with both single and continuous natural infection in the mosquito population. Even though natural infection could occur randomly and would probably be influenced by environmental factors, this thesis examined only the two simple hypotheses of single and continuous natural infection in the mosquito population.

In Chapter 6, various methods of RRV transmission were examined to model outbreaks that have occurred in Southwestern Australia. Single and continuous natural infection in the mosquito population were simulated and compared in Section 6.1.2. Since RRV is endemic in Southwestern Australia, continuous natural infection was more plausible for the study areas.

Since the point of time at which the virus was introduced into the region is unknown, different starting dates for the outbreaks were examined and compared in 6.1.3 and 6.2. The results given in Figures 6.1.16 and 6.2.7 indicated that the time of the introduction of the virus plays an important role in the transmission since the size of the susceptible vector population (initial infective vectors) differs each time.

Results of the ten year simulation based on the 1991/92 outbreak in the Peel district (given in Figure 6.1.18) showed that if the mosquito population is periodic and the size of the human population does not change, then the outbreak is also periodic. However, in reality, the mosquito population during the two year consecutive outbreak of 1991/93 in the Peel district (shown in Figure 6.1.20) was not periodic and the results given in 6.1.22 demonstrated that the reduction in the size of the mosquito population resulted in fewer human infections.

Results with a seasonal human exposure rate to mosquitoes were presented in Section 6.1.6. Even though a variable human exposure rate has not been confirmed by any research, the concept of the rate is obvious (Personal communication, Lindsay). The results given in Figure 6.1.23 implied that a variable human exposure rate would reduce the number of human infections during an outbreak.

In conclusion, the models presented in this thesis suggest that infection rates between hosts and vectors and levels of immunity in host populations in particular play an important role in determining whether an outbreak of human disease can occur. Consequently, such parameters should be more clearly defined in order to provide a better understanding of RRV transmission.

7.2 Future directions

Much of the current research on RRV transmission is not yet complete. However, there are many microbiologists and entomologists working on the mechanics of RRV transmission. It is expected that a more thorough

knowledge of the transmission mechanism will lead to more reliable simulations of the spread of the disease. For example, research on the natural infection rate and human exposure rate should provide better parameter estimates.

Future research areas following from this thesis are :

1. Detailed parameters relating to the populations involved in RRV transmission.

For example, marsupials are presumed to be the major amplifiers of RRV and *Aedes camptorhynchus* is thought to prefer marsupials over humans as a source of blood (Kay *et al.*, 1987; 1989). *Aedes vigilax* was also present during the 1995/96 epidemic (Lindsay *et al.*, 1996). Therefore future modelling should include the marsupial population and both *Aedes camptorhynchus* and *Aedes vigilax* as vectors. The author has already started preliminary research in this area.

2. Spatial modelling of the effect of tourism on RRV in Western Australia.

One of the important features of RRV transmission in Western Australia is the geographical spread of the disease. Since the study areas considered in this thesis are popular places during holidays, especially during summer time, there are many tourists during the period from the Perth metropolitan areas. Modelling this factor should explain the interaction between outbreaks in these regions.

3. Stability analysis of the dynamics with variable parameters.

Smith (1986) has studied the stability analysis of nonlinear systems with periodic parameter functions. Even though malaria models belong to the category of his models, the RRV models do not belong to them because the

removals do not return to the susceptible class. The study of the stability of the dynamics of RRV models when parameters are time-dependent will improve our overall understanding of the simulations.

Finally, to conclude this thesis I personally believe that in spite of the stated future research needs and discussion of the limitations of the existing models, this particular study represents a significant step towards a greater understanding of the dynamics of RRV in Western Australia. We have demonstrated how the meticulous application of disease transmission models coupled with the collaboration of biologists and entomologists working in the field, can provide insights and knowledge both for the applied mathematician and the greater community at large. In the words of N.T.J. Bailey (1957),

'Epidemic theory is a luxury that mankind can ill afford, the world must not only be interpreted, it must be changed.'

References

- Anderson, S.G. & French, E. L. (1957). An epidemic exanthem associated with polyarthritis in the Murray Valley. The Medical Journal of Australia. 148, 113-117.
- Australia, Weekly Epidemiological Record. (1994). Ross River virus infection. 69(13), 98-100.
- Bailey, N.T.J. (1975). The Mathematical Theory of Infectious Diseases. Griffin.
- Bartlett, M.S. (1956). Deterministic and stochastic models for recurrent epidemics, Proc. Third Berkeley Symp. of Math. Statist. 4, 81-109. Berkeley and Los Angeles: Univ. California Press.
- Bartlett, M.S. (1960a). Stochastic Population Models in Ecology and Epidemiology. London: Methuen.
- Bartlett, M.S. (1960b). Some stochastic models in ecology and epidemiology. In Contributions to Probability and Statistics: Essays in Honor of Harold Hotelling (ed. I. Olkin et al.), 89-96. Stanford Univ. Press.
- Bernoulli, D. (1760). Essai d'une nouvelle analyse de la mortalite causee par la petite verole et des avantages de l'inoculation pour la prevenir, Mem. Math. Phys. Acad., 1-45.
- Burden, R. L. & Faires, J. D. (1989). Numerical Analysis (Fourth edition). PWS-KENT.
- Campbell, J., Aldred, J. & Davis, G. (1989). Some aspects of the natural history of Ross River virus in south east Gippsland, Victoria. In: Uren, M. F., Blok, J. & Manderson, L. M. (eds) Arbovirus research in Australia.

- Proceedings of the 5th Symposium, Commonwealth Scientific and industrial Research Organisation and The Queensland Institute of Medical Research, Brisbane. 24-28.
- Capasso, V. (1993). Mathematical Structures of Epidemic Systems. Springer-Verlag.
- Comiskey, C.M. (1988). Mathematical Models for the spread of measles in Ireland, M.Sc. Thesis, Dublin City University, Ireland.
- Comiskey, C.M. (1991). Mathematical models for the transmission dynamics of HIV and AIDS in Ireland, PhD Thesis, Dublin City University, Ireland.
- Condon, R.J. & Rouse, I.L. (1994). Acute symptoms and sequelae of Ross River virus in the south west of Western Australia, 1988-89. Health Statistics Branch, Health Department of Western Australia.
- Doherty, R.L., Barrett, E.J., Gorman, B.M. & Whitehead, R.H. (1971). Epidemic polyarthrititis in the eastern Australia, 1959-1970. The Medical Journal of Australia. 1, 5-8.
- Gard, G., Marshall, I.D. & Woodroffe, G.M. (1973). Annually recurrent epidemic polyarthrititis and Ross River virus activity in a coastal area of New South Wales. The American journal of tropical medicine and Hygenocity. 22, 550-551.
- Geelhoed, E.A. (1995). Economic costs of Ross River virus. Report to the Health Department of Western Australia, Perth, WA, 6.
- Hamer, W.H. (1906). Epidemic disease in England. Lancet, 1, 733-9.

- Hasibeder, G. & Dye, C. (1988). Population dynamics of mosquito-borne disease: Persistence in a completely heterogeneous environment. Theoretical Population Biology, 33(1), 31-53.
- Hawkes, R.A., Pamplin, J., Boughton, C.R. & Naim, H.M. (1993). Arbovirus infections of humans in high-risk areas of south-eastern Australia; a continuing study. The Medical Journal of Australia, 159, 159-162.
- Hethcote, H.W. & Van Ark, J.W. (1987). Epidemiological models for heterogeneous populations : proportionate mixing, parameter estimation and immunization programs. Math. Biosci., 84, 85-118.
- Hirsh, M.W. & Smale, S. (1974). Differential Equations, Dynamical Systems, and Linear Algebra. Academic Press.
- Kandall, D.G. (1956). Deterministic and stochastic epidemics in closed populations. Proceedings of the Third Berkeley Symposium of Mathematics, Statistics and Probability. 4, 149-65.
- Kay, B.H., Saul, A.J. & McCullaugh, A. (1987). A mathematical model for the rural amplification of Murray valley encephalitis virus in southern Australia. American Journal of Epidemiology. 125(4), 690-705.
- Kay, B.H. and Aaskov, J.G. (1989). Ross River virus (epidemic polyarthritis). In: The arboviruses: ecology and epidemiology, IV, T.P. Monath, Ed., CRC Press, Boca Raton, Florida, 1-36.
- Kingsolver, J. G. (1987). Mosquito host choice and the epidemiology of malaria, The American Naturalist, 130(6), 811-827.

- Lindsay, M.D., Coelen, R., Mackenzie, J.S. (1993a). Genetic heterogeneity among Isolates of Ross River virus from different Geographical regions, Journal of Virology, 67(6), 3576-3585.
- Lindsay, M.D., Broom, A.K., Wright, A.E., Johansen, C.A. & Mackenzie, J.S. (1993b). Ross Rive virus isolation from mosquitoes in arid regions of Western Australia: Implication of vertical transmission as a means of persistence of the virus. The American journal of tropical medicine and Hygenocity, 49(6), 686-696.
- Lindsay, M.D. (1995). Ecology and epidemiology of Ross River virus in Western Australia. PhD Thesis. The University of Western Australia, Perth, Western Australia.
- MacDonald, G. (1952). The analysis of equilibrium in malaria, Trop. Dis. Bull. 49, 813-29.
- MacDonald, G. (1957). The Epidemiology and Control of Malaria. London: Oxford Univ. Press.
- MacDonald, G. (1973). Dynamics of Tropical Diseases. London: Oxford Univ. Press.
- Mackenzie, J.S., Smith, D.W., Ellis, T.M., Lindsay, M.D., Broom, A.K., Coelen, R.J. and Hall, R.A. (1994). Human and animal arboviral diseases in Australia. In: Recent advances in microbiology, 2, G.L. Gilbert, Ed., Australian Society for Microbiology, Melbourne, Australia, 1-91.
- May, R. M. (1976). Mathematical aspects of the dynamics of animal populations, in Studies in Mathematical Biology (ed. S.A. Levin), American Mathematical Society.

- Merianos, A., Farland, A. M., Patel, M., Whelan, P., Dentith, H. & Smith, D. (1992). A concurrent outbreak of Barmah Forest and Ross River virus disease in Nhulunbuy, Northern Territory, Comm. Dis. Intell. (Aust.), 16, 110-111.
- Moreira, H. N. (1992). Lienard-type equations and the epidemiology of malaria, Ecological Modelling, 60(2), 139-150.
- Moshvoskii, Sh. D. (1950). A further contribution to the theory of malaria eradication. Bull. Wld Hlth Org., 6, 992-996.
- Mudge, P. R. (1977). A survey of epidemic polyarthritis in the riverland Area, The Medical Journal of Australia, 1, 649-651.
- Muench, H. (1959). Catalytic Models in Epidemiology, Harvard Univ. Press.
- Murray, J.D. (1993). Mathematical Biology, Springer-Verlag.
- Nimmo, J.R. (1928). An unusual outbreak epidemic, The Medical Journal of Australia, 1, 549-550.
- Ross, R. (1911). The Prevention of Malaria (2nd ed.), London: Murray.
- Smith, H.L. (1986). Cooperative systems of differential equations with concave nonlinearities, Nonlinear analysis. Theory, Methods & Applications, 10(10), 1037-1052.
- Soper, H.E. (1929). Interpretation of periodicity in epidemiology, Proc. Fifth Berkeley Symp. Math. Statist. & Prob., 4, 207-215.
- Strauss, J. H. (1991) Togaviridae. In: Classification and nomenclature of viruses: fifth report of the international committee on taxonomy of viruses. Archives of virology: supplementum 2, R.I.B. Franki, C.M.

- Fauquet, D.L. Knudson and F. Brown, Eds., Springer -Verlag, New York, 216-219.
- Tai, K., Whelan, P.I. & Patel, M.S. (1993). An outbreak of epidemic polyarthritis in the Northern Territory during the 1990-1991 wet season, The Medical Journal of Australia, 158(8), 522-525.
- Turell, M.J., Rossi, C.A. and Bailey, C.L. (1985). Effect of extrinsic incubation temperature on the ability of *Aedes taeniorhynchus* and *Culex pipiens* to transmit Rift Valley fever virus. The American Society of Tropical Medicine and Hygiene. 34(6), 1211-1218.
- Turell, M.J. and Lundstrom, J.O. (1990). Effect of environmental temperature on the vector competence of *Aedes aegypti* and *Ae. Taeniorhynchus* for Ockelbo virus. The American Society of Tropical Medicine and Hygiene. 43(5), 543-550.
- Van der Pol, B. (1927). Forced Oscillations in a circuit with non-linear resistance (Receptance with active triode). Edinburgh Dublin Philos. Mag., 3, 65.
- Wilson, E. B. & Worcester, J. (1941). Contact with measles, Proc. Nat. Acad. Sci., Washington, 27, 129-135.
- Wilson, E. B. & Worcester, J. (1945). Damping of epidemic waves. Proc. Nat. Acad. Sci., Washington, 31, 294-8.
- Wolstenholme, J. (1991). Ross River virus disease in Victoria during the summers of 1988/89 and 1989/90. Communicable diseases Intelligence (Australia) 15, 137-139.

Wolstenholme, J. (1992). Ross River virus; an Australian expert?, The Medical Journal of Australia, 156(8), 515-516.

APPENDIX

A.1. The computer program

The computer programs for the simulations in this thesis are all written in C language. In this Appendix, the computer program for the simulation of the host-vector model (7.1.2) with continuous natural infection on mosquito population is presented. The algorithms of the Natural Cubic Spline interpolation and Runge-Kutta method for systems of differential equations are obtained from Burden (1989).

A.2. The computer program listings

```
/* The simulation of the Ross River virus transmission */
/* This model is written for a host vector model (7.1.2) */

#include <stdio.h>
#include <math.h>

/* To define subroutines to calculate differential equations */

/* Human Susceptibles */
double f1(double aa, double bb, double cc, double dd)
{
    return((-1.0) * aa * bb * cc / dd);
```

```
    }

/* Human Infectives */

double f2(double aa, double bb, double cc, double dd, double ee, double ff)

{

    return( aa * bb * cc / ff - dd / ee);

}


/* Mosquito Susceptibles when the total mosquito population is non-zero*/

double f31(double aa, double bb, double cc, double dd, double ee, double ff)

{

    return((-1.0) * aa * bb * cc / ff - ( dd) * bb + ee - bb/(15617.0 * 30.0) );

}


/* Mosquito in latent period when the total mosquito population is non-zero*/

double f32(double aa, double bb, double cc)

{

    return((-1.0) * aa * bb + cc - bb / (15617.0* 30.0));

}


/* Mosquito Susceptibles when the total mosquito population is zero*/

double f41(double aa, double bb, double cc, double dd, double ee, double ff

           , double gg)

{

    return(aa * bb * cc / gg - (ee + 1.0 / ff) * dd + bb/(15617.0 * 30.0));
```

```

    }

/* Mosquito in latent period when the total mosquito population is zero*/
double f42(double aa, double bb, double cc, double dd)
{
    return((-1.0) * ( aa + 1.0/ bb) * cc + dd/(15617.0 * 30.0));
}

/* Mosquito infectives */
double f5(double aa, double bb, double cc, double dd, double ee)
{
    return((1.0 / dd) * bb - aa * cc );
}

/* Main Program */

int main( void )
{
    double human_n, human_x[3000], human_y[3000];
    double mozy_x[3000], mozy_e[3000], mozy_y[3000], step[3000];
    double mozy_i[3000], mozy_n[3000], mozy_I[3000], mozy_N[3000],
        hinff[3000], mozy_death[3000], mozy_birth[3000], mstep[3000],
        ext_incub[3000];
    double hinf_rate, minf_rate, viraemia, ext_incuba, mhtrans, hmtrans;
    double s, time, g[5][5], hx, hy, mx, me, my, md, mb, total, ha[3000],

```

```
ir1, ir2, x[3000], a[3000], alp[3000], b[3000], c[3000], d[3000],  
ta, area, sstep, xx, p, hd, l[3000], mu[3000], z[3000], inf_human;  
  
int sd, istep[1000], stepsize, pp, id, i, j, k;  
  
/* To get the total human population, number of traps, the number of days  
*/  
  
/* from the first July, the total area of the study region */  
  
  
scanf("%lf, %d, %lf\n", &human_n, &stepsize, &hd, &area);  
  
id = stepsize;  
  
/* Calculate the possible number of traps (ta) in the study area  
*/  
  
ta = area / (3.141593 * 0.0025);  
  
/* Natural Cubic Spline Interpolation for the daily mosquito population from  
monthly data */  
  
for (i = 0; i < id; i++){  
    scanf("%lf,%lf\n", &mozy_i[i], &step[i]);  
    istep[i] = (int)step[i];  
}
```



```
mozy_n[i] = sqrt( mozy_i[i]);  
  
};  
  
mhtrans = 0.25 ;  
  
hmtrans = 0.25 ;  
  
  
xx = 0.0;  
  
x[0] = 0.0;  
  
for (i = 0; i < id; i++){  
  
    a[i] = mozy_n[i];  
  
    xx = xx + step[i];  
  
    x[i+1] = xx;  
  
};  
  
for (i = 1 ; i < id - 2; i++){  
  
    alp[i] = 3.0 * ( a[i + 1] * step[i-1] - a[i] * ( x[i + 1] - x[i - 1])  
        + a[i - 1] * step[i] ) / ( step[i-1] * step[i] );  
  
};  
  
  
l[0] = 1.;  
  
mu[0] = 0.;  
  
z[0] = 0.;  
  
  
for (i=1; i < id - 1; i++){
```

```

l[i] = 2.0 * ( x[i + 1] - x[i - 1]) - step[i-1] * mu[i - 1];

mu[i] = step[i] / l[i];

z[i] = (alp[i] - step[i-1] * z[i - 1]) / l[i];

};

l[id - 1] = 1.0 ;

z[id - 1] = 0.0 ;

c[id - 1] = 0.0 ;

for (j = id - 2; j > -1; j--){

    c[j] = z[j] - mu[j] * c[j + 1];

    b[j] = ( a[j + 1] - a[j]) / step[j]

        - step[j] * ( c[j + 1] + 2.0 * c[j]) / 3.0;

    d[j] = ( c[j + 1] - c[j]) / (3.0 * step[j]);

};

k = 0;

for (i = 0; i < id - 1; i++){

    sd = istep[i];

    for (j = 0; j < sd; j++){

        mozy_I[k] = a[i] + b[i] * ( k - x[i]) + c[i] * (k - x[i]) * (k - x[i])

            + d[i] * (k - x[i]) * (k - x[i]) * (k - x[i]);

        k = k + 1;

```

```

    };

};

mozy_I[k] = mozy_n[id - 1];

p = 0.0;

/* To calculate the mortality rate (mozy_death) and the extrinsic incubation
   */

/* period (ext_incub) curves */

for (i = 0; i < k + 1; i++){

    mozy_death[i] = 0.5 * (1.0/5.0 + 1.0/56.0) - 0.5 * (0.2 - 1.0/56.0)*
    cos(2.0 * 3.141592 * ( p + hd) /365.0);

    ext_incub[i] = 0.5 * (21.0 + 3.0) - 0.5 * (3.0 - 21.0) *
    cos(2.0 * 3.141592 * ( p + hd) /365.0);

    p = p + 1.0;

};

/* To get the daily mosquito population (mozy_N), daily recruitment rate
(mozy_birth) */

/* and modified daily mortality rate (mozy_death)
   */

mozy_N[0] = ta* mozy_I[0] * mozy_I[0];

mozy_birth[0] = 0.0;

```

```

i = 0;

printf("%d, %lf, %lf, %lf, %lf\n", i, mozy_N[0], mozy_birth[0],
mozy_death[0], ext_incub[0]);

for (i = 1; i < k + 1 ; i++){

    mozy_N[i] = ta * mozy_I[i] * mozy_I[i];

    mozy_birth[i] = ( mozy_death[i] + 1.0 ) * mozy_N[i] -
mozy_N[i-1];

    if (mozy_birth[i] < 0.0) {

        mozy_death[i] = mozy_death[i] - mozy_birth[i]/mozy_N[i];

        if (mozy_death[i] > 1.0) {

            mozy_death[i] = 1.0;

        }

        mozy_birth[i] = 0.0;

    }

};

/* To input the initial condition for infection rates between humans and
mosquitoes */

minf_rate = 0.5 * 0.05 * mhtrans ;

hinf_rate = 0.5 * 0.6 * (1.0 /0.05) * hmtrans ;

/* To input the initial condition for humans and mosquitoes */

```

```
human_x[0] = (1.0 - 0.25) * human_n;
```

```
human_y[0] = 0.0;
```

```
mozy_y[0] = (1.0 / 15617.0) * mozy_N[0];
```

```
mozy_x[0] = mozy_N[0] - mozy_y[0];
```

```
mozy_e[0] = 0.0;
```

```
/* To input the constant value for the viraemia period */
```

```
viraemia = 4.0;
```

```
sstep = 1.0;
```

```
/* Runge-Kutta 4th method for dynamics to solve the model (6.3.1) */
```

```
for (i=1; i < k + 1; i++){
```

```
hx = human_x[i - 1];
```

```
hy = human_y[i - 1];
```

```
mx = mozy_x[i - 1];
```

```
my = mozy_y[i - 1];
```

```
me = mozy_e[i - 1];
```

```
total = mozy_N[i-1];
```

```
ext_incuba = ext_incub[i];
```

```
md = mozy_death[i];
```

```
mb = mozy_birth[i];
```

```

    ir1 = minf_rate * ha[i];

    ir2 = hinf_rate * ha[i];

    human_x[i] = hx + sstep * f1(ir1, hx, my, human_n);

    human_y[i] = hy + sstep * f2(ir1, hx, my, hy, viraemia,
human_n);

    if (total > 0.0){

        mozy_x[i] = mx + sstep * f31(ir2, mx, hy, md, mb, total);

        mozy_e[i] = me + sstep * f41(ir2, mx, hy, me, md, ext_incuba,
total);

    }

    else {

        mozy_x[i] = mx + sstep * f32(md, mx, total);

        mozy_e[i] = me + sstep * f42(md, ext_incuba, me, mx);

    }

    mozy_y[i] = my + sstep * f5(md, me, my, ext_incuba, mx);

    printf("%d, %lf, %lf, %lf, %lf, %lf, %lf, %lf\n" ,i, human_x[i],
human_y[i],
        mozy_x[i], mozy_e[i], mozy_y[i], mozy_N[i]);

    };

    /* To calculate the total infected humans and to print it and the sero
conversion rate*/

```

```
inf_human = (1.0 - 0.25)* human_n - human_x[k];  
  
printf("Infected human during the period = %lf\n", inf_human);  
  
printf("Infected percentage of human = %lf\n", 100.0 * inf_human /  
      human_n);  
  
return 1;  
  
}
```